Tuberculosis Drug Discovery: Challenges and New Horizons

Guilherme Felipe Santos Fernandes,[1,#,*] Andrew Mark Thompson,[2,#,*] Daniele Castagnolo,[1] William Alexander Denny,[2] and Jean Leandro Dos Santos[3,*]

[1] Department of Chemistry, University College London, 20 Gordon Street, London WC1H 0AJ, United Kingdom.

[2] Auckland Cancer Society Research Centre, Faculty of Medical and Health Sciences, The University of Auckland, Private Bag 92019, Auckland 1142, New Zealand.

[3] São Paulo State University (UNESP), School of Pharmaceutical Sciences, Araraquara, 14800903, Brazil.

[#]These authors contributed equally to this work.

ABSTRACT

Over the past 2000 years, tuberculosis (TB) has claimed more lives than any other infectious disease. In 2020 alone, TB was responsible for 1.5 million deaths worldwide, comparable to the 1.8 million deaths caused by COVID-19. The World Health Organization has stated that new TB drugs must be developed to end this pandemic. After decades of neglect in this field, a renaissance era of TB drug discovery has arrived, in which many novel candidates have entered clinical trials. However, while hundreds of molecules are reported annually as promising anti-TB agents, very few successfully progress to clinical development. In this perspective, we critically review those anti-TB compounds published in the last six years that demonstrate good *in vivo* efficacy against *Mycobacterium tuberculosis*. Additionally, we highlight the main challenges and strategies for developing new TB drugs and the current global pipeline of drug candidates in clinical studies, to foment fresh research perspectives.

KEYWORDS: tuberculosis; *Mycobacterium tuberculosis*; drug discovery; drug resistance; preclinical development; *in vivo* efficacy.

1. INTRODUCTION

Tuberculosis (TB) has killed more individuals in the past two millennia than any other infectious illness around the globe.[1-3] Several significant pandemics that have affected humanity, such as the Black Death, smallpox, and the Spanish flu, or even COVID-19, have had cumulative fatalities that pale in comparison to those of TB, one of the oldest and deadliest diseases that still afflicts people today.[3,4] The causative agents of TB are members of the *Mycobacterium tuberculosis* (*Mtb*) complex, primarily *Mtb*, but also its African variants, *Mycobacterium africanum* and *Mycobacterium canettii*, as well as *Mycobacterium bovis*.[5] Estimates based on synonymous substitution rates point to the likelihood of a common ancestor of these species around 15,000 years ago.[6] However, Hayman has speculated of Jurassic origins more than 150 million years ago.[7] The earliest clear evidence of human TB comes from skeletal remains located in a Neolithic settlement in the Eastern Mediterranean, dating from about 9000 years ago, soon after the development of agriculture.[5] Over the centuries, TB has consistently been linked to a high mortality rate.[2] From 2012 to 2019, *Mtb* was the leading infectious killer, responsible for more deaths annually than the Human Immunodeficiency Virus (HIV/AIDS).[8,9] According to the World Health Organization (WHO), in 2020, TB claimed the lives of 1.3 million HIV-negative people (a 0.1 million increase from 2019), while there were a further 214,000 HIV-positive individuals who died from TB.[10] Moreover, there were an estimated 9.9 million new cases of TB in the same year. In comparison, COVID-19 killed about 1.8 million people during 2020.[11]

Currently, the major global TB challenge for the scientific community is the fight against drug-resistant forms of the disease,[12,13] particularly multidrug-resistant TB [MDR-TB; defined as resistance to at least rifampicin (RIF) and isoniazid (INH)] and extensively drug-resistant TB (XDR-TB). The latter was reclassified by the WHO in January 2021 as being either pre-XDR-TB, meaning MDR-TB plus further resistance to any fluoroquinolone, or XDR-TB, now redefined as MDR-TB plus further resistance to “any fluoroquinolone and at least one additional Group A drug” (see Table 1 below).[14] The latest WHO data for drug-resistant TB are concerning, with an estimated 465,000

new cases and 182,000 deaths from MDR- or RIF-resistant-TB in 2019.[9] Crucially, only 38% of affected patients received proper diagnosis and treatment, and the primary global gaps (41%) were in China and India. The arrival of COVID-19 then led to a 15% decrease in the total number of such cases treated in 2020.[10] In the past two decades, there have also been increasing occurrences of *Mtb* strains with resistance to all available TB drugs, resulting in "programmatically incurable" disease.[15-18] While the WHO has not approved the term "totally drug-resistant TB" (TDR-TB) coined by some authors,[15,16] cases of clinical resistance to even the newest TB drugs are now appearing.[19,20]

Recently, three novel agents have received marketing authorisation by regulatory agencies, representing the first new TB drugs to be approved in more than 40 years (**Figure 1**). Bedaquiline (**1**) (BDQ; Janssen Therapeutics)[21] was approved in 2012 by the U.S. FDA for treating MDR-TB.[22] This compound kills both replicating and nonreplicating mycobacteria by interfering with the synthesis of ATP. Specifically, BDQ binds to subunit *c* of the ATP synthase enzyme (which converts ADP into ATP), blocking its action.[23] Delamanid (**2**) (Otsuka Pharmaceutical Co.) was approved in 2014 by the European Medicines Agency (EMA) for use against MDR-TB,[24] and has subsequently gained regulatory approvals in several other countries. Pretomanid (**3**) (TB Alliance) was approved in 2019 by the FDA, although solely for use in combination with BDQ and linezolid (LZD) for the treatment of highly drug-resistant forms of TB (XDR-TB or treatment-intolerant/non-responsive MDR-TB).[25] Further approvals of **3** were granted by the EMA and the Indian regulatory authority in 2020.

Drugs **2** and **3** are representatives of the nitroimidazole class and both act by inhibiting mycolic acid biosynthesis.[26,27] As prodrugs, they first require specific activation by the mycobacterial F_{420}-deazaflavin–dependent nitroreductase. Upon activation, pretomanid (**3**) has been shown to generate reactive nitrogen species, including nitric oxide, which provides an additional mode of action against nonreplicating *Mtb* by blocking cellular respiration.[27] Transcriptional analysis data for *Mtb* exposed to delamanid (**2**) point to similar effects.[28] However, a new study has suggested the importance of forming adducts with NAD in the anaerobic activity of this drug.[29] While some have questioned the FDA approval of pretomanid (**3**) based on limited data in the pivotal Nix-TB trial,[25] it is noteworthy

that in earlier phase IIa early bactericidal activity (EBA) studies, **3** outperformed **2** as a single agent.[30] Pretomanid (**3**) also displays superior oral pharmacokinetics (suitable for once daily dosing), has much lower plasma protein binding than **2** (~86% vs ~99.5%),[24,25] and is now available at a fraction of the price of **2**. Moreover, a new phase II/III clinical trial that compared the oral combination of **3**, BDQ, LZD and moxifloxacin (MFX) for 6 months with standard therapy for MDR-TB (TB-PRACTECAL, NCT02589782) found that the new regimen was both safer and more effective (89% vs 52% of patients were cured).[31]

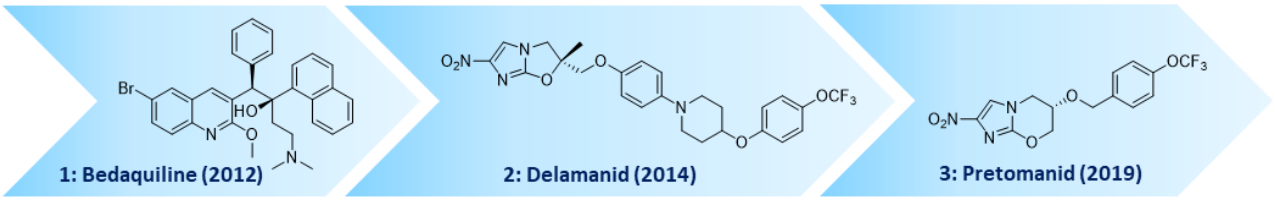

Figure 1. Recently approved drugs for the treatment of MDR-TB.

Each year, hundreds of new molecules are described as promising anti-TB agents, but several questions[32] often remain: 1) How were they designed? 2) What phase of development have they reached? 3) How many agents are likely to reach the clinical development stages and eventually become drugs? This Perspective will first discuss the current challenges faced in TB drug discovery and the strategies used to discover new small molecules as anti-TB agents. Second, it will review the drug candidates in clinical studies in the current TB drug pipeline. Finally, it will describe the latest discoveries of new anti-TB compounds that have reached "validated lead" or preclinical development stages, focusing only on those compounds with significant *in vivo* efficacy against *Mtb* in relevant animal models. Of note, throughout this review, we have converted all MIC, IC_{50} and CC_{50} values to micromolar (μM) to facilitate better comparison between the compounds.

2. CHALLENGES AND STRATEGIES FOR TB DRUG DISCOVERY

From a global perspective, one of the obstacles to better progress in TB drug research is funding. According to the latest Policy Cures Research G-FINDER survey,[33] in 2019, worldwide funding for TB research increased by 4.6% to US$ 670 million, compared to the 2018 data, with reduced industry investment being offset by increased contributions from the Gates Foundation and the German Federal Ministry of Education and Research (BMBF). Another report, provided by the activist organization Treatment Action Group, assessed the 2019 global research funding for TB as reaching US$ 901 million, representing the second highest total ever recorded.[34] Nevertheless, even this amount is still well short of the US$ 2 billion of funding annually that was targeted in the United Nations (UN) Political Declaration on TB during the 2018 "UN High-Level Meeting on the Fight to End TB".[35] Likewise, the Stop TB Partnership's Global Plan to End TB 2018–2022 calls on the world to spend over US$ 2.5 billion per year on TB research (to support further basic science research and the development of new tools), looking toward the goal of eliminating the disease by 2030.[10,36]

These data lead to some critical unanswered questions. Where will we source the remaining US$ 1.1-1.6 billion per year that is needed for TB research? Furthermore, how can we be more productive with the limited available funding?[37] It is broadly accepted that, alongside industry, public–private consortia now play a vital role in successful TB drug development.[38] Several initiatives, partnerships and not-for-profit organizations have emerged since 2000, when few TB drug candidates were in clinical assessment. TB Alliance, Lilly TB Drug Discovery Initiative, TB Drug Accelerator Program, Orchid, New Medicines for Tuberculosis (which became More Medicines for Tuberculosis), the new European Regimen Accelerator for Tuberculosis, UNITE4TB, and Project to Accelerate New Treatments for Tuberculosis, are some examples. Despite the advances these partnerships have achieved (or will achieve), there is still an urgent need for greater, more sustainable and more equitable discovery research funding.[36-39] The annual G-FINDER report shows that over the past 10 years, roughly 63% of research and development funding came from the public sector in high income countries, 20% from philanthropic groups, and 14% from private pharmaceutical and biotechnology companies.[33] In 2019, the top five funding sources for TB research were the US National Institutes

of Health (NIH; US$ 315 million), Gates Foundation (US$ 117 million), aggregate pharmaceutical companies (US$ 83 million), German Federal Ministry of Education and Research (US$ 23 million), and the UK Department for International Development (US$ 17 million).[33] These data provide a final picture of TB research funding before the emergence of COVID-19, an event whose full effect on the research landscape will only be known in the forthcoming years.[34]

Besides the finance issue, there is also the fundamental challenge of working with *Mtb* and our limited grasp of its biology during infection of a human host.[40-42] For instance, *Mtb* is a slow growing bacterium that must be managed under strict containment in facilities (Biosafety Level 3) with the minimum requirements necessary to mitigate risks to laboratory staff. Furthermore, *Mtb* is a highly successful intracellular pathogen that can evade the host immune system by inhibiting several antimicrobial mechanisms of the host, enabling it to survive and replicate inside macrophages, even after been internalized in a phagosome.[43,44] As part of the disease process, the *Mtb*-infected alveolar macrophages penetrate the lung interstitium; here, a growing population of immune cells are recruited to the infection site, engendering a multicellular host response commonly termed a granuloma.[40] As *Mtb* proliferates and inflammation develops, the granuloma structure matures, leading to the destruction of blood vessels, causing increasing necrosis and hypoxia. The ability of macrophages to eliminate the mycobacteria then becomes limited because superoxide and nitric oxide generation is blocked under these conditions.[45] At this stage, if the infection is contained but not eradicated, the mycobacteria can remain in a nonreplicating persistent state or latent state.[40]

The wide range of microenvironments in which *Mtb* survives within the host represents one of the biggest challenges when developing new drugs and should be considered in the drug discovery process.[45] Ideally, a new TB drug should be effective against various physiological states of the bacteria, as differing local conditions (e.g., acidic pH, hypoxia, higher carbon monoxide, or nutrient scarcity) can change their metabolic profile and induce drug tolerance.[42,46] Specialist assays can be used to screen for novel agents that better address this.[45] Bacteria live in diverse lesion and compartment types, including the harder to penetrate caseum of necrotic granulomas (where many

slowly or non-replicating bacilli reside), and can be extracellular or intracellular (in neutrophils and macrophages).[47] Even when the bacteria are successfully reached, the low permeability of the lipid-rich *Mtb* cell wall acts as a barrier, curbing many potential drug candidates from reaching their targets.[42] Besides this, numerous active efflux pumps are expressed and play a crucial role in limiting the anti-TB activity of small molecules, and this represents one of the primary mechanisms of drug resistance in *Mtb*.[48,49] Compounds may also be metabolised within the bacteria, as well as the host. Hence, there are a variety of biological, physical, and pharmacokinetic (PK) factors at play in TB drug discovery, which constrain the development of new lead molecules.

TB is frequently fatal and, in the absence of proper medical treatment, approximately 50% of individuals who develop active TB disease will succumb to it.[50] The current standard medication for drug-susceptible TB (DS-TB) comprises a 6-month course with four first-line antimicrobial drugs: INH, RIF, pyrazinamide (PZA) and ethambutol (EMB). This can achieve cure rates of >95% when administered under directly observed therapy,[51] although global success rates have been consistently lower (86% in 2019).[10,40] Treatment of MDR-TB is far more complex and comprises the use of a cocktail of second-line drugs over 9–12 months for the shorter MDR-TB regimen and at least 18 months for the longer MDR-TB regimens.[12] In 2019, the WHO published new guidelines that brought a major revision and reclassification to the drugs recommended for MDR-TB treatment (**Table 1**).[52] The latest WHO guidelines (2020) have also clarified that the new 6-9 month regimen of pretomanid, BDQ, and LZD can now be used for MDR-TB patients with additional resistance to fluoroquinolone antibiotics (under operational research conditions only).[53] Despite these improvements, shortening treatment times for drug-resistant TB represents one of the main challenges in TB drug discovery. Treatment success here (59% globally in 2018)[10] may be limited by inadequate patient compliance toward the prescribed therapy, due to its greater length, complexity, and adverse side effects. In general, most second-line drugs are more toxic, costly, and less effective than the first-line drugs.[54]

Table 1. Antitubercular drugs recommended by the WHO for the treatment of MDR-TB.[52]

Classification	Drug	Mechanism of action (in *Mtb*)
Group A (Include all three medicines)	Levofloxacin or moxifloxacin	DNA gyrase A inhibitors
	Bedaquiline	Inhibition of ATP synthase
	Linezolid	Protein synthesis inhibition
Group B (Add one or both medicines)	Clofazimine	Release of reactive oxygen species and cell membrane destabilization
	Cycloserine or terizidone	Peptidoglycan biosynthesis inhibition
Group C (Add to complete the regimen and when medicines from Groups A and B cannot be used)	Ethambutol	Arabinogalactan biosynthesis inhibition
	Delamanid	Mycolic acid biosynthesis inhibition
	Pyrazinamide	Coenzyme A biosynthesis inhibition (via target degradation)[55]
	Imipenem–cilastatin or meropenem	Peptidoglycan biosynthesis inhibition (in presence of β-lactamase inhibitor)
	Amikacin or streptomycin	Protein synthesis inhibition
	Ethionamide or prothionamide	Mycolic acid biosynthesis inhibition
	para-Aminosalicylic acid	Inhibition of folic acid and mycobactin biosynthesis

TB treatment in HIV-positive patients is another problematic issue. An estimated 8% of the incident TB cases in 2020 were HIV-positive, and countries on the African continent had the highest proportion of TB cases co-infected with HIV.[10] Furthermore, studies have indicated that HIV-positive patients co-infected with TB face a greater risk of contracting MDR-TB than HIV-negative TB patients.[56] The treatment of these co-infected patients is also more complicated, due to drug-drug interactions between antiretroviral agents and key anti-TB drugs. Such interactions occur between the rifamycin derivatives (RIF, rifabutin and rifapentine) and the drugs that inhibit HIV-protease or reverse transcriptase.[57] For instance, RIF induces the expression of liver enzymes (e.g., CYP3A4) responsible for the metabolism of HIV-protease inhibitors and thus increases the rate of metabolism

196 of these drugs.[56,57] More rapid metabolism can reduce the anti-HIV drug concentration below its
197 optimal range, affecting treatment efficacy.[58]

198 Improving TB therapy remains an urgent research priority and can be summarized in the
199 following goals: i) to make the treatment of DS-TB shorter and simpler, ii) to develop more effective,
200 faster-acting, safe and affordable regimens to cure drug-resistant TB, iii) to discover TB drugs that
201 are more compatible with anti-HIV drugs for treating HIV-coinfected TB patients, and iv) to reduce
202 treatment times for latent *Mtb* infection.[54] These goals are considered vital to improving patient
203 adherence to therapy, thus decreasing the demands on national health systems and minimising the
204 development and spread of resistant strains. Conradie et al. recently reported the results of the Nix-
205 TB trial, an open-label study of 109 patients with XDR-TB or with MDR-TB that was not responsive
206 to treatment (or the therapy had to be discontinued due to drug intolerance).[59] The regimen was daily
207 oral treatment for 26 weeks with BDQ, pretomanid and LZD, followed by a 6-month follow-up
208 period. At the end of that time, 98 of 109 patients (90%) were shown to have a favourable outcome
209 (a negative sputum culture test). Therefore, it is widely recognized that drug discovery has a central
210 role in improving TB therapy and ultimately achieving the 'End TB Strategy' goals.[10,37]

211 TB drug discovery screens can be either target-based or phenotypic/cell-based.[45] Phenotypic
212 screening represents an important strategic approach because it provides the opportunity to discover
213 compounds that inhibit one or more new targets or pathways, or compounds that only become active
214 after enzymatic transformation, such as prodrugs.[42] The main advantage of this cell-based method is
215 that no prior knowledge of the mode of action is required. Moreover, the compounds identified by
216 phenotypic screening display cell permeability and possess structures that can often be modified to
217 improve potency, safety, and PK profile.[43,60,61] Nevertheless, this approach also has some drawbacks,
218 such as the difficulty of hit-to-lead and lead optimisation efforts in the absence of structural data for
219 the target(s) when the cell-based activity depends on multiple parameters.[60] Another weakness is the
220 tendency to repeatedly discover inhibitors of so-called "promiscuous targets",[62,63] as it is now crucial
221 to develop compounds with new mechanisms of action that will not display cross-resistance to other

agents. Target identification can also be problematic. Finally, a recent analysis of active leads against *Mtb* points to limitations around inadequate chemical diversity in the screening libraries used, where, given the likelihood that more than five million compounds have already been tested, there is now a higher risk of rediscovering known inhibitor classes and only modestly improving them.[64]

In contrast to cell-based screening, a target-based drug discovery strategy enables the use and application of *in silico* and other structural approaches to explore a particular molecular proposition.[60,65] The main drawback of this approach is that the selected target may not be essential *in vivo* and vulnerable to drugs.[45] Some targets also develop resistance too readily. Moreover, even when the target is well-validated, it can be challenging to translate potency in cell-free assays into activity in whole cells.[45,61,66] Finding promising anti-TB agents through target-directed screens alone has been relatively unsuccessful.[66] Since publication of the entire *Mtb* genome sequence in 1998,[67] several potential TB drug targets have been pinpointed and validated for use in target-based screening, as reviewed elsewhere.[65,68-72] However, while this strategy has been widely employed in TB drug discovery campaigns, it has so far not produced a single clinically effective anti-TB agent.[60,61,65,66] Truly, not only TB drugs but also most currently used antimicrobial agents had their origins in the phenotypic/cell-based screening strategy, underlining the importance of this latter approach.[60,61] But a more recent tactic of "target-based whole-cell screening" may offer the advantages of both.[45,73]

3. CURRENT STATUS OF NEW TB DRUGS IN CLINICAL DEVELOPMENT

Following the Golden Age of antibiotic discovery (1940s to 1960s), the success of first-line drug regimens in curing TB led to a prolonged period of low activity in TB drug discovery.[51] However, by the early 1990s, a resurgence of TB due to increasing drug-resistance and HIV coinfection prompted the WHO in 1993 to declare the disease a global emergency.[74] In February 2000, public and private sector representatives and donors assembled in Cape Town, South Africa and discussed the urgent need to develop better treatments for TB.[54,74] Today, after two decades of renewed efforts in this area,

the situation has improved (**Figure 2**), with seventeen drug candidates now listed as being in various stages of clinical development.[75] Of these, up to ten might qualify as "radical innovation" due to their novel mechanisms of action (although four agents have the same target, two being from the same chemical class; **Table 2**). The remaining seven candidates are re-optimised versions of existing TB drugs. This illustrates the point made by Nobel Prize winner, Sir James Black, that "the most fruitful basis for the discovery of a new drug is to start with an old drug".[76] It is also in line with a recent analysis of published clinical candidates from the *Journal of Medicinal Chemistry*, which concluded that the most common lead generation approach in these cases was to start from a previously known compound (43%); random screening was ranked as the second most common strategy (29%).[77]

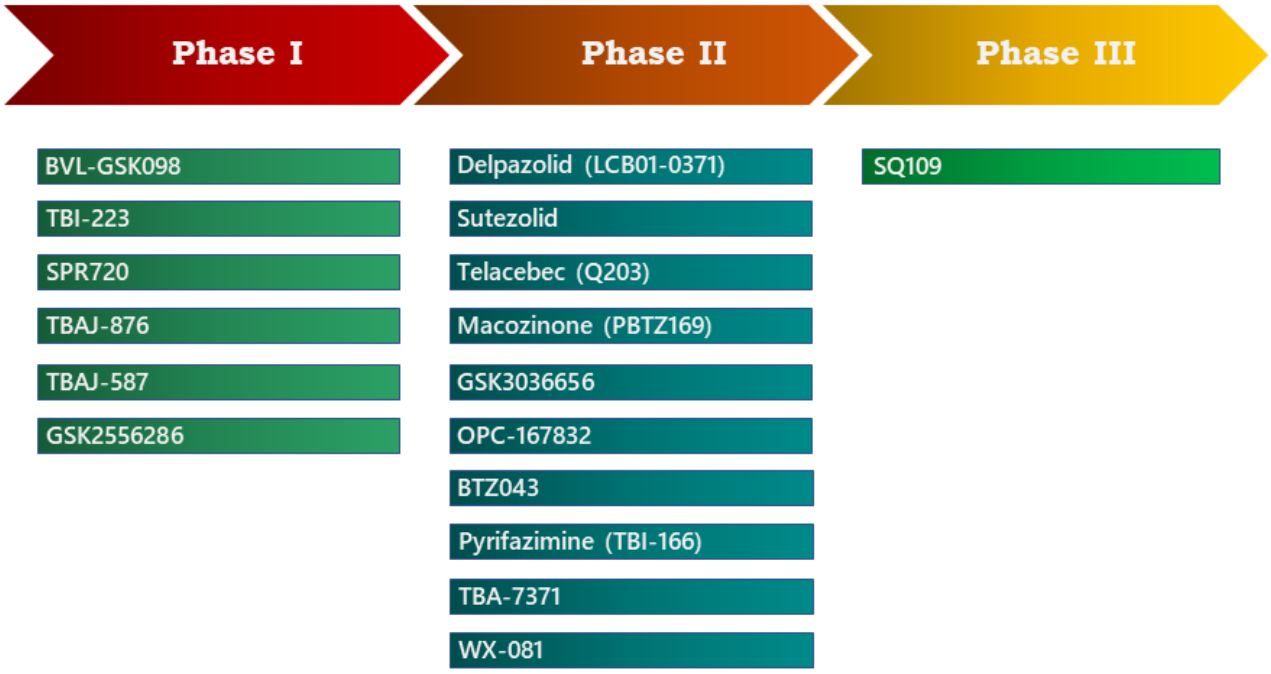

Figure 2. Current global pipeline of new tuberculosis drugs based on information provided by the Working Group for New TB Drugs (WGND)[75] and Treatment Action Group.[78]

Table 2. Current global pipeline of new tuberculosis drugs in clinical development.

Name	Structure	Chemical class	Phase	Target

SQ109 (**4**)	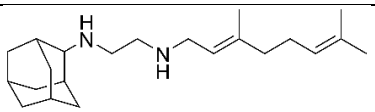	Ethylenediamine	IIb/III	MmpL3 and energy production
Delpazolid (**5**) (LCB01-0371)	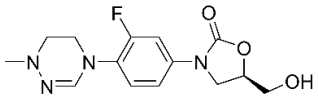	Oxazolidinone	IIb	Protein synthesis (50S ribosomal subunit)
Sutezolid (**6**)	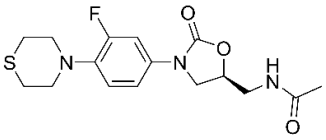	Oxazolidinone	IIb	Protein synthesis (50S ribosomal subunit)
Telacebec (**7**) (Q203)	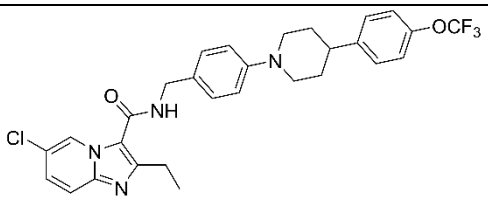	Imidazopyridine amide	IIa	Energy production (QcrB subunit of cytochrome *bcc*)
Macozinone (**8**) (PBTZ169)	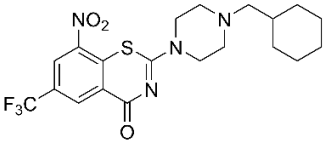	Benzothiazinone	IIa	Arabinogalactan synthesis (DprE1)
GSK3036656 (**9**)	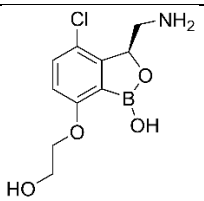	Benzoxaborole	IIa	Protein synthesis (Leucyl-tRNA synthetase)
TBA-7371 (**10**)	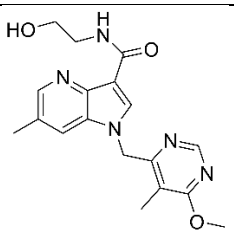	1,4-Azaindole	IIa	Arabinogalactan synthesis (DprE1)
Pyrifazimine (**11**) (TBI-166)	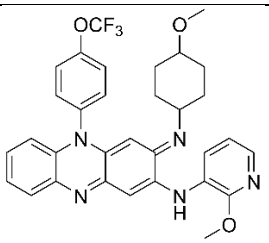	Riminophenazine	IIa	Energy production (release of reactive oxygen species)

OPC-167832 (**12**)	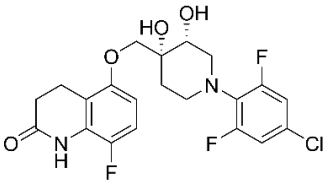	3,4-Dihydro-carbostyril	I/IIa	Arabinogalactan synthesis (DprE1)
BTZ043 (**13**)	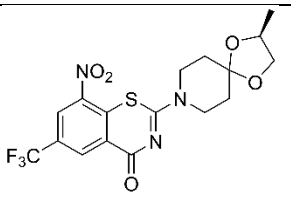	Benzothiazinone	I/IIa	Arabinogalactan synthesis (DprE1)
SPR720 (**14**)	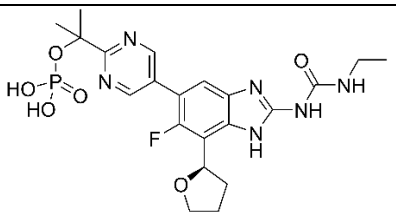	Benzimidazole urea	I	DNA synthesis (GyrB)
TBI-223 (**15**)	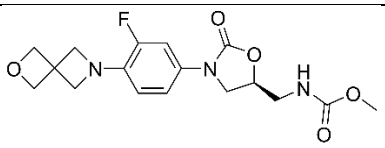	Oxazolidinone	I	Protein synthesis (50S ribosomal subunit)
TBAJ-876 (**16**)	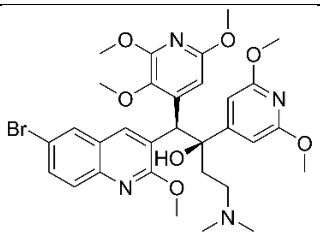	Diarylquinoline	I	Energy production (ATP synthase)
TBAJ-587 (**17**)	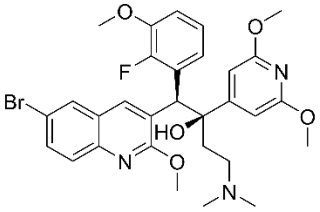	Diarylquinoline	I	Energy production (ATP synthase)
GSK2556286 (**18**)	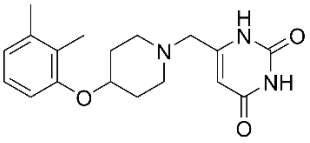	Pyrimidine-2,4-dione	I	Cholesterol catabolism
BVL-GSK098 (**19**)	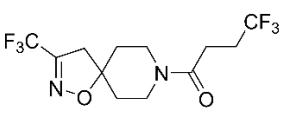	Amido-piperidine	I	Mycobacterial transcriptional regulator

262

SQ109 (**4**) is a 1,2-ethylenediamine derivative that has produced mixed efficacy results in phase IIa, IIb, and IIb/III combination trials for DS and MDR-TB, respectively, with only the latter one showing significant promise (more extensive phase III trials are planned).[78,79] This lead was initially discovered by Sequella, Inc. and the Laboratory of Host Defenses, National Institute of Allergy and Infectious Diseases (NIH) via high-throughput screening (HTS) of a large combinatorial library of EMB analogues having 1,2-ethylenediamine as the pharmacophore.[80] Despite its broad structural similarity to EMB, **4** retained good activity against EMB-resistant *Mtb* strains (MIC 2.4 µM, *cf.* 1.2 µM against H37Rv), implying that the two compounds must have distinct mechanisms of action. Candidate **4** acts in part by inhibiting MmpL3, a transmembrane transporter protein involved in exporting trehalose monomycolate from the cytoplasm to the outer membrane during *Mtb* cell wall biosynthesis.[81,82] Additionally, **4** is believed to affect energy production (inhibiting the menaquinone biosynthesis enzymes, MenA and Men G, and blocking respiration and ATP synthesis). It may also inhibit other *Mtb* efflux pumps (by dissipating the pH gradient and membrane potential that powers them).[83] The inhibition by **4** of multiple targets may explain why spontaneous drug-resistant mutants could not be generated.[81,83] *In vitro* studies have shown that **4** synergizes with several other TB drugs, including INH, RIF, BDQ (**1**), and sutezolid (**6**), and has efficacy superior to EMB *in vivo*, both alone and in combination therapy.[79,80,84] A new investigation has also confirmed that it is the parent molecule and not a metabolite that provides the antitubercular activity.[85]

Delpazolid (**5**) (LegoChem Biosciences, Inc.), sutezolid (**6**) (Sequella, Inc. and TB Alliance) and TBI-223 (**15**) (TB Alliance and Institute of Materia Medica) are broad-spectrum antibiotics from the oxazolidinone class that are currently being developed for the treatment of both drug-resistant and DS-TB.[78] The structural design of these new candidates originated from LZD, the first oxazolidinone to be FDA-approved and now an established Group A medicine for the treatment of MDR- and XDR-TB.[52,53] The mechanism of action of this class of drugs involves inhibiting protein synthesis.[86] Specifically, oxazolidinone derivatives bind selectively to the A-site on the 50S subunit of the bacterial ribosome and block the binding of incoming aminoacyl tRNA.[87] In phase I clinical trials, **5**

was found to have better safety (milder side effects) than LZD due to its more rapid clearance,[88] although final results from a phase IIa EBA study may suggest lower efficacy than both LZD and sutezolid (**6**).[89,90] A phase IIb clinical trial of **5** in combination with delamanid (**2**), BDQ (**1**) and MFX for DS-TB commenced in October 2021 (NCT04550832). Sutezolid (**6**) showed good safety and promising anti-TB activity in a phase IIa EBA study,[91] but further clinical development of this drug had stalled for reasons relating to its ownership.[78] However, Sequella (with the PanACEA consortium) has recently launched a phase IIb trial of **6** in combination with delamanid (**2**), BDQ and MFX for DS-TB (NCT03959566). Lastly, TBI-223 (**15**), another LZD analogue with suitable activity against *Mtb* and reduced toxicity, is currently completing phase I clinical trials (NCT04865536).[89,92]

Telacebec (**7**) (Q203; Qurient, Inc.) is an optimised imidazopyridine amide derivative (MIC_{50} 2.7 nM against *Mtb* H37Rv), based on a starting hit that was identified from a commercial library through whole-cell screening in *Mtb*-infected macrophages.[93] This compound has an innovative mechanism of action, which involves interference with energy generation in *Mtb*. Specifically, **7** targets the cytochrome *bcc* complex at the QcrB subunit (the menaquinol-binding Q_P site, as confirmed by a cryo-electron microscopy structure),[94] disrupting the electron transport chain that is essential for ATP synthesis in both replicating and nonreplicating *Mtb*.[93] While **7** displays valuable activity in mouse models of TB,[93] considerably improved bactericidal effects were observed in combination with BDQ and clofazimine (CFZ)[95] or with inhibitors of the alternative cytochrome *bd* oxidase.[96] A recent phase IIa EBA clinical trial of **7** demonstrated satisfactory dose-dependent efficacy, with acceptable safety,[97] and planning is underway for a phase IIb combination trial against drug-resistant TB.[89] Q203 (**7**) has also received orphan drug designation from the FDA as a treatment for Buruli ulcer (based on its outstanding efficacy in mice against infection by *M. ulcerans*)[98] and is now under appraisal as a possible therapy for COVID-19 in a phase II study (NCT04847583).

Macozinone (**8**) (PBTZ169) and BTZ043 (**13**) are benzothiazinone derivatives that are being developed by Nearmedic Plus, Ltd. and the PanACEA Consortium, respectively.[78,99] The class was initially discovered through identifying and testing the metabolites formed after incubating an

antimicrobial dithiocarbamate derivative with *M. smegmatis.*[100] Macozinone (**8**), which is an optimized analogue of the earlier lead BTZ043 (**13**), has an MIC_{99} value of ~0.0007 μM against *Mtb* H37Rv (3-fold lower than the MIC_{99} of **13**)[99] and displays synergism with several anti-TB drugs, including BDQ, CFZ, delamanid (**2**), and sutezolid (**6**).[101] Candidate **8** also has reduced cytotoxicity and better *in vivo* efficacy than **13** (~1.1 vs 0.6 $\log_{10}$ CFU reduction in lungs at 50 mg/kg in a chronic *Mtb* infection mouse model, where CFU means colony forming units),[99] albeit this activity level is still considered only moderate, given its low MIC value. The extraordinary *in vitro* potency of these benzothiazinones (BTZs) is due to their covalent mode of inhibition, as well as the cellular location of their target, decaprenylphosphoryl-β-D-ribose 2'-epimerase (DprE1), an enzyme required for arabinan biosynthesis during mycobacterial cell wall construction.[102] BTZs act as "suicide substrates" for the reduced DprE1 enzyme; this occurs through partial nitro group reduction to generate nitroso intermediates that react with an active site cysteine (Cys387 in *Mtb*), forming stable semimercaptal adducts, which block the enzymatic action.[100] Intriguingly, reversible ring reduction to an oxygen-sensitive Meisenheimer complex is also evident *in vivo* (as a common metabolite formed in whole blood), complicating PK analyses with these drugs.[103] Macozinone (**8**) has shown good tolerability and safety in phase I studies and exhibited significant efficacy in a pilot phase IIa study in Russia (another is planned by the Innovative Medicines for Tuberculosis).[89,100] Meanwhile, BTZ043 (**13**) began a phase I/IIa clinical trial in South Africa in November 2020 (NCT04044001).

GSK3036656 (**9**) (also referred to as GSK656 and GSK070; GlaxoSmithKline)[104] is the first boron-containing compound in the current pipeline and was developed from two screening hits identified by testing a small library of benzoxaboroles against *Mtb*.[105] Like the antifungal drug tavaborole, this molecule acts by selectively targeting leucyl-tRNA synthetase (LeuRS). The boron atom is essential for the activity because it binds covalently to the *cis* diol of adenosine nucleotide Ade76 of $tRNA^{Leu}$ in *Mtb*, trapping one end of the enzyme in the editing site. This in turn inhibits leucylation and thus protein synthesis.[104,105] Candidate **9** has good potency against *Mtb* H37Rv (MIC 0.08 μM) and displayed excellent *in vivo* PK (low clearance, high exposure, and 100% oral

bioavailability), as well as impressive efficacy in a chronic *Mtb* infection mouse model (2.1 $\log_{10}$ CFU reduction in lungs at 10 mg/kg).[104] In a phase I clinical study, **9** was found to be well tolerated,[106] and a phase IIa EBA assessment that started in 2019 has just been completed (NCT03557281).

TBA-7371 (**10**) is a 1,4-azaindole derivative that was initially discovered by AstraZeneca (India) through a scaffold morphing strategy, followed by lead optimisation, starting from an analogue of Q203 (**7**) in the imidazopyridine amide class.[107] Compound **10** is a noncovalent inhibitor of the *Mtb* DprE1 enzyme (IC_{50} 10 nM), not cross-resistant to the benzothiazinones,[107] having weaker potency against cultured *Mtb* (MIC_{80} 1.6 μM) but reasonable *in vivo* efficacy in a chronic *Mtb* infection rat model (~1 $\log_{10}$ CFU reduction in lungs at 100 mg/kg).[108] This candidate has a sound overall profile; albeit moderate off-target activity against phosphodiesterase 6 (IC_{50} 4 μM) raised some concerns regarding the possible risk of ocular side effects.[108,109] Nevertheless, TB Alliance completed a phase I clinical trial of **10** in 2018[78] and a phase IIa EBA clinical assessment (sponsored by the Bill & Melinda Gates Medical Research Institute) began in January 2020 (NCT04176250).[89]

Pyrifazimine (**11**) (TBI-166) is a riminophenazine derivative related to CFZ that is being developed by the Institute of Materia Medica in China.[110] This molecule was discovered through lead optimisation work with the TB Alliance, involving more than 500 new CFZ analogues. Compound **11** showed very high potencies against *Mtb* H37Rv and a panel of clinical isolates, ~4-fold superior to CFZ, with MIC_{90} values ranging from <0.008 μM to 0.34 μM. In an acute *Mtb* infection mouse model, **11** displayed primarily bacteriostatic activity, equivalent to or better than CFZ.[110,111] However, in the chronic *Mtb* infection model, delayed bactericidal activity was observed for both compounds (with minimal efficacy in the first 2 weeks of treatment), and **11** appeared to be slightly less efficacious than CFZ (1.7 vs 2.2 $\log_{10}$ CFU kill at 20 mg/kg after 4 weeks of treatment). Further *in vivo* experiments revealed that the combination of **11** with BDQ and LZD was particularly effective.[112] Importantly, it was demonstrated that **11** caused lower skin discoloration in mice than CFZ and several other analogues,[113] this being an unwelcome effect that hinders the use of CFZ in anti-TB therapy.[110] The mode of action of CFZ (and **11**) was thought to involve the production of

reactive oxygen species (ROS), following its reduction by the respiratory enzyme type II NADH dehydrogenase (NDH-2) and *in situ* reoxidation by oxygen.[114] However, more recent data on a knockout strain of *Mtb* in which both NDH-2 encoding genes (*ndh* and *ndhA*) were deleted shows that the activity of CFZ does not require NDH-2.[115] TBI-166 (**11**) completed phase I clinical evaluation in China and is currently in the final stage of a phase IIa EBA study (NCT04670120).

OPC-167832 (**12**) (Otsuka Pharmaceutical Co., Ltd.) is another noncovalent DprE1 inhibitor (IC_{50} 0.26 μM), resulting from the identification and optimisation of carbostyril-based screening hits.[116] This compound exhibited outstanding MIC_{99} values against *Mtb* H37Rv and a panel of mono-resistant strains, with values ranging from 0.00053 to 0.0044 μM. Further experiments showed that **12** was bactericidal and had excellent *in vivo* efficacy in a chronic *Mtb* infection mouse model [>1 log_{10} CFU reduction in lungs at 2.5 mg/kg; equivalent to delamanid (**2**) and superior to macozinone (**8**)]. Moreover, the four-drug regimen of **12**, **2**, MFX and BDQ (**1**) reduced the CFU count in the lungs of ICR mice infected with *Mtb* Kurono to undetectable levels after 8 weeks of treatment, without subsequent relapse. Additionally, a new *in vivo* study comparing **12** with macozinone (**8**) and TBA-7371 (**10**) head-to-head in *Mtb*-infected C3HeB/FeJ mice (which develop caseous necrotic lung lesions) confirmed the superior efficacy of **12**, even at low doses.[117] OPC-167832 (**12**) has almost completed the last stage of a phase I/IIa clinical trial for uncomplicated DS-TB (NCT03678688), which also aimed to assess two- or three-drug combinations with delamanid (**2**) and BDQ (**1**).[89]

SPR720 (**14**) is an orally bioavailable phosphate prodrug of the active drug SPR719 (VXc-486), which belongs to the class of benzimidazole urea DNA gyrase inhibitors and was developed by Vertex Pharmaceuticals, then later acquired by Spero Therapeutics (2016).[118,119] This antibacterial class was first discovered through HTS of a compound library in an ATPase assay to target gyrase B, then further optimised by SAR studies using structure-based design.[120] SPR719 has decent potency levels against *Mtb* (MIC_{90}s 0.07-0.58 μM), including strains resistant to fluoroquinolones (e.g., MFX), which target DNA gyrase A. In a murine chronic *Mtb* infection model, the prodrug form (**14**) displayed more potent bactericidal activity than the parent alcohol (SPR719), comparable to MFX

when dosed twice daily at 100 mg/kg (2.5 $\log_{10}$ CFU reduction),[118] and was sterilizing in combination with RIF and PZA.[119] Candidate **14** showed good tolerability and safety during a phase I clinical trial in 2019[89] and began a phase IIa EBA study in November 2020 against the non-tuberculous mycobacterium, *M. avium* (NCT04553406). Unfortunately, this trial was terminated in early 2021, following FDA concerns about preclinical toxicology findings in non-human primates. Nevertheless, the company has expressed optimism about relaunching its SPR720 clinical program. In 2019, Spero Therapeutics assigned the Bill & Melinda Gates Medical Research Institute a sole license to develop and eventually market **14** for use against TB in poor to middle-income countries.[78]

Two novel BDQ analogues, TBAJ-876 (**16**) and TBAJ-587 (**17**),[121] commenced Phase I clinical trials in June and December 2020 (NCT04493671 and NCT04890535). These next generation candidates were developed by researchers at The University of Auckland, New Zealand, through an extensive lead optimisation programme conducted in partnership with the TB Alliance, aiming to improve activity and PK profiles, reduce lipophilicity, and decrease cardiotoxicity risk. Compounds **16** and **17** displayed excellent MIC_{90} values against *Mtb* H37Rv (0.006 and 0.01 μM, respectively), 7- to 12-fold more potent than BDQ, despite having lower calculated lipophilicities (by 1.5-2.1 log units).[121] Furthermore, these compounds retained excellent efficacies in mouse models of TB. For example, TBAJ-587 (**17**) was more effective than BDQ against both wild-type *Mtb* H37Rv and a resistant *Rv0678* mutant strain, either alone or combined with other drugs; it also rendered the regimens less prone to the emergence of drug resistance.[122] Importantly, both **16** and **17** showed a lower risk of inducing QT prolongation, due to reduced inhibition of hERG (by >19-fold[121] in the former case). Recent mode of action studies demonstrated that TBAJ-876 (**16**) binds to the same sites as BDQ on the mycobacterial ATP synthase, blocking its action, but has much weaker proton-shuttling ability than BDQ, suggesting that the latter effect is not essential for bactericidal activity.[123,124] Interestingly, another second generation BDQ-like candidate, WX-081, began phase II clinical trials in September 2020 (NCT04608955). This compound was derived from a collaboration between Cisen Pharmaceutical Co., Ltd. and WuXi AppTec (Shanghai),[125] although the current trial

is sponsored by a different company (Shanghai Jiatan Pharmatech Co., Ltd.). No information is available on the structure or profile of WX-081, but a 2017 patent application by the original collaborators claims BDQ-like molecules in which the bromoquinoline moiety has been replaced by 5-(4-chlorophenyl)-2-methoxypyridine.[126]

Two other drug candidates with innovative mechanisms of action that entered phase I clinical studies at the end of 2020 are GSK2556286 (**18**) (NCT04472897) and BVL-GSK098 (**19**) (NCT04654143).[89] GSK2556286 (**18**) is a pyrimidine-2,4-dione derivative discovered by GlaxoSmithKline (GSK), in collaboration with the Bill & Melinda Gates Foundation's TB Drug Accelerator Program, using library HTS in *Mtb*-infected macrophages.[127] The mechanism of action of **18** is related to the catabolism of host-derived cholesterol (which *Mtb* employs as a carbon source).[128,129] This candidate selectively kills *Mtb* in macrophages (MIC <0.1 μM) and has moderate *in vivo* efficacy in several animal models, more significant in combination with other TB drugs.[127] Lastly, BVL-GSK098 (**19**) is an amido-piperidine derivative that Bioversys AG has developed, in collaboration with GSK, the Pasteur Institute Lille, and the University of Lille, France.[75] Compound **19** boosts the bactericidal activity of two important Class C prodrugs that are used for the treatment of MDR-TB, ethionamide (ETH) and prothionamide, and restores sensitivity toward bacterial strains that have become resistant to these drugs.[130] While full details of the mechanism have yet to be disclosed, it appears that **19** acts on one of several transcriptional regulators in *Mtb* (VirS), stimulating the expression of an additional enzyme activator for ETH (MymA).[130,131] Based on the *in vivo* results, a reduction in the efficacious oral dosage of ETH by at least three-fold is predicted in humans.[130] A phase IIa EBA study of **19** and ETH in comparison to INH has been planned for 2022.[131] The clinical development of **19** represents the climax of an extensive program in this area, as discussed in Section 4.1.3 below.

4. PRECLINICAL PROMISES

Notwithstanding the recent exit of several major pharma from TB research (e.g., Pfizer, AstraZeneca, and Novartis),[132,133] in the past two decades the development of new drugs for TB has recaptured substantial global interest, resulting in the identification of many new lead candidates. Many reviews have been published addressing novel compounds with potent *in vitro* activity in the early stages of development (discovery),[71,134-140] and others have described the drug candidates in clinical studies.[92,141,142] Nevertheless, there is a scarcity of reviews covering the anti-TB compounds that have progressed to "validated lead" or preclinical development status and, to the best of our knowledge, no article to date has specifically covered those compounds from a drug candidate profiling perspective. This section reviews the anti-TB compounds published in the last six years that have reached such stages (arising from hit-to-lead, lead optimisation, and other preclinical investigations), focusing solely on those with proven efficacy against *Mtb* in animal models. To simplify this task, we will restrict our attention to so-called "small molecules" obtained wholly by chemical synthesis. The lead compounds presented herein were selected from the Stop TB Partnership's Discovery Pipeline (https://www.newtbdrugs.org/pipeline/discovery) and literature reports identified manually or via scientific database searching. These molecules will be discussed in various subsections, according to their reported mode of action.

4.1 Compounds Targeting Cell Wall Biosynthesis

An essential requirement in developing any anti-TB drug is that the compound can cross the lipid-rich cell wall surrounding the bacterium and reach its intended target(s). The cell envelope of mycobacteria is distinctive, incorporating the so-called "mycomembrane" or outer membrane, which is abundant in long-chain fatty acids (mycolic acids), as well as lipoglycans, phospholipids, and glycopeptidolipids (**Figure 3**).[143] This outer membrane is organizationally similar to that of Gram-negative bacteria, even though *Mtb* is a Gram-positive organism.[144] The complete cell envelope can be broadly represented as comprising three domains: i) an exterior layer ("capsule") of proteins and

some glucan; ii) a cell wall with an outer membrane attached to an arabinogalactan-based polysaccharide layer joined to peptidoglycan; iii) an internal plasma membrane.[143-148]

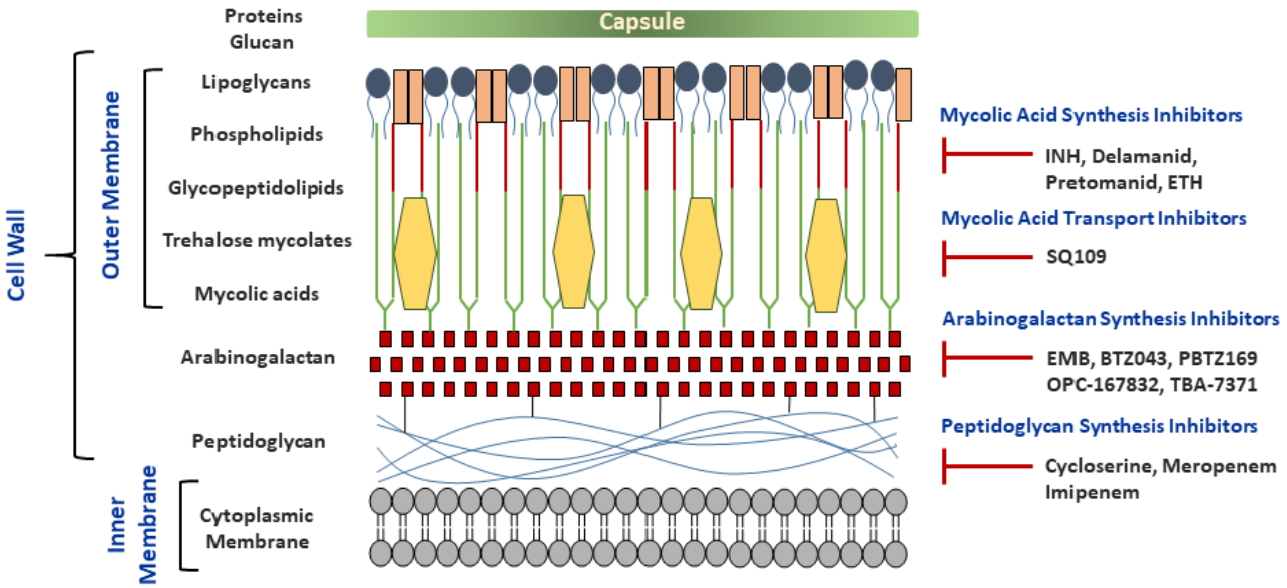

Figure 3. Schematic model of the *Mtb* cell envelope and some approved or candidate TB drug inhibitors, based on the information provided by several authors.[143,145-148]

The distinctive and complex architecture of the mycobacterial cell envelope has rendered it a rich source of novel targets for TB drug discovery.[145-147] It is estimated that there are at least 60 potential enzyme targets in the cell wall of *Mtb*.[149] Recent comprehensive research into the construction of this cell wall has shed light on many important biochemical and structural features. This has spurred renewed efforts to find new anti-TB agents that inhibit the biosynthesis of essential components of this structure in *Mtb*.[150] Some examples of agents known to do this include the two front line drugs, INH and EMB, the MDR-TB drugs ETH, delamanid (**2**), pretomanid (**3**), cycloserine, imipenem, and meropenem, as well as several drug candidates in clinical studies, such as macozinone (**8**), TBA-7371 (**10**), OPC-167832 (**12**), and BTZ043 (**13**).[145,147]

4.1.1 DprE1

The flavoprotein DprE1 is an oxidising enzyme that plays a critical role in the biosynthesis of arabinogalactan, one of the essential building blocks for the cell wall.[151] A reductase, DprE2, is also involved in this. First, DprE1 converts decaprenylphosphoryl-D-ribose into decaprenylphosphoryl-2-ketoribose, then the latter is reduced by DprE2 to form decaprenylphosphoryl-D-arabinose (DPA). DPA is the sole known source of D-arabinofuranosyl units, which are required to create the arabinan chains of arabinogalactan.[145,151] Numerous crystal structures of *Mtb*-derived DprE1 have been published, with most featuring the enzyme bound to an inhibitor.[152]

Many promising novel compounds are known to target the DprE1 enzyme.[62,152] For instance, in 2019, researchers working at AstraZeneca in India (in collaboration with the TB Alliance, before the site closure in 2014[132]) reported benzimidazole derivative **20** (**Figure 4**) as a DprE1 inhibitor.[153] This compound was discovered using the scaffold morphing strategy, by replacing the azaindole core of their earlier lead, TBA-7371 (**10**),[109] with a benzimidazole moiety, and adjusting the position of the amide side chain. Compound **20** showed an MIC_{80} value of 1.6 μM against *Mtb* H37Rv (equal to that of **10**), and high potency against the enzyme itself (IC_{50} 0.034 μM, *cf.* 0.010 μM for **10**).[109,153] The activity was specific for mycobacteria, as **20** was ineffective against various Gram-negative and Gram-positive bacteria.[153] Benzimidazole **20** displayed good aqueous solubility (152 μM) and lower human plasma protein binding than **10** (68% vs 78%); it also exhibited a sound safety profile (IC_{50} >33 μM against the hERG channel and IC_{50} >50 μM against a panel of five CYPs). Rat PK studies revealed excellent oral bioavailability (100%) and an acceptable clearance rate. Oral dosing of **20** at 30 mg/kg for 4 weeks in a chronic *Mtb* infection BALB/c mouse model reduced the lung bacterial burden by 1.5 $\log_{10}$ CFU, relative to untreated control levels.

Several teams have also prepared new BTZ derivatives as analogues of the covalent DprE1 inhibitors macozinone (**8**) and BTZ043 (**13**), attempting to improve key aspects such as solubility, metabolic stability, and *in vivo* PK and efficacy. For example, Piton et al. devised the less lipophilic sulfonyl-piperazine analogue **21** (**Figure 4**), which retained high potency, having an MIC_{99} value of 0.0065 μM against *Mtb* H37Rv (15-fold decreased, relative to **8**), and showed modest cytotoxicity

against HepG2 cells (CC_{50} 17 μM), resulting in an excellent selectivity index (SI of 2,615).[154] Notably, although its solubility was inferior (19 vs 68 μM for **8**), **21** displayed much better stability than **8** toward mouse and human liver microsomes. However, the efficacy of **21** in the chronic *Mtb* infection BALB/cByJ mouse model was disappointing, with oral dosing at 50 mg/kg for 4 weeks giving a lung bacterial load reduction of only 0.5 $\log_{10}$ CFU (relative to the untreated control), compared to a 1.0 $\log_{10}$ CFU decrease for **8** (25 mg/kg).

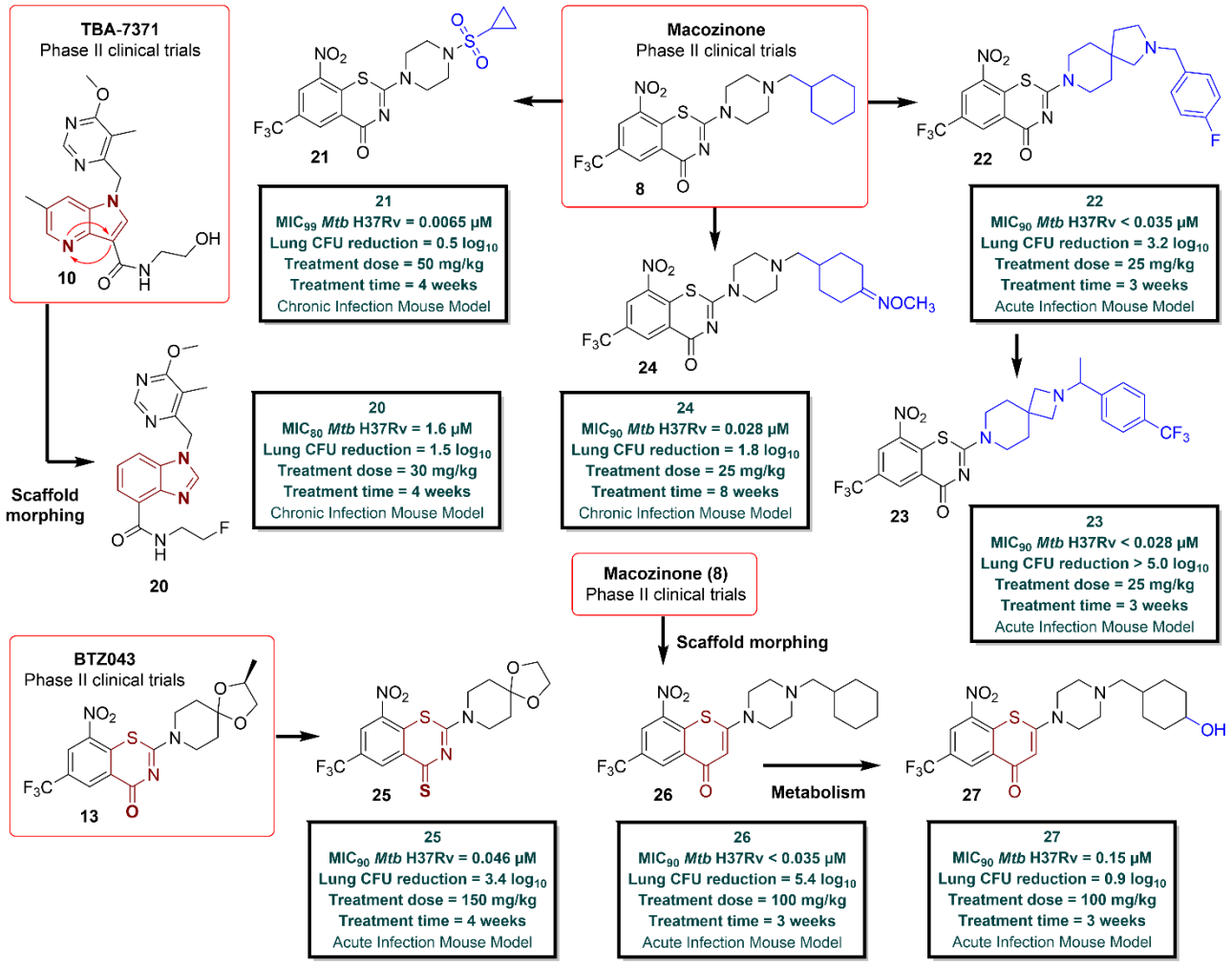

Figure 4. Benzimidazole **20**, BTZ derivatives **21-24**, benzothiazinethione **25**, and benzothiopyranones **26** and **27** as DprE1 inhibitors.

Another research team, based in China, explored BTZs with spirocyclic amine-based side chains, e.g., IMB1603 (**22**) (**Figure 4**).[155,156] Lead **22** exhibited potent activity against *Mtb* H37Rv (MIC_{90}

<0.035 μM, the same as **8** in their assay) and minimal cytotoxicity against Vero cells (CC_{50} 811 μM). Comparable solubility values were measured for **8** and **22** at a pH value of ~2.0 (2.0 and 2.1 mM, respectively) and the two molecules displayed almost identical mouse PK profiles.[155] Compound **22** was subsequently assessed for efficacy in the BALB/c mouse model of acute *Mtb* infection. Here, oral dosing at 25 mg/kg for 3 weeks gave a notable 3.2 $\log_{10}$ CFU decrease in lung bacterial burden (relative to the untreated control).[156] Nevertheless, further testing revealed **22** to be a strong hERG inhibitor (96% at 10 μM vs 42% for **8**) and to cause some acute toxicity in mice at 500 mg/kg.[155,156]

A new study by these investigators pinpointed compound **23** (**Figure 4**) as an improved lead.[157] This molecule provided similar MIC_{90} potency against *Mtb* H37Rv (<0.028 μM), was non-cytotoxic to Vero cells (CC_{50} >112 μM) and was well tolerated by mice at 2 g/kg. Compared to **8**, **23** also provided a superior mouse PK profile, with a slightly longer half-life (6.7 h vs 5.1 h for **8**) and much greater oral bioavailability (42% vs 12% for **8**). In the acute *Mtb* infection BALB/c mouse model, treatment with **23** (25 mg/kg for 3 weeks) reduced the CFU count in lungs by >5.0 $\log_{10}$ (relative to the untreated control), leaving no detectable bacteria. The authors finally identified **23** as a possible preclinical candidate, although the paper did not disclose any information about hERG inhibition.

In 2019, this team also reported the results of an alternative SAR strategy, focusing on side chains bearing an alkoxyimino group (*cf.* gemifloxacin and zabofloxacin).[158] The best lead, TZY-5-84 (**24**) (**Figure 4**), showed an MIC_{90} value of 0.028 μM against *Mtb* H37Rv (~65-fold less potent than **8**),[159] with no cytotoxicity (CC_{50} >128 μM on VERO cells), minimal inhibition of hERG (IC_{50} 48 μM) or CYPs (IC_{50} 7.8 μM for 2C19; others had IC_{50} >10 μM), and no mutagenicity (Ames test). Similar to **23**, in mouse PK studies of **24** and **8**, **24** demonstrated better oral absorption (7- to 9-fold greater C_{max}) and much higher oral bioavailability (37% vs 9% for **8**).[158,159] This translated into almost equivalent efficacy for both compounds, following oral dosing at 25 mg/kg for 3 weeks in a BALB/c mouse model of acute *Mtb* infection (lung CFU reductions of 4.0 $\log_{10}$ for **24** and 3.8 $\log_{10}$ for **8**, compared to the untreated control group).[158] A chronic *Mtb* infection experiment was then conducted in C3HeB/FeJ mice, which develop more refractory necrotic granulomas.[160] Here, dosing of compound

552 **24** or **8** at 25 mg/kg for 8 weeks also yielded equivalent efficacy (a lung burden reduction of 1.8 $\log_{10}$
553 CFU, relative to the control group at the start of treatment).[159] These data reinforce the potential
554 benefits of improving PK profiles in this class. Lead **24** was selected for further preclinical evaluation.
555 Additional promising lead compounds have been generated through modifications to the BTZ
556 scaffold itself. Gao et al. reported SKLB-TB1001 (**25**) (**Figure 4**), which is structurally related to
557 BTZ043 (**13**) but features a thione moiety on the thiazine ring (the chiral methyl group on the side
558 chain is also absent).[161] This new analogue was equipotent to **13** against *Mtb* H37Rv (an MIC_{90} of
559 0.046 μM in the assay used) but was at least 4-fold less cytotoxic than the latter drug toward A549
560 cells (CC_{50} values >231 μM and 58 μM, respectively). Another difference was that **25** displayed *in*
561 *vitro* synergy with RIF, whereas **13** gave an additive effect. A rat PK investigation further revealed
562 that **25** had better oral bioavailability than **13** (44% vs 30%), although other parameters, such as half-
563 life (1.5 h vs 1.2 h) and AUC (847 vs 899 ng·h/mL), were comparable. Moreover, lead **25** also showed
564 substantial efficacy in an acute infection (*Mtb* Erdman) BALB/c mouse model, with oral dosing at
565 150 mg/kg for 4 weeks delivering a 3.4 $\log_{10}$ CFU reduction in lungs (relative to the vehicle control),
566 whereas **13** (150 mg/kg) was surprisingly ineffective. The favourable activity of **25** was confirmed in
567 other acute infection models.[162] However, a comprehensive *in vivo* metabolism study later identified
568 three metabolic pathways, each involving reduction of the nitro group to inactive amine derivatives,
569 which may have broader implications for the BTZ class.[163] High human plasma protein binding
570 (99.4%, similar to data for **8**), poor solubility (<2.3 μM), and a low lung:plasma distribution in mice
571 (1:2.7) were other issues for this molecule, which was initially described as a preclinical candidate.[161]
572 Another excellent example of scaffold switching is compound **26** (**Figure 4**), in which the
573 thiazine ring of macozinone (**8**) has been replaced by a thiopyran ring. This lead was derived from a
574 wider medicinal chemistry study conducted by investigators at the Institute of Materia Medica, China,
575 who concurrently explored benzoxazinones and benzopyranones as alternative scaffolds.[164] While
576 SARs varied across these classes, compound **26** was the most active of the three direct analogues of
577 **8** (MIC_{90} <0.035 μM against *Mtb* H37Rv, the same as **8**) and the least cytotoxic one (CC_{50} >140 μM

on VERO and HepG2 cells). Surprisingly, this new molecule (**26**) showed only modest potency against the DprE1 enzyme (IC_{50} 4.5 μM, *cf*. 0.20 μM for **8**). Compound **26** exhibited good stability toward human and mouse liver microsomes (comparable to **8**); it also displayed a substantially prolonged half-life in mice (7.3 h vs 1.9 h for **8**), although, like **8**, its oral bioavailability was low (13%). Furthermore, in a BALB/c mouse model of acute *Mtb* infection, oral dosing of **26** at 100 mg/kg for 3 weeks provided an impressive 5.4 $\log_{10}$ reduction in lung CFU (relative to the untreated control). The excellent *in vivo* results for **26**, supported by favourable safety data (hERG IC_{50} >30 μM and IC_{50} >50 μM against a panel of five CYPs), suggest significant potential for this novel class.

The same investigators have recently reported a new study based around one of the proposed metabolites of **26** in hepatocytes, alcohol **27** (**Figure 4**).[165] This active metabolite (MIC_{90} 0.15 μM against *Mtb* H37Rv) was considerably less lipophilic than **26** (ClogP was lowered by 2 log units) and had much better solubility in water (18 μM vs <0.2 μM for **26**). These results prompted an assessment of its *in vivo* efficacy, using the acute *Mtb* infection BALB/c mouse model. However, in comparison to **26**, alcohol **27** showed only modest utility, with oral dosing at 100 mg/kg for 3 weeks giving a 0.9 $\log_{10}$ reduction in lung CFU. New ester and amide leads based on **27** are currently being evaluated.[165]

Meanwhile, Borthwick et al. (2020) disclosed novel morpholino-pyrimidine derivatives **29** and **30** (**Figure 5**) as potent non-covalent DprE1 inhibitors with enhanced physicochemical properties in comparison to the original HTS hit, **28** (**Figure 5**).[166] Compounds **29** and **30** respectively exhibited MIC_{90} values of 0.6 and 1.7 μM against *Mtb* H37Rv and IC_{50} values of 0.025 and 0.050 μM against the DprE1 enzyme. These leads also displayed low cytotoxicity toward HepG2 cells, with CC_{50} values of 50 and 32 μM, respectively. Additionally, both compounds showed suitable aqueous solubility (160 and ≥364 μM for **29** and **30**, respectively) but there was a big difference in their stabilities toward mouse and human liver microsomes, with **29** demonstrating moderate or high clearance, whereas **30** gave low clearance values. Mouse PK studies further revealed that both compounds had short half-lives (0.45 and 1.0 h) but excellent oral bioavailabilities (100% and 79%). These two leads were evaluated for efficacy in a rapid acute assay,[167] using C57BL/6 mice infected with *Mtb* H37Rv. Here,

the candidates were administered orally at multiple doses for 8 days, starting one day post-infection, and activity was quantified by ED_{99} values (where ED_{99} is the dosage that decreases mycobacterial load at day 9 post-infection by 99%, compared to the untreated group, a 2.0 log_{10} CFU reduction). Compounds **29** and **30** gave ED_{99} values of 30 and 29 mg/kg, implying significant promise.[166]

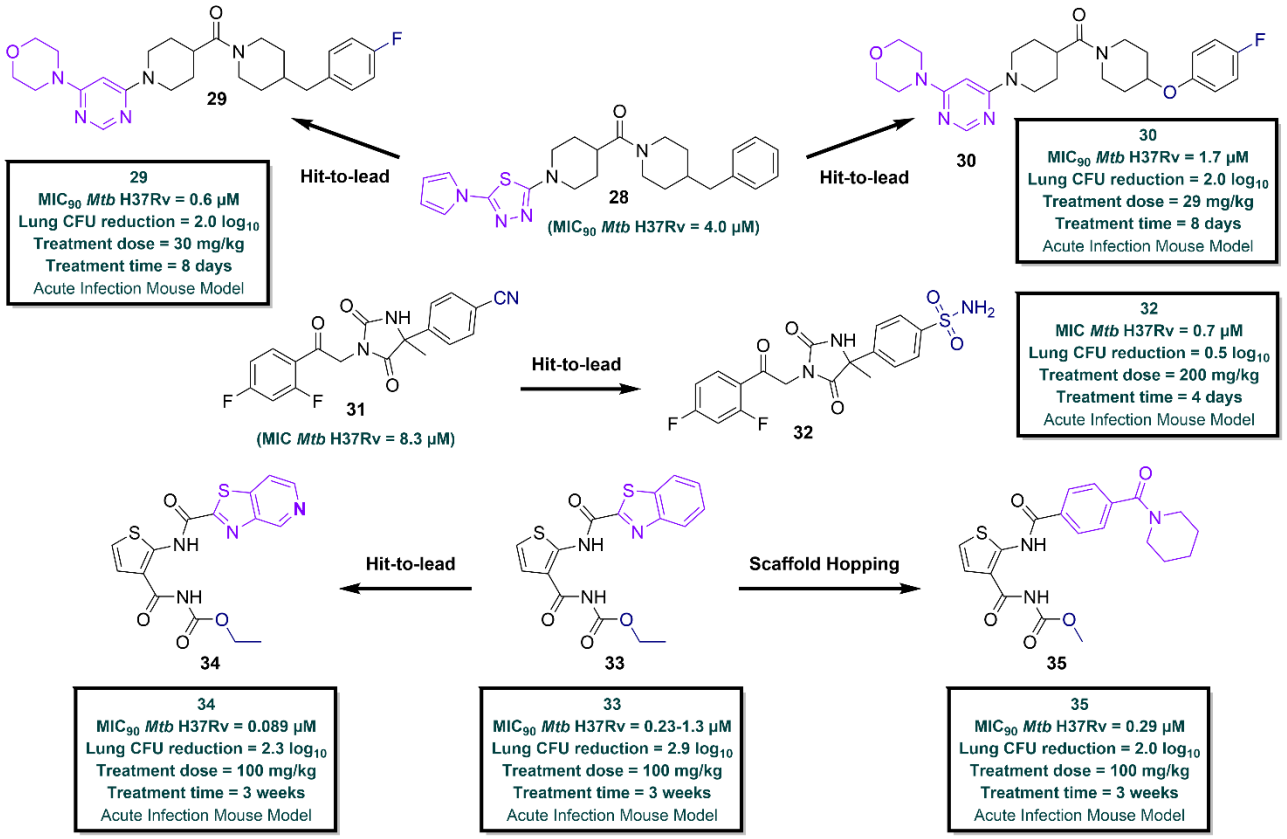

Figure 5. Morpholino-pyrimidine derivatives **29** and **30**, hydantoin **32**, and thiophene amide derivatives **33-35** as DprE1 inhibitors.

The hydantoin derivative **32** (**Figure 5**) is another noncovalent DprE1 inhibitor identified by researchers at GSK.[168,169] This compound was discovered through a target-based HTS strategy, followed by further optimisation of the initial hit **31**[169] (**Figure 5**). Compound **32** provided an MIC value of 0.7 µM against *Mtb* H37Rv and was not cytotoxic (CC_{50} >100 µM on HepG2 cells).[168] It also demonstrated high potency against the DprE1 enzyme (IC_{50} 0.063 µM) and did not interact markedly with the hERG potassium channel (IC_{50} >50 µM). Lead **32** was nicely water soluble (≥486

μM) and displayed moderate or low clearance upon exposure to mouse and human liver microsomes. An *in vivo* assessment of **32** in the rapid acute *Mtb* infection assay[167] (using C57BL/6J mice), dosing orally at 200 mg/kg for just 4 days (starting 5 days post-infection), led to a modest 0.5 $\log_{10}$ decrease in lung CFU (relative to the untreated control).[168] This outcome was despite plasma levels remaining above the MIC for 24 h after a single dose. However, it is important to note the brevity of this experiment and that only the *R*-enantiomer of compound **32** contributes to the activity.

Liu et al. (2017) reported the new thiazolo[4,5-*c*]pyridine amide lead TCA007 (**34**) (**Figure 5**) as a promising DprE1 inhibitor.[170] This molecule was obtained by structure-guided optimisation of the *in vivo* active screening hit TCA1 (**33**) (**Figure 5**), which the team had disclosed a few years earlier.[171] Lead **34** gave an improved MIC_{90} value of 0.089 μM against *Mtb* H37Rv (*cf.* 0.23 μM for **33**) and was 9-fold more potent than **33** against the DprE1 enzyme derived from *M. smegmatis* (IC_{50} 0.0053 μM).[170] Compound **34** also displayed no cytotoxicity toward HepG2 or Vero cells (CC_{50} >100 μM) and no hERG inhibition (IC_{50} >30 μM). Although explicit data were not provided, it was noted that **34** showed enhanced PK properties, so it was tested in BALB/c mouse models of acute and chronic infection (against *Mtb* Erdman). In the acute infection experiment, oral dosing of **34** at 100 mg/kg for 3 weeks resulted in a 2.3 $\log_{10}$ CFU reduction in lung bacterial burden (relative to vehicle control). Similarly, dosing with **34** at 200 mg/kg for 4 weeks in the chronic model led to a >1.7 $\log_{10}$ CFU decrease. Overall, compound **34** showed an excellent *in vitro* and *in vivo* profile but, unfortunately, it was found to inhibit one of the major CYP enzymes, 2C9 (IC_{50} 0.1 μM). Because TB treatment requires the combination of multiple drugs, such an effect could produce problematic drug-drug interactions. Hence, structure-based design is being used to find a more suitable candidate.

A different group of investigators recently developed the 4-substituted benzamide analogue **35** (**Figure 5**) through a systematic SAR study of the same hit (**33**).[172] This new molecule (**35**) also displayed strong cellular activity (relative to **33**), with an MIC_{90} value of 0.29 μM against *Mtb* H37Rv (a 4-fold improvement). Additionally, **35** exhibited reduced cytotoxicity toward Vero cells (CC_{50} >154 μM vs 85 μM for **33**), providing a superior SI value (>531 vs 66 for **33**); it also showed slightly

lower hERG inhibition (IC_{50} 23 vs 18 μM). However, **35** was 8-fold less effective than the starting hit **33** at inhibiting DprE1 (IC_{50}s 2.2 and 0.27 μM, respectively). The *in vivo* efficacy of both compounds was evaluated using the BALB/c mouse model of acute *Mtb* infection. Following oral dosing at 100 mg/kg for 3 weeks, the new lead **35** reduced the bacterial burden in the lungs by 2.0 $\log_{10}$ CFU, compared to the untreated group (whereas identical dosing of hit **33** gave a 2.9 $\log_{10}$ CFU lung burden decrease in a repeat experiment). Notwithstanding this activity, **35** displayed a shorter half-life than **33** (0.85 vs 2.2 h), inferior oral absorption (C_{max} 22-fold less than data for **33**), and very poor oral bioavailability (7.9 vs 43% for **33**), indicating that further improvement may be needed.

4.1.2 MmpL3

Like DprE1, the inner membrane transporter protein MmpL3 is another "promiscuous" but important drug target in cell wall biosynthesis.[62] Specifically, MmpL3 is responsible for the export and delivery of mycolic acids (as trehalose monomycolate) to the outer membrane of the cell envelope.[82] It has been shown that MmpL3 is essential for *Mtb* growth and survival, with its depletion affecting surface permeability.[173] Several crystal structures of MmpL3 derived from *M. smegmatis* have been solved, with or without small molecule inhibitors such as SQ109 (**4**).[62] Nevertheless, the additional effect of some reported MmpL3 inhibitors on dissipating the transmembrane charge or proton gradients required to drive such transporters may further explain their mode of action.[82]

One of the many interesting MmpL3 inhibitor classes published in the past decade[62] is *N*-benzyl spirocyclic compounds, or "spiros". These stemmed from a HTS hit, **36** (**Figure 6**), which was further elaborated into the preferred lead **37** (**Figure 6**) by investigators from GSK.[174,175] This molecule exhibited high potency against *Mtb* H37Rv (MIC_{90} 0.06 μM), modest cytotoxicity (CC_{50} 36 μM on HepG2 cells), and a favourable PK profile (good oral exposure, with an oral bioavailability of 55%).[174] Further assessment of **37** in the rapid acute *Mtb* infection assay[167] (using C57BL/6 mice and dosing orally at up to 50 mg/kg for 8 days, starting 1 day post-infection) revealed impressive efficacy (a maximal 4.2 $\log_{10}$ CFU decrease in lung bacterial burden, relative to the untreated control, and an

671 ED_{99} value of 12 mg/kg).[175] However, the authors cited various concerns about hERG inhibition (IC_{50}
672 1.5 or 10 µM), hepatotoxicity risk, and limited *in vivo* tolerability, together with low solubility (6
673 µM) and high lipophilicity (ClogP 6.2), such that their work on this class was terminated. Recently,
674 Ray et al. described their optimisation of a similar pyrazole based spirocyclic HTS hit from the Lilly
675 collection, but although lipophilicity, HepG2 cytotoxicity, and hERG inhibition were nicely reduced
676 for a zwitterionic lead, it showed no efficacy in the acute infection BALB/c mouse model.[176]
677

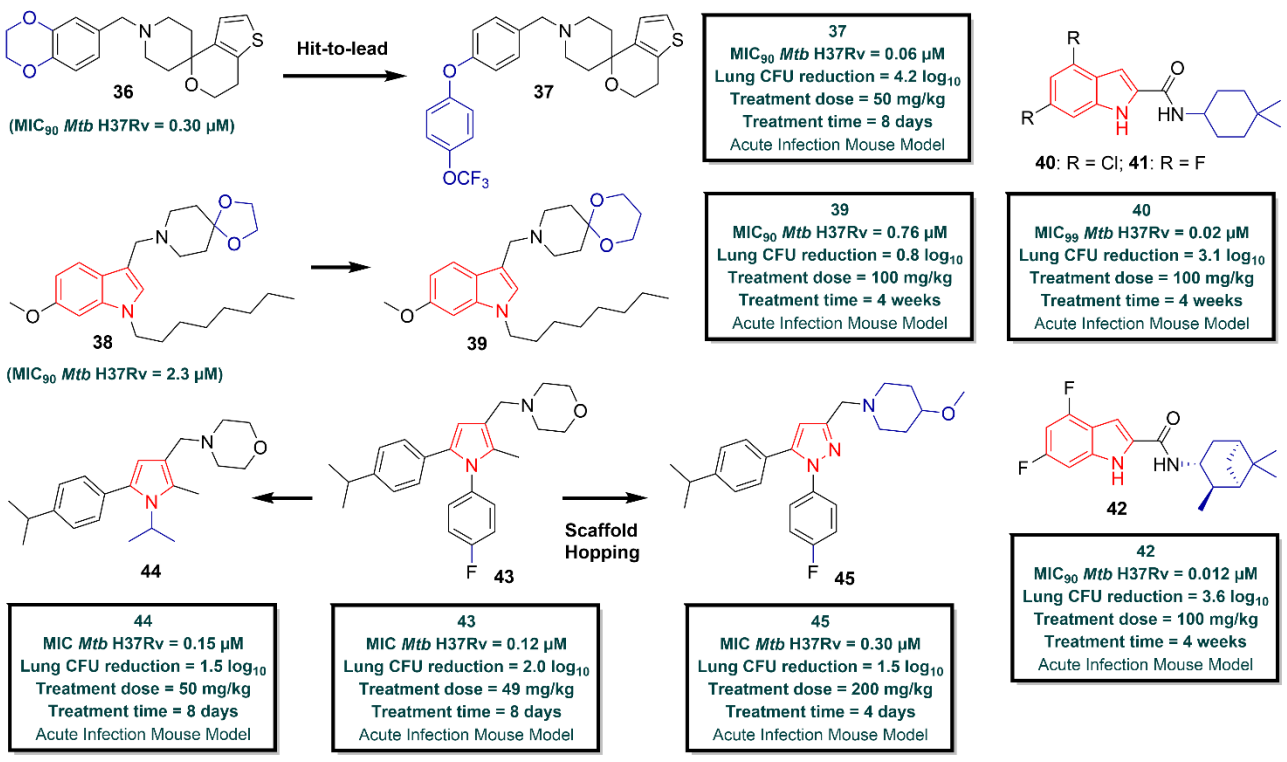

678

679 **Figure 6.** Aryl azaspirocyclic derivatives **37** and **39**, indole-2-carboxamides **40** and **42**, and 1,5-
680 disubstituted-(pyrrole or pyrazole) derivatives **43-45** as MmpL3 inhibitors
681

682 In 2018, a team based at the National University of Singapore reported a study about structurally
683 related indole derivatives containing a spiroketal moiety as potent anti-TB agents.[177] Out of 98 newly
684 synthesized analogues derived from their previous lead **38**, compound **39** (**Figure 6**) was the most
685 promising. It displayed an MIC_{90} of 0.76 µM against *Mtb* H37Rv and low cytotoxicity toward Vero
686 cells (CC_{50} 29 µM; an SI of 38). Further studies of **39** revealed adequate solubility (28 µM),

687 acceptable rat microsomal stability (a half-life of 28 min), and strong partitioning into lung tissue in
688 CD1 mice (due to its high lipophilicity: ClogP 5.7). A ^{1}H NMR study of **39** treated with the thiol
689 cysteamine (run in deuterated DMSO containing 1% acetic acid) also indicated good stability over
690 24 h, suggesting that loss of the Mannich base side chain would not be problematic. In the acute *Mtb*
691 infection BALB/c mouse model, oral dosing of **39** at 100 mg/kg for 4 weeks reduced the bacterial
692 load in lungs by 0.8 $\log_{10}$ CFU, relative to the untreated control. Recent mode of action studies
693 demonstrated that in addition to the various membrane disruptive effects found with non-spirocyclic
694 indolyl Mannich bases (e.g., inducing permeabilization and upregulating a stress reporter promoter),
695 compound **39** directly inhibits MmpL3, without affecting the membrane charge or proton gradients.[178]
696 Another well-known class of MmpL3 inhibitors is indole-carboxamides, including NITD-304
697 (**40**) and NITD-349 (**41**) (**Figure 6**), which were disclosed by Novartis as preclinical candidates in
698 2013 and provided to the TB Alliance in the following year.[92,133] Stec et al. (2016) reported the new
699 analogue **42** (**Figure 6**), following optimisation of their earlier cyclooctylamide lead.[179] This
700 compound (**42**) showed impressive potency against *Mtb* H37Rv (MIC_{90} of 0.012 μM) and negligible
701 cytotoxicity toward Vero cells (CC_{50} ≥192 μM). It also did not significantly inhibit major CYPs or
702 hERG (IC_{50} >30 μM). Mouse PK studies of **42** and **40** suggested greater oral exposure for **42** (with
703 preferential accumulation in lungs over plasma), so both leads were advanced into *in vivo* efficacy
704 testing. In this acute *Mtb* infection experiment, BALB/c mice were orally dosed with **42** or **40** at 100
705 mg/kg for 4 weeks, starting one day post-infection, leading to reductions in lung bacterial load of 2.1
706 and 1.1 $\log_{10}$ CFU (relative to untreated control), respectively. Additionally, a combination of RIF
707 and **42** displayed synergy in the same model. Nevertheless, use of a suboptimal oral formulation
708 (0.5% carboxymethylcellulose in water) cast some doubt on the efficacy differences observed.
709 To resolve this uncertainty regarding the best indole-carboxamide candidate, new *in vivo* studies
710 were conducted, in collaboration with the TB Alliance.[180] The use of an optimized formulation for **42**
711 (4:1 propylene glycol: Tween 80) dramatically improved both its oral bioavailability (from 22% to
712 96%) and efficacy in the acute *Mtb* infection BALB/c mouse model (a 4.7 $\log_{10}$ lung CFU reduction,

relative to untreated control, was observed after dosing with **42** at 50 mg/kg for 4 weeks). Finally, a head-to-head efficacy comparison of **42** and **40** was made in BALB/c mice infected with *Mtb* via a high-dose aerosol (acute model). After 4 weeks of oral dosing with **42** or **40** at 100 mg/kg (using a lipid-based formulation developed by Novartis in each case), the lung bacterial load decreased by 3.6 and 3.1 $\log_{10}$ CFU, respectively, relative to untreated control, confirming the slight superiority of **42**.

The known class of 1,5-diarylpyrroles, exemplified by the first reported MmpL3 inhibitor BM212,[63,82] has also been explored recently. Starting with the *in vivo* active compound BM635 (**43**) (**Figure 6**),[181] Poce et al. developed *N*-isopropyl analogue **44** (**Figure 6**) as a new lead.[182] While the *in vitro* activity and toxicity profiles of **43** and **44** were comparable (*Mtb* MIC values of 0.12 and 0.15 µM, CC_{50} values of 40 and 20 µM vs HepG2 cells, and hERG IC_{50} values of 10 and 16 µM, respectively), the kinetic aqueous solubility of **44** was greatly improved (199 µM, *cf.* <1 µM for **43**). Additionally, membrane permeability was increased 3-fold for **44** and human serum albumin binding was reduced (to 94.1% from 98.4% for **43**). Compound **44** was tested for efficacy in the 9-day rapid acute assay,[167] using C57BL/6 mice infected with *Mtb* H37Rv. Compared to the untreated control, oral dosing with **44** at 50 mg/kg for 8 days lowered the lung CFU count by 1.5 $\log_{10}$.[182] However, poor oral bioavailability (1% in C57BL/6 mice) was an unresolved issue for this molecule.

In a subsequent attempt to improve this class, the above investigators turned to scaffold hopping. They discovered that the central pyrrole ring could be replaced by pyrazole and identified **45** (**Figure 6**) as the best lead.[183] Compound **45** was only 2-fold less potent than **44** (MIC of 0.30 µM vs *Mtb* H37Rv) and displayed low cytotoxicity (CC_{50} 32 µM vs HepG2 cells), although it proved to be a moderate inhibitor of hERG (IC_{50} 6.3 µM). This compound also showed good aqueous solubility (152 µM) but slightly greater binding to human serum albumin (96.4%). Further assessment of **45** in the same 9-day rapid acute *Mtb* infection assay (but dosing orally at 200 mg/kg for 4 days, starting 5 days post-infection) again resulted in a 1.5 $\log_{10}$ CFU reduction in bacterial load (relative to untreated control). With SARs varying between pyrroles and pyrazoles, the mode of action of **45** was studied by whole genome sequencing of resistant *Mtb* mutants, and MmpL3 was confirmed as the target.

4.1.3 InhA

Enoyl-ACP reductase (InhA) is an enzyme involved in the elongation of long chain fatty acids.[184] Specifically, it catalyses the double bond reduction of 2-*trans*-enoyl substrates of at least 16 carbons in length, the last step in the type II fatty acid synthase (FAS-II) pathway. Inhibition of InhA, such as with the first-line TB drug INH, blocks mycolic acid biosynthesis.[185] Because most clinical resistance to INH can be traced to mutations in KatG, the enzyme that activates this prodrug, direct inhibitors of InhA have recently been sought as potential alternative drug candidates for TB.

Screening of the GSK compound collection against InhA had initially identified the thiadiazole hit GSK625 (**46**) (**Figure 7**) and further optimisation produced the lead compound GSK693 (**47**) (**Figure 7**).[185] This molecule was a low nanomolar inhibitor of InhA (IC_{50} 0.007 μM) and showed good activity against *Mtb* H37Rv both within and outside of macrophages (MIC 0.2 μM). Compound **47** was not cytotoxic to HepG2 cells (CC_{50} >50 μM) and displayed no inhibition of hERG (IC_{50} >50 μM). Pleasingly, aqueous solubility was markedly improved (413 μM for **47** vs 9 μM for **46**) and metabolic liabilities observed in hit **46** were reduced, leading to a better mouse PK profile (a half-life of 56 min and an oral bioavailability of 92%). This new lead (**47**) was tested in the 9-day rapid acute *Mtb* infection assay,[167] where oral dosing at 100 mg/kg for 8 days gave a large decrease in lung bacterial load (~3.0 $\log_{10}$ CFU vs untreated control).[185] Dosing of **47** at 300 mg/kg for 8 weeks in a chronic *Mtb* infection model also led to excellent efficacy (3.0 $\log_{10}$ CFU reduction in lungs, relative to the untreated control), comparable to that of INH (25 mg/kg). Finally, a much lower frequency of generating resistance to **46** (4×10^{-8} mutants/CFU vs ~10^{-5} for INH) further validated this approach.

Xia et al. (2018) reported the discovery of optimised diazaborine AN12855 (**49**) (**Figure 7**) as a potent InhA inhibitor, after screening against purified *Mtb* InhA had identified the weak hit **48** (**Figure 7**).[186] Compound **49** exhibited an IC_{50} value of 0.03 μM against InhA (a 2633-fold improvement over **48**), an MIC_{90} value of 0.09 μM against *Mtb* H37Rv, and very low cytotoxicity against HepG2 cells (CC_{50} >100 μM). It also retained high potencies against MDR clinical isolates

765 resistant to INH. A cocrystal structure with InhA revealed that **49** occupied both substrate- and
766 cofactor-binding sites of the enzyme (in contrast to earlier inhibitors like **46**, which occupied only the
767 former location). Diazaborine **49** displayed a satisfactory mouse PK profile (a half-life of 3.5 h and
768 an oral bioavailability of 53%) and was progressed into *in vivo* efficacy assessments. In the acute *Mtb*
769 infection model (C57BL/6 mice), oral dosing of **49** at 50 mg/kg for 9 days led to a decreased lung
770 burden of 3.7 $\log_{10}$ CFU, relative to the untreated control. Moreover, in the chronic *Mtb* infection
771 model (BALB/c mice), prolonged dosing of **49** at 100 mg/kg for 8 weeks reduced the lung bacterial
772 load by 1.7 $\log_{10}$ CFU, relative to the untreated control. An additional experiment using the more
773 stringent C3HeB/FeJ mouse model confirmed this efficacy; dosing of **49** at 100 mg/kg for 4 weeks
774 provided a 1.5 $\log_{10}$ CFU reduction in lung burden, relative to the control at the start of treatment.[187]
775 Importantly, it was shown that **49** was taken up early and retained well in caseum and necrotic lung
776 lesions, where most extracellular bacteria are located. Lead **49** also had a much lower tendency to
777 generate resistance than INH, both *in vitro* (4×10^{-7}) and *in vivo* (0.04% resistance to **49** and 29%
778 resistance to INH was seen at the end of the last efficacy experiment). Taken together, these data
779 indicate that **49** has promising attributes as a possible alternative to INH in TB therapy.

780 Aside from direct inhibitors of InhA, there are also compounds that have an indirect but similar
781 overall effect. Like INH, the Group C MDR-TB drug ETH is a prodrug that when activated by the
782 enzyme EthA forms a covalent adduct with NAD, which binds to InhA and inhibits its activity.[130] As
783 noted in Section 3, phase I candidate BVL-GSK098 (**19**) boosts the activity of ETH and overcomes
784 acquired ETH resistance by interacting with a specific transcriptional regulator in *Mtb*, triggering the
785 expression of a second enzyme activator for ETH (MymA).[131] Boosting ETH activity would enable
786 the use of lower drug doses that minimize side effects, increasing patient compliance to therapy. This
787 novel approach is being led by researchers at the Pasteur Institute Lille and the University of Lille.
788

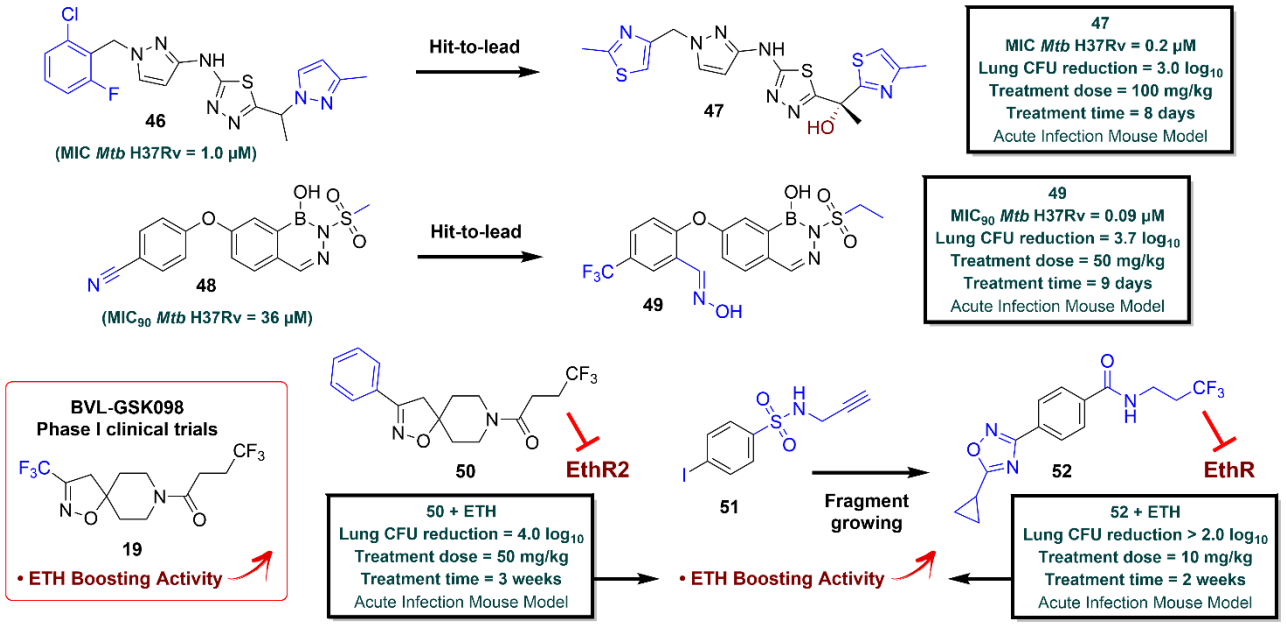

Figure 7. Pyrazolylamino-thiadiazole **47** and diazaborine derivative **49** as direct InhA inhibitors, and spiroisoxazoline analogue **50** and oxadiazole derivative **52** as ETH boosters.

In 2017, these investigators had reported the discovery of another spiroisoxazoline analogue named SMARt-420 (**50**) (**Figure 7**) that also boosted the activity of ETH.[188] In this case, the molecule **50** promoted the expression of a new enzyme activator for ETH (EthA2) through binding to its transcriptional repressor, EthR2. A cocrystal structure of **50** in EthR2 revealed changes to the conformation of EthR2 such that it could no longer bind to its DNA target and prevent elevated expression levels of EthA2. This had the effect of providing more efficient ETH activation, meaning more potent inhibition of InhA. Thus, the MIC of ETH alone against *Mtb* H37Rv was 12 µM, whereas the combination of ETH and **50** (at 10 µM) gave an MIC of 0.30 µM. Similarly, ETH resistant MDR/XDR clinical strains yielded MICs for ETH alone of 48-1540 µM, whereas in the presence of **50** (at 10 µM), these MIC values were 0.15-3 µM. In an *Mtb*-infected macrophage assay, **50** displayed an EC_{50} of ~0.020 µM (where EC_{50} was defined as the concentration of inhibitor that allowed ETH at 0.6 µM to inhibit 50% of *Mtb* growth). The activity-boosting effect of **50** was not observed for non-thioamide TB drugs and was further validated in an acute infection BALB/c mouse model using an ETH-resistant Beijing strain of *Mtb*. Here, 3 weeks of oral dosing with ETH alone (at 50 mg/kg)

807 reduced lung bacterial load by 1.0 $\log_{10}$ CFU, whereas the combination of ETH and **50** (both at 50
808 mg/kg) produced a 4.0 $\log_{10}$ CFU decrease, relative to the untreated control. Compound **50** alone (50
809 mg/kg) had negligible efficacy in this experiment. These results provided excellent proof of principle,
810 especially given that the mouse PK data for **50** were not ideal (e.g., a half-life of only 19 min).

811 The University of Lille team recently reported a further example of this strategy,[189] with the
812 oxadiazole derivative BDM71339 (**52**) (**Figure 7**) being identified as a potent EthR inhibitor and
813 ETH booster. This compound was discovered through a combination of fragment-based drug design,
814 *in silico* docking, and further optimisation,[130] starting from a cocrystal structure of fragment **51**[189]
815 (**Figure 7**) and EthR, the transcriptional repressor of EthA. The EthR inhibitor **52** displayed an EC_{50}
816 of 0.072 μM and possessed sufficient solubility (30 μM) and mouse microsomal stability ($t_{1/2}$ 19 min)
817 to evaluate its *in vivo* boosting capability in the acute *Mtb* infection BALB/c mouse model. In this
818 experiment, **52** and ETH were coencapsulated in poly(*β*-cyclodextrin) nanoparticles and administered
819 6 times over 2 weeks via the endotracheal route, using a microsprayer. The effectiveness of this
820 method had already been proven for an earlier ETH booster, BDM41906.[190] Dosing at 10 mg/kg for
821 both **52** and ETH reduced the mycobacterial burden in lung by more than 2.0 $\log_{10}$ CFU, compared
822 to the untreated control group, about 1 log unit more than for ETH alone.[189] Collectively, these studies
823 revealed the considerable potential of transcriptional repressor inhibitors to boost ETH activity, which
824 will now be tested in clinical trials of BVL-GSK098 (**19**).
825
826 **4.1.4 KasA**
827 Like InhA, β-ketoacyl-ACP synthase I (KasA) is an enzyme that plays an important role in the
828 elongation of long chain fatty acids, which is essential for mycolic acid biosynthesis.[184] KasA
829 catalyses the first step in the FAS-II pathway in which the growing acyl chain undergoes a
830 condensation reaction with malonyl-ACP. Published natural product inhibitors were not sufficiently
831 selective for KasA and were poorly active against *Mtb* or displayed unfavourable toxicities.[139]

Abrahams et al. (2016) reported that one of the open-source screening hits[191] derived from the GSK library, GSK3011724A (**53**) (**Figure 8**) was a selective KasA inhibitor.[192] Compound **53** had acceptable MIC potency against *Mtb* H37Rv (0.8 µM; *cf.* MIC >479 µM for other bacteria), was non-cytotoxic to HepG2 cells (CC_{50} >100 µM) and displayed no hERG liability (IC_{50} >50 µM). It also showed excellent solubility (>550 µM) and sufficiently suitable mouse PK properties to evaluate *in vivo* efficacy. In the 9-day rapid acute assay,[167] using C57BL/6 mice infected with *Mtb* H37Rv, oral dosing of **53** at 200 mg/kg for 8 days lowered the bacterial load in lungs by 3.5 $\log_{10}$ CFU, compared to untreated controls.[192] Furthermore, a 2.4 $\log_{10}$ CFU bacterial burden reduction in lungs was recorded in the chronic *Mtb* infection model, after dosing with **53** at 100 mg/kg for 8 weeks.

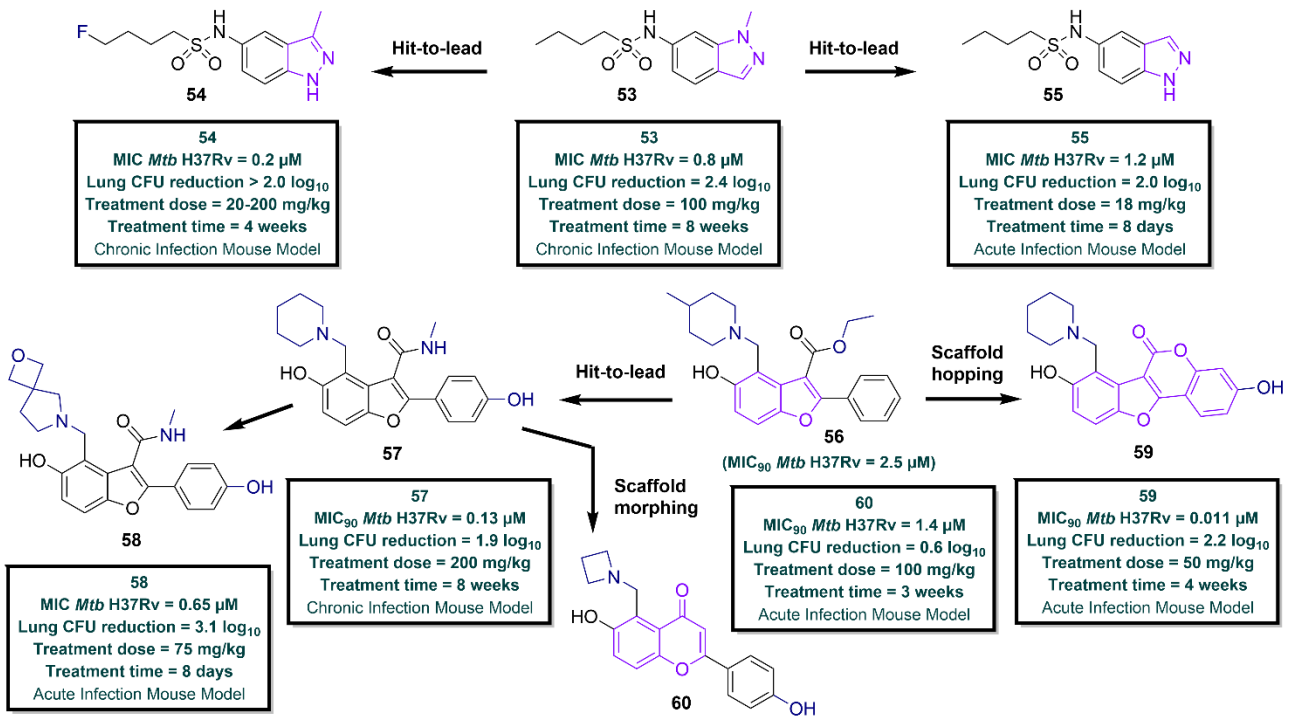

Figure 8. Indazole sulfonamides **53-55** as KasA inhibitors, and benzofuran, coumestan and chromen-4-one derivatives **56-60** as Pks13 inhibitors.

An independent study on **53** (DG167), published in 2018, delivered several new findings.[193] First, analysis of a cocrystal structure with its target found that **53** had a unique dual binding mode to KasA, occupying two different sites in the substrate-binding channel. Second, hit **53** displayed synergistic

activity in combination with INH, both *in vitro* and *in vivo*. Third, it was shown that the predominant metabolite of **53** (upon exposure to mouse liver microsomes) was its N-demethylated derivative, which was completely inactive. These investigators subsequently identified the transposed indazole JSF-3285 (**54**) (**Figure 8**) as an optimised preclinical candidate.[194] This new lead (**54**) displayed an MIC value of 0.20 μM against *Mtb* H37Rv (a 2-fold improvement over **53** in their assay) and a CC_{50} of 170 μM against Vero cells. Notably, **54** demonstrated good solubility (175 μM) and significantly better mouse microsomal stability than **53** ($t_{1/2}$ 28 vs 10 min), leading to much greater oral exposure in mice. Additionally, **54** exhibited only moderate binding to human plasma proteins (77%) and did not inhibit hERG or a panel of 5 CYPs (IC_{50}s >50 μM). When this new lead was tested in the acute *Mtb* infection BALB/c mouse model, dosing orally at 100 mg/kg for 4 weeks, the lung bacterial load was lowered by ~2 $\log_{10}$ CFU, relative to the level at the start of treatment (a benchmark for cidality). In the chronic *Mtb* infection BALB/c mouse model, administration of **54** at doses ranging from 20-200 mg/kg for 4 weeks led to >2 $\log_{10}$ CFU reductions in lung burden, relative to the level when dosing began. Compound **54** also had a low tendency to generate resistance (6×10^{-8}). Overall, these data nicely supported KasA as a drug target in *Mtb* and the advancement of **54** as a TB drug candidate.

Nevertheless, in one final twist to the story, the original researchers from GSK recently reported their own optimisation studies on **53**.[195] Coincidentally, they also identified a transposed indazole derivative, (**55**) (**Figure 8**), as a new lead (MIC 1.2 μM vs *Mtb* H37Rv). This molecule displayed improved microsomal stability and 2-fold superior dose potency in their rapid acute mouse model[167] (ED_{99} 18 mg/kg vs 38 mg/kg for **53**). However, further profiling revealed a key liability with this inhibitor class, due to the mutagenicity of the parent indazole amines in the Ames assay. These amines were detected as metabolites in the urine of rats treated with **53** or **55**. Unfortunately, all attempts to remove this liability failed, due to the very narrow SAR, and GSK eventually abandoned this series.

4.1.5 Pks13

Another essential enzyme of the more than 20 involved in *Mtb* mycolic acid biosynthesis is polyketide synthase 13 (Pks13), which catalyses a final step Claisen-type condensation to give the required 2-alkyl-3-hydroxy fatty acids.[184,196] In 2017, the benzofuran derivative TAM16 (**57**) (**Figure 8**) was disclosed as a novel Pks13 inhibitor.[197] This molecule was developed from screening hit TAM1 (**56**) (**Figure 8**), which was readily susceptible to hydroxylation of the phenyl ring and ester hydrolysis. A cocrystal structure of **56** bound to the thioesterase domain of Pks13 assisted the initial optimisation work. The new lead (**57**) showed improved potency (an MIC_{90} value of 0.13 μM against *Mtb* H37Rv and an IC_{50} value of 0.19 μM against Pks13), with no cytotoxicity toward human dermal fibroblasts (CC_{50} >100 μM). It also displayed acceptable solubility (74 μM), safety (hERG IC_{50} 21 μM), and mouse PK properties ($t_{1/2}$ of 1 h, oral bioavailability of 28%), and the Mannich substructure was not reactive toward glutathione. Daily oral administration of **57** (200 mg/kg) to BALB/c mice having a high dose acute *Mtb* infection reduced the lung mycobacterial burden by 0.9 $\log_{10}$ CFU after 2 weeks, compared to the level at the start of treatment (untreated control mice had to be euthanized after 1 week due to their poor condition). Moreover, in the chronic *Mtb* infection model, BALB/c mice treated with **57** at 200 mg/kg for 8 weeks had a 1.9 $\log_{10}$ CFU lower lung bacterial load than the vehicle control group. Finally, **57** exhibited a ~100-fold lower frequency of generating resistance than INH. These data gave valuable proof of principle for inhibiting this new target.

Interestingly, the findings of a new lead optimisation study of **57** have just been released, where the researchers were seeking to identify a suitable preclinical candidate with a reduced hERG liability.[198] This work was motivated by revised hERG data for **57** (IC_{50} 6.9 μM) and gave rise to several *in vivo* active analogues; of these, **58** (**Figure 8**) was considered to have the best overall profile. Compared to **57**, new lead **58** was similarly active against Pks13 (IC_{50} 0.27 μM) but was 8-fold less potent against *Mtb* H37Rv (MIC 0.65 vs 0.08 μM for **57**) and exhibited minimal hERG inhibition (only 25% at 30 μM). Both **57** and **58** displayed equivalent (moderate) stability toward mouse liver microsomes, therefore, these compounds were further assessed in the 9-day rapid acute assay[167] (using C57BL/6 mice infected with *Mtb* H37Rv). Here, oral dosing of **57** at 58 mg/kg for 8

days provided a 3.9 log_{10} CFU decrease in lung bacterial burden, relative to the untreated control, whereas similar dosing of **58** at 75 mg/kg gave a 3.1 log_{10} CFU reduction. During this efficacy experiment, the 24 h exposures of both molecules were monitored and found to be essentially the same. Subsequent testing demonstrated that **57** was ~3.5-fold more dose-potent than **58** in this acute infection model (ED_{99} 13 mg/kg vs 46 mg/kg for **58**). Lead **58** was also evaluated in the BALB/c mouse model of chronic *Mtb* infection, where dosing at 500 mg/kg for 4 weeks gave a lung burden reduction of 1.1 log_{10} CFU, relative to the untreated control. Nevertheless, following an additional assessment of **58** in an *ex vivo* cardiotoxicity study, the investigation team concluded that the safety window for this lead was still too small and have therefore terminated development of this series.

Meanwhile, Zhang et al. described their own SAR studies to optimise hit **56**, resulting in a set of innovative coumestan derivatives as Pks13 inhibitors.[199] Lead compound **59** (**Figure 8**) displayed a very potent MIC_{90} value of 0.011 μM against *Mtb* H37Rv (*cf.* **56**: MIC_{90} 2.5 μM in the same assay) and a CC_{50} of 11 μM against Vero cells, giving an SI value of 10^3 (less cytotoxicity was recorded for cell lines of human origin). Strong bactericidal activity was also demonstrated *in vitro*.[200] However, a mouse PK assessment of **59** revealed lower than expected oral bioavailability (19%) and only modest oral absorption and exposure, although the half-life was fine (4.5 h). In the acute *Mtb* infection model (BALB/c mice), oral dosing of **59** at 50 mg/kg for 4 weeks (starting only 1 day after infection) reduced the lung mycobacterial load by 2.2 log_{10} CFU (relative to untreated control). Conversely, in the chronic *Mtb* infection model, **59** alone (25 mg/kg) was ineffective (a 0.3 log_{10} CFU decrease in lungs after 8 weeks) but when combined with RIF (10 mg/kg) it achieved an additional 0.6 log_{10} CFU reduction in bacterial burden (compared to RIF alone), suggesting a synergistic effect.

The chromen-4-one derivative **60** (**Figure 8**) was also recently confirmed as a Pks13 inhibitor, having been designed by structure-guided scaffold morphing of benzofuran **57**.[201,202] *In vitro* studies on **60** revealed an MIC_{90} value of 1.4 μM against *Mtb* H37Rv, low cytotoxicity against Vero cells (CC_{50} 164 μM), and superb stability toward mouse liver microsomes (96% parent after 30 min).[201] The PK profile of **60** in BALB/c mice was also considered acceptable (a half-life of 1.4 h and an oral

bioavailability of 21% at 100 mg/kg). Nevertheless, in the BALB/c mouse model of acute *Mtb* infection, oral dosing of **60** at 100 mg/kg for 3 weeks reduced the lung bacterial load by only 0.6 $\log_{10}$ CFU (compared to the untreated group), suggesting that further optimisation would be needed.

4.1.6 FadD32

The enzyme FadD32 has an important dual role immediately before Pks13 in mycolic acid synthesis. As an acyl-AMP ligase it first converts fatty acid substrates into reactive adenylate intermediates,[184] then (as an acyl-ACP synthetase) it relocates these intermediates to Pks13 for the final step condensation.[203] In 2018, Fang et al. described the discovery of quinoline derivative **62** (**Figure 9**) as a FadD32 inhibitor.[204] The group had earlier reported the identification of a 4,6-diaryl coumarin lead (**61**) (**Figure 9**) as an *in vivo* active anti-TB agent and found that it inhibited the synthetase activity of FadD32.[203] However, **61** showed chemical reactivity due to the presence of the lactone ring (a potential toxicity risk) so the coumarin scaffold was finally replaced with a quinoline moiety.[204] New lead **62** displayed an MIC_{90} value of 0.8 µM against *Mtb* H37Rv and a CC_{50} value of 60 µM against HepG2 cells. On-target FadD32 inhibition was confirmed by its 8-fold lower activity against a mutant *Mtb* strain with resistance to hit **61**. Quinoline **62** further demonstrated adequate microsomal stability, modest solubility (15 µM), and excellent dose-dependent efficacy in the rapid acute assay,[167] using C57BL/6J mice infected with *Mtb* H37Rv. After 8 days of oral dosing (starting one day post-infection), compound **62** (50 mg/kg) reduced the mycobacterial burden in the lungs by ~4.0 $\log_{10}$ CFU, compared to the untreated control.[204] The ED_{99} value for this lead was 7.8 mg/kg.

4.1.7 PptT

Phosphopantetheinyl transferase (PptT) is an essential enzyme involved in the activation of acyl carrier proteins (ACPs) for the biosynthesis of virulence factors and cell wall lipids (including mycolic acids).[205] The role of PptT is to relocate 4′-phosphopantetheine (Ppt) from coenzyme A (CoA) onto these ACPs, providing a thiol attachment point for various acid substrates (as thioesters).

952

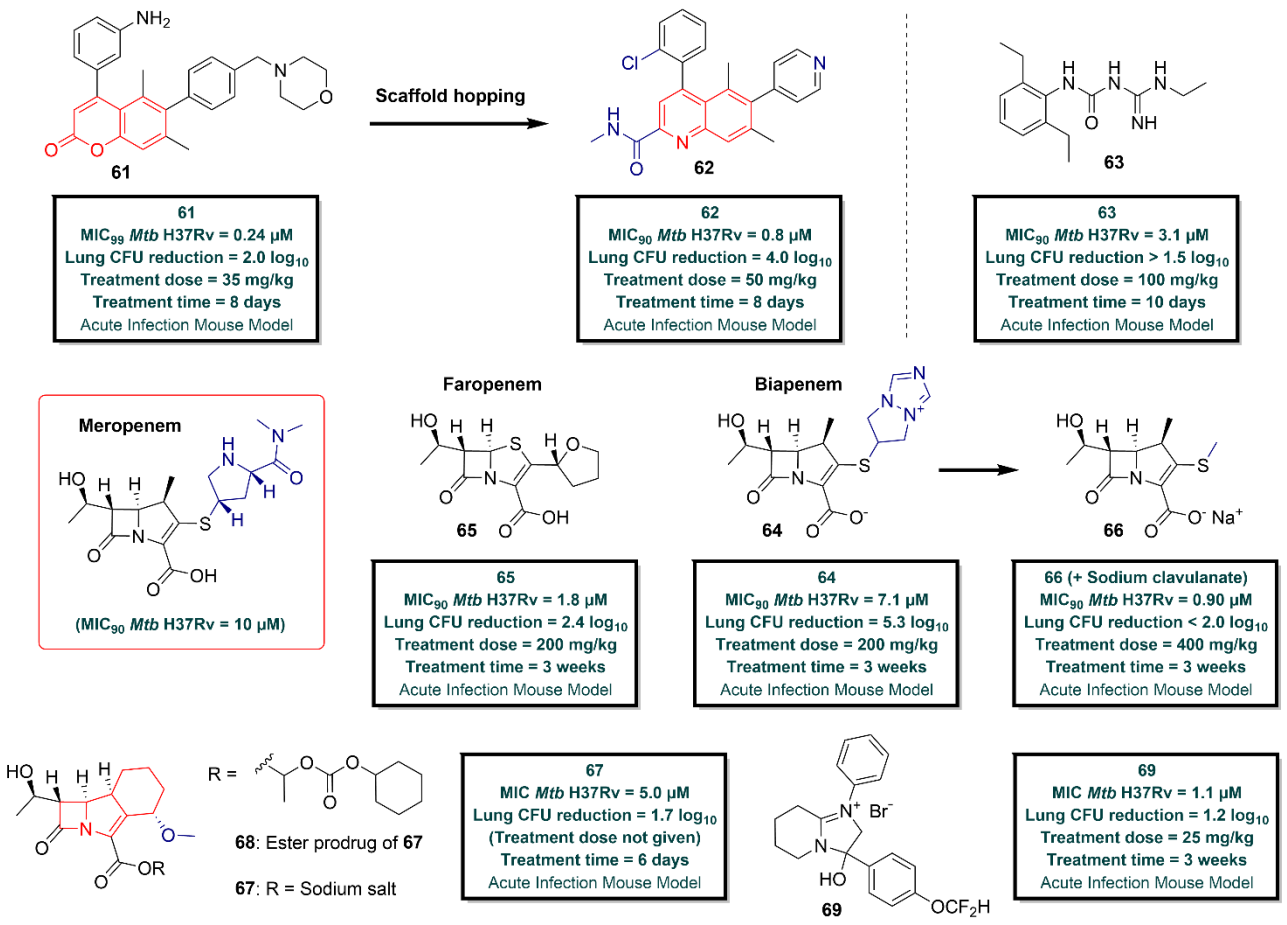

953

954 **Figure 9.** Quinoline derivative **62** as a FadD32 inhibitor, amidino-urea **63** as a PptT inhibitor, β-
955 lactam antibiotics **64**-**68** as transpeptidase inhibitors, and **69** as a DdlA inhibitor.

956

957 The amidino-urea derivative AU 8918 (**63**) (**Figure 9**) was identified through HTS of a >90,000-
958 member Sanofi library.[206] It exhibited an MIC_{90} value of 3.1 µM against *Mtb* H37Rv but was inactive
959 against other Gram-negative and Gram-positive bacteria (MIC_{90} >100 µM) and noncytotoxic to
960 HepG2 cells (CC_{50} >30 µM). A mouse PK experiment determined that **63** was orally bioavailable,
961 with a fine half-life (6.7 h) and extensive accumulation in lung tissue (42:1 over plasma). Moreover,
962 in an acute *Mtb* infection BALB/c mouse model, oral dosing of **63** at 100 mg/kg (8 times in 10 days,
963 starting 1-day post-infection) led to a bacterial burden decrease in lungs of >1.5 log_{10} CFU (relative
964 to the vehicle-only control), equivalent to the efficacy of RIF (10 mg/kg). Resistance to compound
965 **63** was infrequent (3×10^{-7}) but pointed to PptT as the target, although subsequent studies with the

966 purified enzyme indicated non-competitive and partial inhibition (IC_{50} 2.5 μM). A cocrystal structure
967 found that **63** occupied a deep lipophilic pocket in the active site of PptT where the Ppt portion of
968 CoA was normally located, explaining the weaker enzymatic activity. Additional resistance to **63**
969 from mutations in an adjacent gene finally led to the discovery of a Ppt hydrolase, whose function
970 was to remove Ppt from ACPs. Synergistic activity between **63** and Ppt hydrolase was postulated as
971 the reason that partial inhibition of PptT was sufficient to terminate lipid synthesis and kill *Mtb*.
972 Further results on **63** have just been released, including that while this compound does not inhibit
973 CYP3A4 or hERG (IC_{50}s >30 μM), it does cause cardiotoxicity through inhibition of two other ion
974 channels (Ca^{2+} and Na^{+}).[207] However, initial SAR studies revealed that appropriate *para*-substitution
975 of the phenyl ring can substantially diminish these interactions without reducing *in vitro* potency.
976 These findings provide optimism for the future development of PptT inhibitors as anti-TB agents.
977
978 **4.1.8 Transpeptidases**
979 Transpeptidases are enzymes that carry out the final step cross-linking in the synthesis of
980 peptidoglycan, another key constituent of the cell wall.[208] In *Mtb*, most of these cross-linkages are
981 formed by a family of five L,D-transpeptidases, although D,D-transpeptidases are also employed.
982 Both types are uniquely and covalently inhibited by carbapenems, broad-spectrum antibacterial
983 agents from the β-lactam class; two such drugs, meropenem and imipenem, are listed in Table 1 as
984 Group C medicines for the treatment of MDR-TB. However, the need to give those drugs every 8 or
985 12 h by slow infusion (optimally with a β-lactamase inhibitor, to minimise metabolism by the *Mtb* β-
986 lactamase BlaC) has limited their clinical use, stimulating further research to find more suitable
987 analogues.[209] Several co-crystal structures of carbapenem L,D-transpeptidases with inhibitors have
988 afforded a better understanding of mechanistic and physical details relevant to this task.[210,211]
989 Biapenem (**64**) (**Figure 9**) is a newer, more stable carbapenem (approved in Japan, China and
990 India) that has recently been evaluated for use against DS and RIF-resistant *Mtb*.[211-213] Biapenem
991 alone displayed an MIC_{90} value of 7.1 μM against *Mtb* H37Rv, and this was lowered to 1.7 μM in

992 the presence of clavulanic acid (a β-lactamase inhibitor).[212] In the BALB/c mouse model of acute *Mtb*
993 infection, treatment with **64** at 200 mg/kg (given twice daily for 3 weeks by subcutaneous injection,
994 starting 2 days after infection) notably reduced the lung bacterial load by 5.3 $\log_{10}$ CFU, relative to
995 the untreated control group. Identical dosing with a related antibiotic, faropenem (**65**) (**Figure 9**), led
996 to a more modest 2.4 $\log_{10}$ CFU decrease.[211] Moreover, combining **64** with RIF produced much
997 greater bactericidal activity in the same mouse experiment (a lung bacterial load reduction of 8.6 $\log_{10}$
998 CFU, relative to the untreated control). In further experiments using BALB/c mice acutely infected
999 with either *Mtb* H37Rv or one of two RIF-resistant strains, dosing with **64** at 300 mg/kg (twice daily
1000 for 8 weeks) led to equivalent efficacy in all three cases.[213] Curiously, a co-crystal structure of **64**
1001 complexed with L,D-transpeptidase-2 revealed that the final covalent adduct formed after opening
1002 the β-lactam ring by the catalytic cysteine was a considerably degraded 8-carbon fragment in which
1003 the bicyclotriazoliumthio group had been eliminated.[210] It was suggested that this mechanism could
1004 be capitalised upon by S-linking a synergistic antibacterial agent to the carbapenem core.

1005 Mouse efficacy studies of known carbapenems have often been limited by PK issues, particularly
1006 short half-lives (~0.3 h for **64**, ~0.5 h for meropenem).[209,211,213] As part of the above investigations, a
1007 small set of additional analogues was prepared and JSF-2204 (**66**) (**Figure 9**) was identified as the
1008 best lead. This molecule showed improved potency against *Mtb* H37Rv (MIC_{90} 0.90 μM vs 10 μM
1009 for meropenem) and, unlike **64**, gave a stable adduct with L,D-transpeptidase-2 based on the entire
1010 molecule (confirmed by a co-crystal structure).[211] Although the half-life of **66** in mice (0.24 h)
1011 remained an issue, this compound was further tested alongside meropenem in the acute *Mtb* infection
1012 BALB/c mouse model.[209] Both drugs were administered subcutaneously at 400 mg/kg (twice daily
1013 for 3 weeks, together with the β-lactamase inhibitor sodium clavulanate at 75 mg/kg), resulting in
1014 equivalent but moderate efficacy (<2.0 $\log_{10}$ CFU reduction in lung bacterial burden, compared to the
1015 untreated control). Therefore, **64** seems to be the better carbapenem for treating TB.

1016 Interestingly, a related tricyclic β-lactam antibiotic named sanfetrinem (**67**) (**Figure 9**) has been
1017 advanced to preclinical studies for TB. This compound was first developed by GSK more than 27

years ago (as GV 104326), but the original clinical investigations for respiratory infections ceased in 2009 after phase II trials.[214,215] This antibiotic has several advantages, particularly its oral ester prodrug formulation (**68**), as well as its resistance toward β-lactamases and improved stability (a half-life of 2.0 h in humans following a 500 mg oral dose).[215] However, one significant drawback for repurposing as a potential TB drug might be its higher distribution into plasma over lung tissue (4:1 in mice).[216] Compound **67** was rediscovered for TB via HTS of ~2000 β-lactams, where it was the most potent hit at killing *Mtb* H37Rv in THP-1 cells (MIC_{90} 5.6 μM); it also displayed equivalent activity in the standard broth assay (MIC 5.0 μM).[214,217] A comparative assessment of meropenem plus clavulanate and **67** (given subcutaneously) with **68** (given orally) in an acute *Mtb* infection model (using 129sv dehydropeptidase-1 knockout mice and dosing twice daily for 6 days) found similar efficacy, with the lung bacterial burden being lowered by 1.7, 1.7, and 1.4 $\log_{10}$ CFU, respectively, compared to the untreated control group. A phase IIa EBA clinical study for TB is now planned.[214]

4.1.9 DdlA

D-Alanine-D-alanine ligase A (DdlA) is an essential enzyme in *Mtb*, required for peptidoglycan biosynthesis.[218] It couples together two molecules of D-alanine to form a dipeptide, which is then attached to a tripeptide portion of the peptidoglycan.[150] The Group B MDR-TB drug D-cycloserine has DdlA as its primary target, although it also inhibits alanine racemase, the previous enzyme in the pathway.[218] Nevertheless, D-cycloserine can cause severe side effects (e.g., peripheral neuropathy, seizures) that result from NMDA receptor binding in the brain, implying the need for safer inhibitors.

Meng et al. recently published the results of their HTS against DdlA that identified IMB-0283 (**69**) (**Figure 9**) as a new competitive inhibitor (IC_{50} 6.2 μM).[219] This hit compound displayed good activity against *Mtb* H37Rv (MIC 1.1 μM vs 157 μM for D-cycloserine) and low cellular toxicity (CC_{50} 263 μM for HepG2 cells). Oral dosing of **69** (25 mg/kg for 3 weeks) to BALB/c mice with an acute *Mtb* infection led to an encouraging 1.2 $\log_{10}$ CFU reduction in lung bacterial load (relative to the vehicle control), whereas D-cycloserine (25 mg/kg) exhibited no efficacy in the same experiment.

4.2 Compounds Targeting Amino Acid Biosynthesis and Metabolism

While a major focus for TB drug discovery has been cell wall biosynthesis, another promising and novel area is amino acid biosynthesis and metabolism. *Mtb* possesses the toolset required to prepare all 20 standard acids.[220] Moreover, the ability of *Mtb* to survive and induce disease is often reliant upon the integrity of these pathways. The frequent absence of human equivalent targets is also attractive as it implies a lower toxicity risk for inhibitors (from mechanism-based side effects).[221]

4.2.1 Tryptophan Synthase

In *Mtb*, L-tryptophan is formed through a six-step biosynthetic pathway in which the enzyme tryptophan synthase (TrpAB) performs the last two catalytic steps.[221] First, TrpA severs indole from a 3-glycerol side chain, then TrpB condenses indole with L-serine to make L-tryptophan. Current evidence suggests that TrpAB may be vital for *Mtb* survival *in vivo*.[221,222] Sulfolane **71** (**Figure 10**) was reported in 2017 as a TrpAB inhibitor, following optimisation of HTS hit **70** (**Figure 10**).[223] Lead **71** exhibited an MIC value of 2.3 μM against *Mtb* H37Rv and was not cytotoxic to HepG2 cells (CC_{50} >100 μM). It also displayed high solubility (434 μM) and excellent microsomal stability; hence, it was further assessed in the 9-day rapid acute assay[167] (using *Mtb*-infected C57BL/6J mice). Oral dosing of **71** (350 mg/kg) for 8 days, starting one day post-infection, decreased the lung bacterial burden by 1.4 $\log_{10}$ CFU, relative to the untreated control.[223] These data verify the importance of this pathway *in vivo*. A recent cocrystal structure of hit **70** with TrpAB has confirmed that **70** binds to an allosteric site between the two subunits, likely blocking indole transfer to the TrpB catalytic site.[224]

4.2.2 ArgJ

Ornithine acetyltransferase (ArgJ) is one of eight essential enzymes within the L-arginine biosynthesis pathway, which is critical for *Mtb* survival.[225] The role of ArgJ is to recycle an acetyl

moiety by catalytically transferring this group from *N*-acetyl ornithine to the L-glutamate starting material.[225,226] In 2019, Mishra and co-workers reported the first inhibitors of *Mtb* ArgJ.[226] Pranlukast (**72**) (**Figure 10**), an asthma medication having widespread use in Japan, was identified as the best hit from a library of approved drugs, following *in silico* screening and assessment in enzyme assays. This drug was shown to be a non-competitive ArgJ inhibitor (K_i 139 μM), binding to an allosteric pocket on the enzyme surface. It displayed a modest MIC_{90} value of 10 μM against *Mtb* H37Rv but was highly effective in combination with RIF and INH (particularly in infected macrophages, where the bactericidal effects of **72** through ArgJ inhibition may be boosted by its downregulation of *Mtb* pro-survival pathways in the host cells, e.g., 5-lipoxygenase signalling). Pranlukast (**72**) was also tested in the chronic *Mtb* infection BALB/c mouse model, with intraperitoneal dosing at 40 mg/kg for 24 days reducing the lung mycobacterial load by 0.5 $\log_{10}$ CFU, compared to the untreated control group. Furthermore, an additional ~1 $\log_{10}$ CFU load reduction was found in combination with RIF (10 mg/kg), compared to treatment with RIF alone, suggesting some drug repurposing potential.

4.2.3 Aspartate Semialdehyde Dehydrogenase

The aspartate pathway in *Mtb* converts L-aspartate into several other essential amino acids (L-isoleucine, L-lysine, L-methionine, and L-threonine) and *meso*-diaminopimelic acid, a central component in peptidoglycan cross-links.[227] The second step is catalysed by aspartate semialdehyde dehydrogenase (ASADH), an enzyme shown to be crucial for *Mtb* growth and pathogenicity. Very recently, the nitrofuran derivative IMB-XMA0038 (**73**) (**Figure 10**) was identified as a new inhibitor of *Mtb* ASADH (IC_{50} 2.0 μM), following target-based HTS.[227] This compound demonstrated good anti-TB potency (MIC 1.7 μM vs *Mtb* H37Rv) that modulated in response to ASADH expression levels. It also failed to show any cytotoxicity to HepG2 or Vero cells (CC_{50} >218 μM) and did not cause acute toxicity in mice when dosed orally at 500 mg/kg. Moreover, hit **73** was also efficacious in a BALB/c mouse model of acute *Mtb* infection, with oral dosing at 25 mg/kg for 3 weeks decreasing the lung bacterial burden by 1.7 $\log_{10}$ CFU, compared to the vehicle control group.

However, because nitrofuranylamides are a known class of anti-TB agents[134,228] that are reductively activated, it seems unlikely that inhibition of *Mtb* ASADH is the only mechanism of action of **73**.

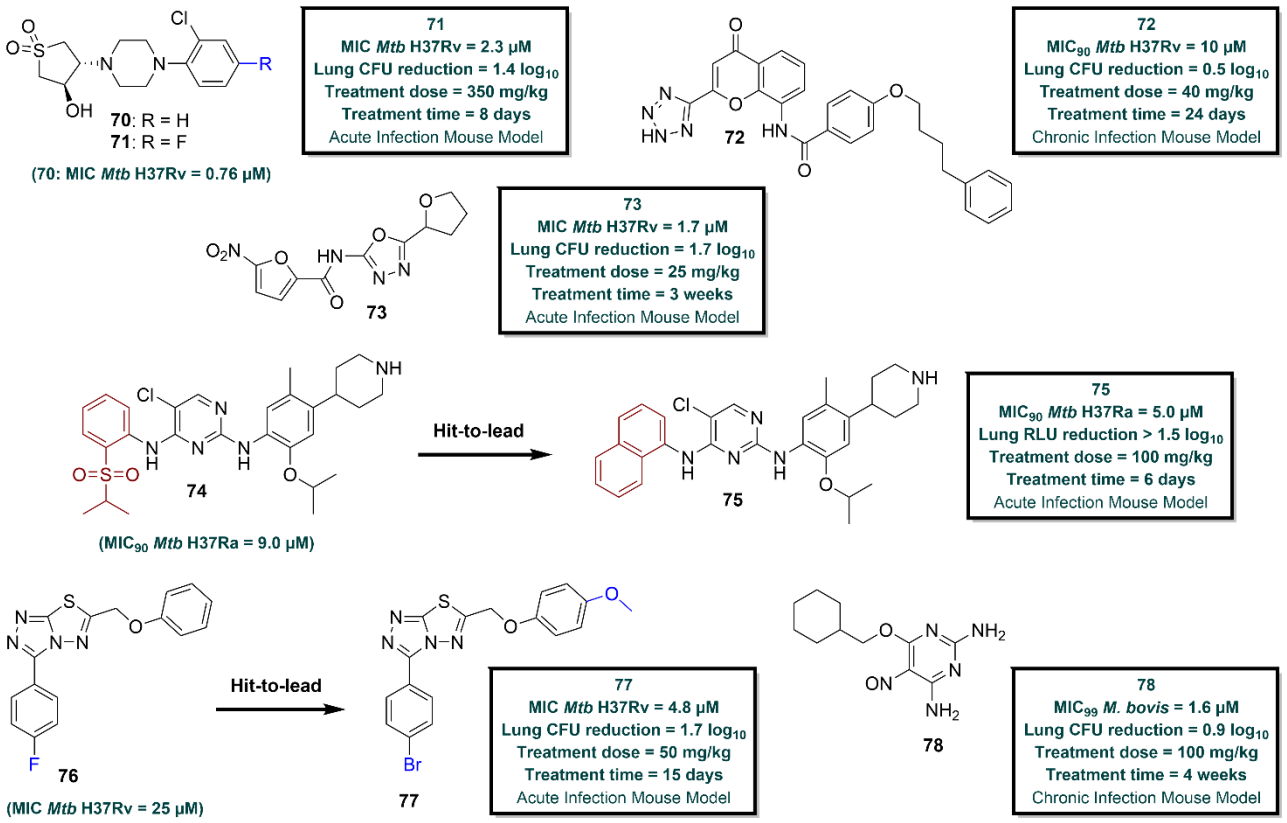

Figure 10. Sulfolane **71**, pranlukast (**72**), nitrofuran **73**, ceritinib analogue **75**, triazolothiadiazole **77**, and diaminopyrimidine **78** as inhibitors of amino acid biosynthesis and metabolism.

4.2.4 Dihydrofolate Reductase

The enzyme dihydrofolate reductase (DHFR) has a crucial role in the folate biosynthesis pathway, as it catalyses the final step production of tetrahydrofolate from dihydrofolate.[229] Tetrahydrofolate derivatives carrying one extra carbon are cofactors in many cellular processes, such as the manufacture L-methionine and purines.[230] The Group C MDR-TB drug *para*-aminosalicylic acid acts as both a substrate and prodrug in the folate pathway, with DHFR being one of its targets.[229]

Ceritinib analogue **75** (**Figure 10**) was reported by Liu et al. (2019) as a putative DHFR inhibitor with moderate anti-TB activity.[231] The original HTS hit, ceritinib (**74**) (**Figure 10**), an anaplastic

lymphoma kinase inhibitor approved for use against lung cancer (NSCLC), was modestly active against autoluminescent *Mtb* H37Ra (MIC_{90} 9.0 μM). However, **74** was ineffective in an acute infection (*Mtb* H37Ra) BALB/c mouse model when dosed orally at 100 mg/kg for 6 days and was too toxic at 300 mg/kg; therefore, an SAR study was conducted. The best analogue (**75**), having a ClogP value of 8.3, showed higher potency against *Mtb* H37Ra (MIC_{90} 5.0 μM) and was non-toxic to mice at 300 mg/kg daily for 6 days. In the same acute infection model, oral administration of **75** at 100 mg/kg for 6 days reduced the lung mycobacterial burden by at least 1.5 $\log_{10}$ relative light units (RLU), compared to the untreated control group. The possible inhibition of DHFR by **75** was inferred from molecular docking studies and a demonstration of partial synergism with sulfamethoxazole, a known inhibitor of another enzyme in the folate biosynthesis pathway, dihydropteroate synthase.[230]

4.2.5 Shikimate Dehydrogenase

Shikimate dehydrogenase (SD) is the middle enzyme in the seven-step shikimate pathway leading to chorismic acid, an essential biochemical intermediate used to produce many key aromatic molecules in *Mtb* (e.g., tyrosine, tryptophan, and phenylalanine).[232] This enzyme converts 3-dehydroshikimate into shikimate by transferring a hydride ion from NADPH. All enzymes in the shikimate pathway are vital to *Mtb* survival, making them appealing targets for TB drug discovery.

In 2018, Deng et al. reported additional assessments of IMB-SD62 (**77**) (**Figure 10**),[233] a novel *Mtb* SD inhibitor, selected from a set of triazolothiadiazoles that the team had prepared earlier (based on the target-based HTS hit **76**; **Figure 10**).[234] Compound **77** exhibited an MIC value of 4.8 μM against *Mtb* H37Rv and an IC_{50} value of 29 μM against *Mtb* SD; it also showed low cytotoxicity toward HepG2 cells (CC_{50} 50 μM). Moreover, in a BALB/c mouse model of acute *Mtb* infection, oral dosing of **77** at 50 mg/kg for 15 days reduced the lung bacterial load by 1.7 $\log_{10}$ CFU, relative to the untreated control group.[233] Nevertheless, further lead profiling studies exposed several deficiencies in **77**. The compound inhibited CYPs 1A2, 2C9 and 2C19 (IC_{50}s 0.56-5.9 μM) and was rapidly metabolised by liver microsomes ($t_{1/2}$ 1.1, 12 and 17 min in human, mouse, and rat), where the major

metabolites were identified as products from oxidation and dealkylation reactions. A rat PK study also revealed a short half-life (1.1 h) and low oral bioavailability (14%), while the solubility of **77** was described as "limited". Hence, this molecule may need additional refinement as a drug candidate.

4.2.6 PknD and PknG

Another promising approach in this area is the inhibition of Ser/Thr protein kinases (STPKs), phosphorylating enzymes involved in regulating numerous cellular functions.[235] There are 11 SPTKs in *Mtb*, of which three (protein kinases A, B and G) are necessary for survival. Protein kinase D (PknD) has been shown to mediate signalling in response to osmotic stress, leading to adaptive modifications in cell wall structure and virulence factor synthesis.[236] In contrast, protein kinase G (PknG) regulates glutamate metabolism in response to signals for amino acid availability.[237]

The diaminopyrimidine derivative NU-6027 (**78**) (**Figure 10**) was reported by Kidwai et al. (2019) as a dual inhibitor of *Mtb* PknD and PknG.[238] This molecule (**78**), a known CDK1/2, DNA-PK and ATR kinase inhibitor, was the most useful new hit obtained from screening a set of 1,280 pharmacologically active compounds against *M. bovis*. It showed an MIC_{99} value of 1.6 µM against *M. bovis* BCG and was not cytotoxic toward THP-1 macrophages at 25 µM. A brief SAR assessment confirmed that the nitroso group was essential for the antibacterial activity. In autophosphorylation assays against all but one of the *Mtb* SPTKs, **78** inhibited the activities of PknD and PknG only, and this was rationalised using docking studies. Furthermore, treatment of *M. bovis*-infected macrophages with **78** not only inhibited bacterial growth, but it also increased apoptosis levels in the host cells, reducing bacterial survival. An *in vivo* PK assessment in BALB/c mice determined that **78** had a short half-life (~1 h) and provided modest oral exposure. Nevertheless, in a chronic infection model using BALB/c mice infected with *Mtb* H37Rv, oral dosing of **78** at 100 mg/kg for 4 weeks decreased the lung bacterial burden by 0.9 $\log_{10}$ CFU, relative to the control group. These data affirm that targeting *Mtb* STPKs and enhancing host cell apoptosis can be valuable approaches for anti-TB drug discovery.

4.3 Compounds Targeting Energy Generation and ATP Synthesis

Unquestionably, the FDA approval of ATP synthase inhibitor BDQ (2012) has stimulated more intense interest in energy generation and ATP synthesis as a fruitful target area for anti-TB drug discovery.[239-242] Oxidative phosphorylation is at the heart of this and is essential for *Mtb* survival and growth.[243] In the "OxPhos" pathway, electrons are typically transferred from the oxidation of organic substrates, through a series of protein complexes, to oxygen (the "electron transport chain"), and protons are transported across the inner membrane. This creates a "proton motive force" (PMF) or transmembrane electrochemical potential (comprising an electrical potential gradient and a proton gradient). The PMF provides the proton flow that drives ATP synthase to phosphorylate ADP, producing ATP.[241,244] In *Mtb*, the protein complexes include complex I (NADH dehydrogenase), complex II (succinate dehydrogenase) and supercomplex III_2IV_2 (complex III, cytochrome *bcc*; complex IV, aa_3-type cytochrome *c* oxidase) (**Figure 11**).[244] A cryo-electron microscopy structure of the supercomplex III_2IV_2 from *M. smegmatis* has furnished new insight into its dimeric architecture and the design of its 20 subunits.[245] Here, cytochrome *bcc* (complex III) transfers electrons derived from menaquinol oxidation to the aa_3-type cytochrome *c* oxidase (complex IV) for reduction of oxygen.[241,245] A less efficient enzyme, cytochrome *bd* oxidase, can perform the same role and a long-awaited cryo-electron microscopy structure of the *Mtb* enzyme has just been published.[246,247]

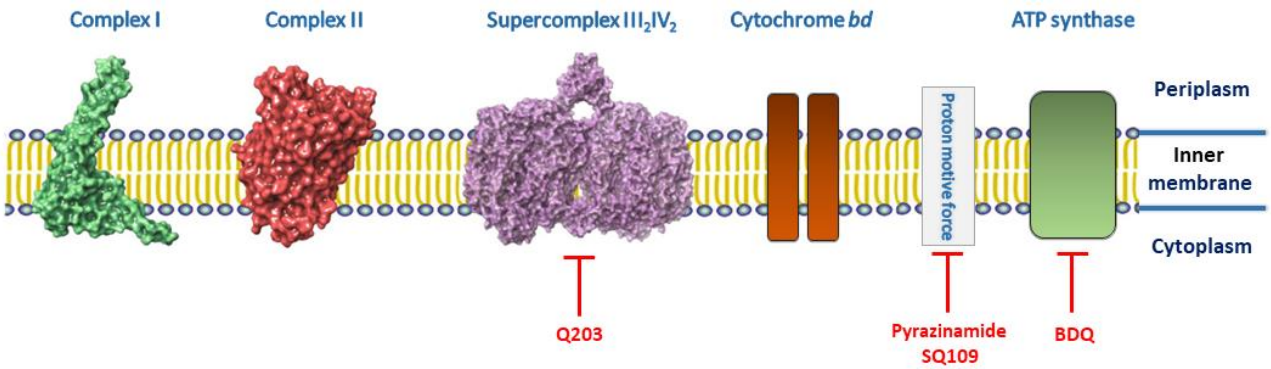

Figure 11. Schematic representation of the oxidative phosphorylation pathway of *Mtb*, based on the description given by several authors[241-243] and modified from Bahuguna et al.[248] (reproduced with permission. Copyright © 2021, John Wiley and Sons).

4.3.1 QcrB

The QcrB subunit of cytochrome *bcc* (complex III) has been reported as the target of several small molecules with favourable anti-TB activity, including the drug candidate Q203 (**7**) in phase II clinical trials.[92,94,241,242,248] The morpholino-thiophene amide **80** (**Figure 12**), derived from an Eli Lilly HTS hit (**79**) (**Figure 12**), was revealed by Cleghorn et al. (2018) to be a potent cytochrome *bcc* inhibitor at QcrB.[249] Compound **80** displayed an MIC_{90} value of 0.24 µM against *Mtb* H37Rv and modest cytotoxicity toward VERO cells (CC_{50} 39 µM). While this molecule had minimal aqueous solubility (2.4 µM), it demonstrated high permeability and acceptable oral exposure in mice, with an oral bioavailability of 18%. Metabolism studies found that oxidation of the morpholine ring was the main issue contributing to a short half-life in rats (0.5 h). In a 9-day rapid acute *Mtb* infection assay[167] (using C57BL/6 mice), oral dosing of **80** at 100 mg/kg for 4 days (starting 5 days post-infection) reduced the lung bacterial load by 0.8 $\log_{10}$ CFU, relative to the untreated control group.[249]

The unsaturated piperazine amide derivative AX-35 (**81**) (**Figure 12**), one of the open-source screening hits[191] obtained from the GSK library, was also found to inhibit QcrB, but with a distinct binding mode.[250] This compound exhibited an MIC_{90} value of 0.14 µM against *Mtb* H37Rv, with low cytotoxicity toward HepG2 cells (CC_{50} 140 µM), although it was rapidly metabolised by mouse liver microsomes. That led to weak efficacy in an acute *Mtb* infection BALB/c mouse model, where oral dosing of **81** at 200 mg/kg for 10 days decreased lung bacterial load by only 0.4 $\log_{10}$ CFU, compared to the untreated control group. Replacement of the thiophene ring in **81** by thiazole (**82**) (**Figure 12**) was acceptable *in vitro* (MIC_{90} 0.84 µM against *Mtb* H37Rv; HepG2 CC_{50} 210 µM) and resulted in better *in vivo* activity in the acute model, with oral dosing of **82** at 100 mg/kg for 10 days reducing the lung bacterial burden by 0.9 $\log_{10}$ CFU, relative to the control group. However, **82** was inactive

in the chronic TB infection model, possibly due to reduced target expression. The lack of bactericidal activity for these and other QcrB inhibitors is attributed to the presence of cytochrome *bd* oxidase, which is upregulated when cytochrome *bcc* is inactivated and during low oxygen conditions.[115,247]

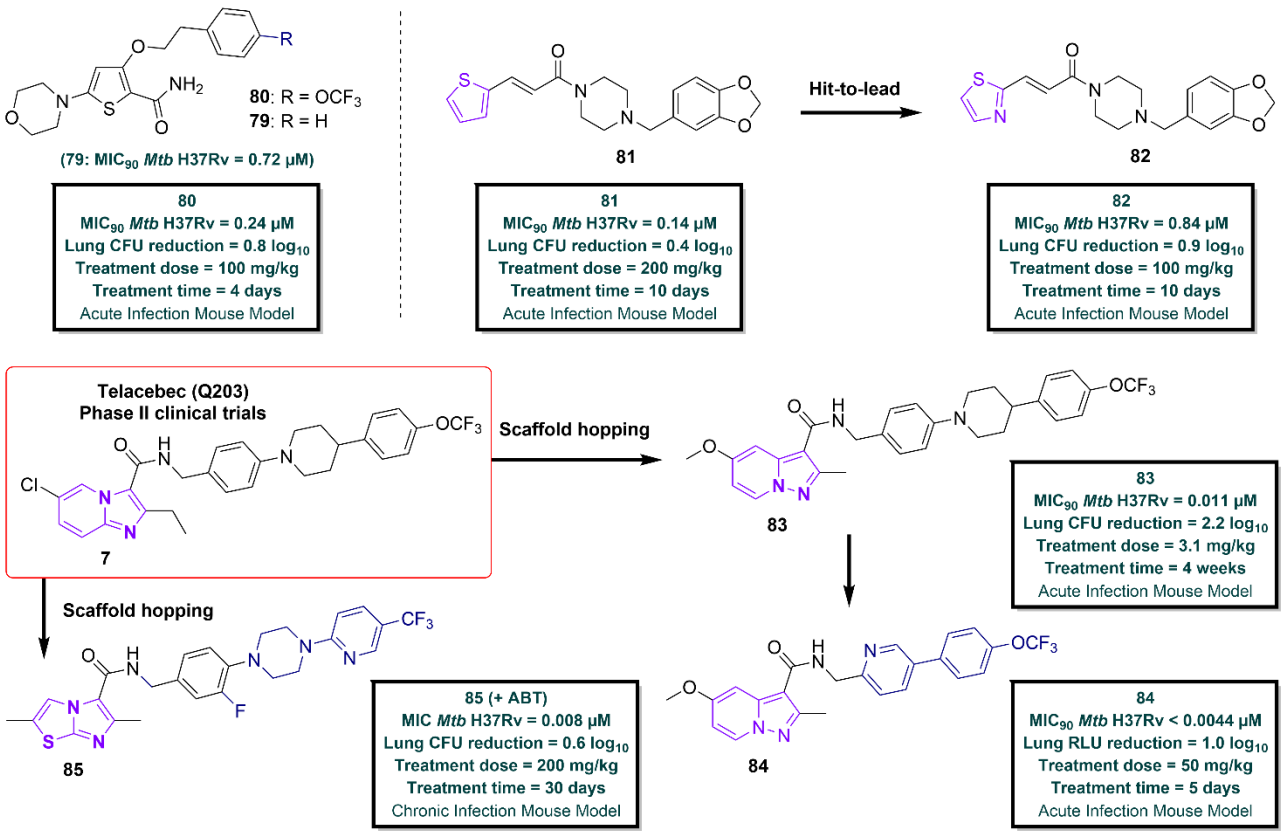

Figure 12. Morpholino-thiophene **80**, piperazine amides **81** and **82**, pyrazolo[1,5-*a*]pyridines **83** and **84**, and imidazo[2,1-*b*]thiazole **85** as QcrB inhibitors.

In 2019, Lu et al. published additional assessments of the QcrB inhibitor TB47 (**83**) (**Figure 12**), a Q203 mimic designed by scaffold hopping that was disclosed by these investigators in 2015.[251,252] Pyrazolo[1,5-*a*]pyridine **83** was non-cytotoxic (CC_{50} >100 µM on Vero and HepG2 cells) and displayed high potency, equal to that of Q203 (**7**), against *Mtb* H37Rv (MIC_{90} 0.011 µM).[252] Remarkably, the Caco-2 permeability of **83** was negligible and it was 100% bound to human plasma proteins, yet it still demonstrated an excellent rat PK profile, with a half-life of 19 h and an oral bioavailability of 94%. This lead showed no early toxicity liabilities (hERG IC_{50} >30 µM and IC_{50}s

>20 μM for a panel of 7 CYPs) and provided an MTD of >2 g/kg in rats. Furthermore, **83** was efficacious in a BALB/c mouse model of acute *Mtb* infection; oral administration for 4 weeks (starting one day after infection) gave lung bacterial burden reductions ranging from 2.2 $\log_{10}$ CFU at 3.1 mg/kg up to 3.9 $\log_{10}$ CFU at 200 mg/kg (relative to the vehicle control group). Synergistic effects were also seen in the same model when **83** (25 mg/kg) was combined with RIF (10 mg/kg) or PZA (150 mg/kg). However, **83** appeared to be somewhat less active than **7** in the chronic *Mtb* infection BALB/c mouse model after dosing at 50 mg/kg for 8 weeks (0.3 and 0.6 $\log_{10}$ CFU reductions in lung bacterial load, respectively, relative to the vehicle control). More recent acute infection mouse studies have focused on the benefits of combining **83** with CFZ in various treatment regimen for MDR-TB.[253,254] Like **7**, **83** also exhibited outstanding *in vivo* efficacy against *M. ulcerans* (the causative agent for Buruli ulcer).[255] A cryo-electron microscopy structure of *Mtb* cytochrome *bcc* bound to **83** confirmed that the inhibitor occupies the same menaquinol-binding Q_P site pocket in QcrB as **7**.[256] This promising lead candidate is currently completing preclinical safety studies.[253]

During their search for a backup candidate to **83**,[242] the same investigators developed the heterobiaryl side chain analogue **84** (**Figure 12**).[257] Compound **84** demonstrated improved potency (an MIC_{90} value of <0.0044 μM against *Mtb* H37Rv) and was not cytotoxic to Vero cells (CC_{50} >110 μM). It also displayed a suitable half-life (5.1 h) and respectable oral bioavailability (41%) in rats; hence, it was further evaluated against autoluminescent *Mtb* H37Ra in an acute infection BALB/c mouse model. Oral dosing of **84** at 50 mg/kg for 5 days (starting one day post-infection) led to a 1.0 $\log_{10}$ RLU decrease in the lungs (relative to solvent control), suggesting some potential as a new lead.

Recently, Moraski et al. reported further profiling of the imidazo[2,1-*b*]thiazole derivative ND-11543 (**85**) (**Figure 12**), a QcrB inhibitor that the team had unveiled in 2016 as part of a scaffold hopping SAR study.[258,259] Lead **85** exhibited MIC values of 0.008 μM and 1.1 μM against replicating *Mtb* (strain H37Rv) and non-replicating *Mtb* (LORA assay), respectively. It was also non-cytotoxic toward Vero cells (CC_{50} >100 μM) and did not inhibit the major CYPs (IC_{50} >10 μM). Being less lipophilic than Q203 (**7**) (ClogP values 5.4 vs 7.6), it was interesting to note that **85** had reasonable

solubility (50 μM) and moderate stability toward human liver microsomes ($t_{1/2}$ 28 min), but low Caco-2 permeability (<1 x 10^{-6} cm/s) and 100% binding to human plasma proteins. In BALB/c mice, oral dosing of **85** at 200 mg/kg led to slow absorption and a long half-life ($t_{1/2}$ >24 h); moreover, drug exposure was more than 3-fold higher in the presence of the pan CYP inhibitor 1-aminobenzotriazole (ABT), suggesting a metabolism issue. Unfortunately, poor efficacy was seen for **85** in the chronic *Mtb* infection BALB/c mouse model after 30 days of oral dosing at 200 mg/kg (an insignificant 0.3 $\log_{10}$ CFU reduction in lung bacterial burden, relative to the untreated control). When ABT (100 mg/kg) was added, some efficacy was seen for **85** at 200 mg/kg (0.6 $\log_{10}$ CFU reduction) but little at 100 mg/kg (0.3 $\log_{10}$ CFU reduction). However, given the modest efficacies of Q203 (**7**) and **83** in this model and the use of an appreciably different side chain (potentially less effective *in vivo*), the future utility of this new scaffold remains unclear. Ideally, the optimised Q203 side chain would be employed for a head-to-head assessment of all three scaffolds in the acute infection model.

From 76 analogues of the GSK HTS hit **86**[191] (**Figure 13**), Lupien et al. found lead quinazoline **87** (**Figure 13**). This class targets both QcrB and QcrA, based on the sequencing of resistant *Mtb* mutants (albeit the menaquinol-binding Q_P site was implicated in all cases).[260] Compound **87** showed an MIC_{99} value of 0.20 μM against *Mtb* H37Rv and negligible cytotoxicity toward HepG2 cells (CC_{50} 153 μM) but its human microsomal stability was only moderate. When **87** was tested in an acute *Mtb* infection BALB/cByJ mouse model, dosing orally at 150 mg/kg for 10 days (starting one day post-infection), it gave a 0.5 $\log_{10}$ CFU reduction in lung bacterial load, compared to the solvent control. Further optimisation may be needed to improve metabolic stability and better contact both target sites.

4.3.2 ATP Synthase

Following on from the clinical success of BDQ, the commencement of phase I clinical trials for two analogues [TBAJ-876 (**16**) and TBAJ-587 (**17**)] having higher potencies, reduced lipophilicities, and lower cardiotoxicity risk (Section 3) represents a notable advance.[92,242] Furthermore, in 2017, a team from AstraZeneca (in collaboration with the TB Alliance) disclosed squaramide **89** (**Figure 13**)

as a novel ATP synthase inhibitor.[261] This lead was developed from the hit **88** (**Figure 13**), which was identified through HTS of AstraZeneca's 900K compound library for inhibition of mycobacterial ATP synthesis. Compound **89** was highly potent at inhibiting ATP synthesis in membrane vesicles from *M. smegmatis* (IC_{50} 0.03 μM) and had an SI value of 782 over ATP synthesis inhibition in bovine mitochondria. It was not cytotoxic toward A549 cells (CC_{50} >100 μM) and did not cause membrane damage in *M. bovis* BCG cells (IC_{50} >100 μM). Lead **89** also exhibited an MIC_{80} value of 0.5 μM against *Mtb* H37Rv and retained sensitivity toward two BDQ-resistant strains, suggesting differences in its binding mode compared to that of BDQ. Sequencing of *Mtb* mutants resistant to **89** indicated that sites on two subunits (*a* and *c*) of ATP synthase were involved in inhibitor binding. Mouse PK studies of **89** in the presence of pan CYP inhibitor ABT (both at 100 mg/kg) demonstrated oral exposure above the MIC for more than 15 h; therefore, this lead was assessed in an acute *Mtb* infection BALB/c mouse model. Here, oral dosing of **89** (200 mg/kg, with ABT at 100 mg/kg) for 2 weeks provided a >2.0 $\log_{10}$ CFU reduction in lung bacterial burden, compared to the untreated control group. These findings suggest some potential for this class if the PK issues can be overcome.

These AstraZeneca researchers had earlier discovered pyrazolopyrimidine **91** (**Figure 13**) by scaffold morphing and optimisation of a non-selective hit from the same HTS, **90** (**Figure 13**).[262] Compound **91** selectively inhibited ATP synthesis in *M. smegmatis*-derived membrane vesicles (IC_{50} 0.5 μM; 20-fold better than the value for inhibiting ATP synthesis in bovine mitochondria), reduced ATP levels, and did not induce membrane damage in *M. bovis* BCG cells (IC_{50} >100 μM). It also displayed moderate potencies against *Mtb* H37Rv and two BDQ-resistant strains (MIC_{80} 6.2 and 6.3-12.5 μM, respectively) and was bactericidal under both standard and low oxygen conditions. In the BALB/c mouse model of acute *Mtb* infection, **91** showed good oral exposure, and 2 weeks of oral dosing at 100 mg/kg gave a ~1.5 $\log_{10}$ CFU smaller lung bacterial load than the vehicle control group. But while docking results supported ATP synthase as the target of **91**, this still requires further study.

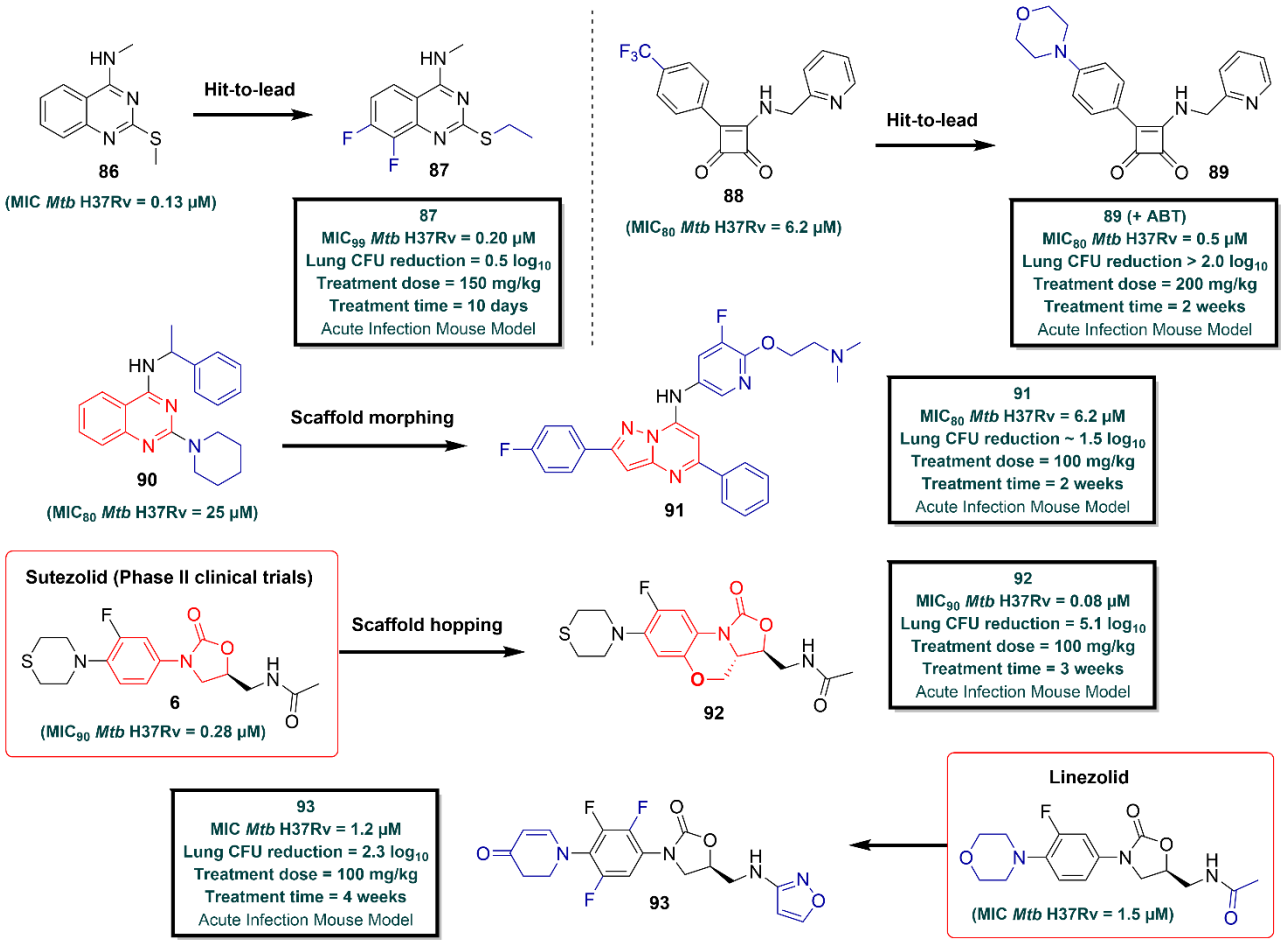

Figure 13. Quinazoline **87** as a QcrA/B inhibitor, squaramide **89** and pyrazolopyrimidine **91** as ATP synthase inhibitors, and oxazolidinone derivatives **92** and **93** as protein synthesis inhibitors.

4.4 Compounds Targeting Protein Synthesis

Protein synthesis is essential for survival and replication of biological life and is responsible for approximately 50% of the total energy used in growing bacteria.[263] The final stage in protein synthesis, RNA translation, occurs on the bacterial 70S ribosome. The latter is comprised of two subunits (30S and 50S) and a bridging interface area that hosts a trio of binding sites for tRNA (A, P and E).[92] Organism-specific differences within the translational machinery can enable the development of new drugs with high selectivity for the *Mtb* target, e.g., the LeuRS inhibitor GSK656 (**9**), in phase II clinical trials.[92,263]

Several structural studies have identified that oxazolidinone derivatives bind to the A-site of the bacterial ribosome.[87] Nevertheless, LZD concomitantly inhibits mitochondrial protein synthesis, leading to toxic side effects; these are exacerbated by longer treatment times (>1-2 months) and contribute to its more restricted clinical application against severe (MDR) infections only.[87,90,264] For example, in the recent Nix-TB trial against MDR/XDR-TB [combining LZD with BDQ (**1**) and pretomanid (**3**)], 81% of patients experienced LZD-related myelosuppression (e.g., anaemia and thrombocytopenia) and 48% had LZD-related peripheral neuropathy (2% with optic neuritis). Therefore, most Nix-TB study participants had to switch to a lower dose of LZD or temporarily cease taking it.[59] However, the new ZeNix trial (evaluating lower dosages or shorter treatment duration with LZD) has shown that such toxicities can be reduced without compromising the superb efficacy of this regimen against MDR/XDR-TB.[265] In the past two decades, numerous oxazolidinone derivatives have been studied, and three candidates with better safety are now in clinical trials for TB [delpazolid (**5**), sutezolid (**6**), and TBI-223 (**15**); see Section 3].[87,88,266]

In 2020, Zhao et al. reported the development of a conformationally restricted derivative of sutezolid (**6**) that had been advanced to preclinical testing.[267] This new drug candidate, named OTB-658 (**92**) (**Figure 13**), was inspired by some reported antibacterial agents that possessed the same fused tricyclic scaffold and had favourable activity and PK profiles. Compound **92** showed improved potency against *Mtb* H37Rv (an MIC_{90} of 0.08 μM *cf.* 0.28 μM for **6** and 1.3 μM for LZD) and was non-cytotoxic (CC_{50} >168 μM for Vero and HepG2 cells). A *trans* configuration (3*S*,3*aS*) in the benzoxazinyl-oxazolidinone core (confirmed by an X-ray structure) was crucial for its activity. Crucially, **92** demonstrated much weaker inhibition of mitochondrial protein synthesis than sutezolid (**6**) and LZD (IC_{50} >100 μM *cf.* 8.2 and 8.0 μM, respectively) and a decreased inhibition of monoamine oxidases A and B (IC_{50}s >45 and 3.2 μM, respectively, *cf.* 13 and 0.7 μM for **6**). Furthermore, this lead exhibited high membrane permeability, suitable microsomal stability, low hERG risk (IC_{50} >30 μM) and minimal CYP inhibition (IC_{50}s >45 μM for a panel of five isoforms). Additionally, **92** displayed a favourable mouse PK profile (a prolonged oral half-life of 15 h and 56%

oral bioavailability), although significant oxidation to the less active sulfoxide derivative was apparent. In the acute *Mtb* infection BALB/c mouse model, oral dosing of **92** at 100 mg/kg for 3 weeks remarkably reduced the lung bacterial burden by 5.1 $\log_{10}$ CFU, in comparison to the untreated group, whereas LZD (100 mg/kg) achieved a lesser reduction of 3.0 $\log_{10}$ CFU. Moreover, the *in vivo* efficacy of **92** also surpassed that of sutezolid (**6**) in this model. These findings prompted further assessment of **92** and LZD in a chronic *Mtb* infection experiment using BALB/c mice.[268] After 8 weeks of treatment, **92** (at 25 mg/kg) was superior to LZD (50 mg/kg), while dosing of **92** at 50 mg/kg led to a lung bacterial burden reduction of ≥3.0 $\log_{10}$ CFU, relative to the solvent control. Finally, **92** exhibited a low frequency of generating resistant mutants (9×10^{-9} to 3×10^{-8})[268] and in a four-week rat toxicity study showed a decreased risk of myelosuppression, compared to LZD.[267] This impressive candidate currently appears poised to commence phase I clinical trials for MDR-TB in China.[268]

Another antibacterial oxazolidinone-based clinical candidate, contezolid (MRX-I, **93**) (**Figure 13**), was evaluated by Shoen et al. for utility against *Mtb*.[269] This drug has recently been approved in China to treat problematic soft tissue and skin infections.[270] It has better safety than LZD, due to its weaker tendency to induce myelosuppression or inhibit monoamine oxidases A and B.[270,271] In this current study, **93** and LZD were found to be similarly active against *Mtb* H37Rv (MICs 1.2 and 1.5 μM, respectively) and a panel of clinical isolates.[269] An earlier report had also revealed that **93** exhibited an acceptable mouse PK profile, with a half-life of 1 h and an oral bioavailability of 69%.[271] Therefore, this molecule was further assessed, alongside LZD, in a BALB/c mouse model of acute *Mtb* (Erdman) infection.[269] In this experiment, head-to-head oral dosing of **93** and LZD at 100 mg/kg for 4 weeks achieved statistically equivalent lung bacterial load reductions of 2.3 and 2.4 $\log_{10}$ CFU, respectively, relative to the untreated group. Furthermore, once-daily dosing of **93** at 100 mg/kg was much more effective than twice-daily dosing at 50 mg/kg. Collectively, the outcomes shown by compounds **92** and **93** are very encouraging, given the importance of developing a safer oxazolidinone-based drug as an alternative to LZD for the treatment of MDR- and XDR-TB.

Fernandes et al. (2017) reported a new generation of heterocyclic *N*-oxide derivatives, including benzofuroxans, furoxans, and quinoxaline 1,4-di-*N*-oxides, as potent anti-TB agents.[272] The lead compound, benzofuroxan BZ8 (**94**) (**Figure 14**) provided MIC_{90} values of 1.1 µM and 6.6 µM against replicating and nonreplicating *Mtb* H37Rv, respectively. It was also active against a panel of monoresistant strains of *Mtb* and did not show cytotoxicity toward MRC-5 cells (CC_{50} 519 µM). Time-kill kinetic experiments further revealed that **94** was bactericidal, sterilizing *Mtb* cultures after treatment for 48 h. This molecule exhibited moderate human plasma protein binding (54%), adequate permeability, and minimal CYP inhibition (IC_{50}s >15 µM against four isoforms). Notably, in the acute infection BALB/c mouse model (against *Mtb* Erdman), oral dosing of **94** at 200 mg/kg for 3 weeks reduced the lung bacterial burden to undetectable levels, a >6.0 log_{10} CFU decrease, compared to the solvent control. Transcriptional profiling studies pinpointed an upregulation in most ribosomal genes (and all ATP synthase-coding genes), leading the authors to suggest that **94** blocks the initiation step of protein synthesis. However, the exact target and mode of action have yet to be determined.

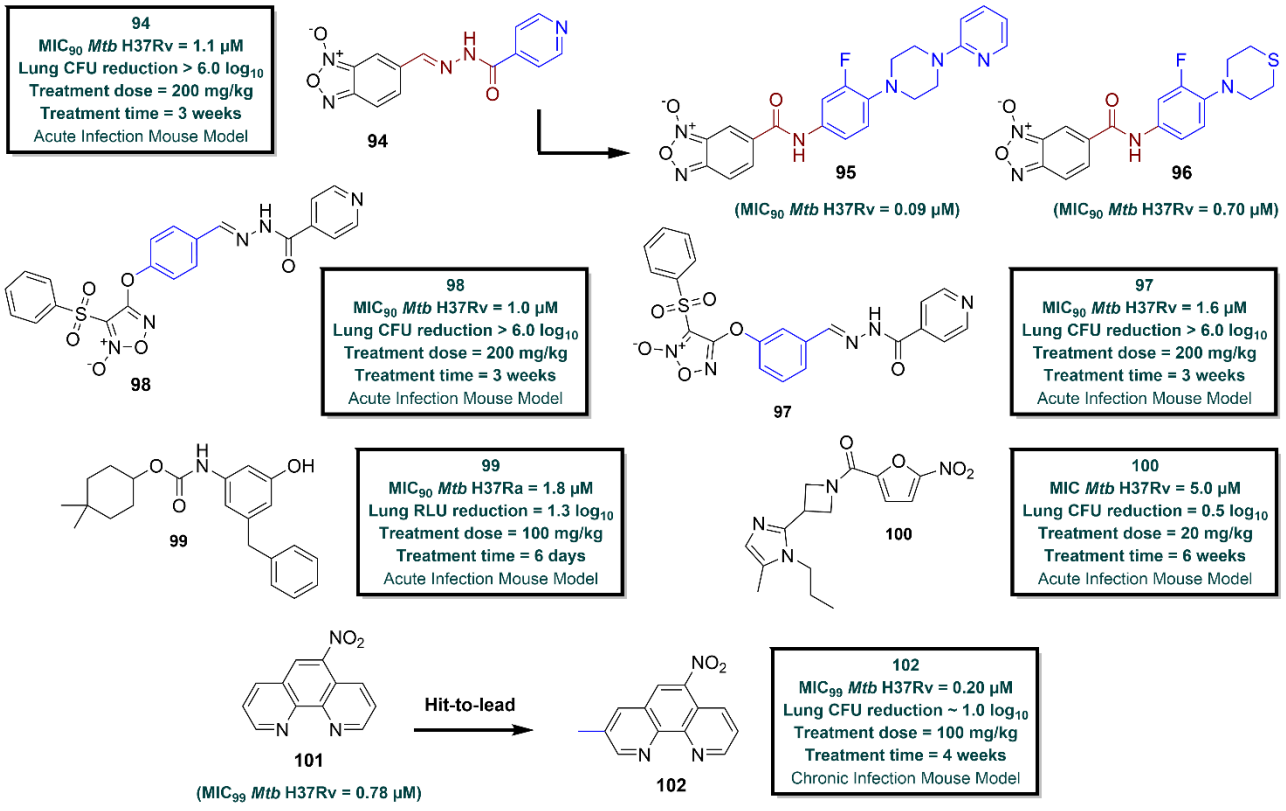

Figure 14. Benzofuroxan **94**, furoxans **97** and **98**, carbamate **99**, nitrofuran **100**, and nitrophenanthroline **102** with *in vivo* anti-TB activity.

Despite the impressive sterilizing activity of **94**, some concerns remained about its cytotoxicity to Hep G2 cells (CC_{50} 16 μM) and its chemical stability, due to the *N*-acylhydrazone moiety. Hence, these authors have recently developed novel analogues, e.g., **95** and **96** (**Figure 14**) with amide-linked aminoaryl side chains, which are more effective than **94** against MDR strains of *Mtb* (MIC_{90}s <0.27-2.2 μM).[273] *In vivo* efficacy studies are underway and the results will be published in due course.

4.5 Compounds with Miscellaneous or Unknown Targets

While phenotypic drug discovery approaches have successfully delivered many novel agents to treat TB and other infectious diseases, elucidating the molecular targets and mechanisms of action of these compounds can often be labour-intensive and challenging.[274,275] For example, the generation of spontaneous drug-resistant mutants may be difficult or even impossible.[66,275] However, knowing the targets of promising screening hits can also assist with prioritization decisions, accelerate the lead optimisation process, and help to establish whether leads possess appropriate selectivity and safety.

Prior to their work on **94** (described above), Fernandes et al. designed and evaluated a new class of hybrid furoxan analogues as nitric oxide donors.[276] Compounds **97** and **98** (**Figure 14**) displayed MIC_{90} values of 1.6 and 1.0 μM against *Mtb* H37Rv and modest cytotoxicity toward MRC-5 cells (CC_{50} values of 30 and 43 μM). Nitric oxide release was confirmed through the detection of nitrite in the MIC assay medium and was evidently critical for the anti-TB activity, as the latter could be abolished by adding a nitric oxide scavenger (giving MIC_{90}s >62 μM). Subsequent studies reported in 2020 found that **97** and **98** were also active against nonreplicating *Mtb* (MIC_{90}s 6.7 and 9.8 μM, respectively) and various monoresistant and MDR strains.[277] Both compounds were not mutagenic (Ames test) and did not induce toxicity in mice. When BALB/c mice infected with *Mtb* Erdman (acute

model) were orally dosed with either compound at 200 mg/kg for 3 weeks, no bacteria could be detected in the lungs (as seen for **94**, a >6.0 $\log_{10}$ CFU decrease, compared to the solvent control). Nevertheless, chemical stability might be a concern for these compounds because they also possess the *N*-acylhydrazone moiety. In fact, all three compounds (**94**, **97** and **98**) were orally administered to mice using a nanostructured lipid-based formulation that afforded better solubility and stability.

Carbamate **99** (**Figure 14**) was published in 2019 as part of an SAR study.[278] This molecule showed an MIC_{90} value of 1.8 μM against autoluminescent *Mtb* H37Ra but had weaker activity against *Mtb* H37Rv and MDR strains (MICs 11-23 μM) and low cytotoxicity against A549 cells (CC_{50} 64 μM). Unfortunately, **99** was rapidly metabolised in mouse liver microsomes, with a 1.8 min half-life indicating faster clearance than their original amide congeners, which had shown no *in vivo* activity. Nevertheless, the authors elected to perform a brief efficacy study in the acute infection model, using BALB/c mice infected with autoluminescent *Mtb* H37Ra. Surprisingly, dosing **99** orally at 100 mg/kg for 6 days (starting one day post-infection) achieved a respectable reduction of the bacterial burden in mouse lungs of 1.3 $\log_{10}$ RLU, relative to the untreated control group.

From a newly synthesized series of reductively activated[228] nitrofuranylamides conjugated to alkylimidazoles, Krasavin et al. reported the novel anti-TB lead **100** (**Figure 14**).[279] Compound **100** exhibited MIC values of 5.0 μM and 2.5-9.7 μM against *Mtb* H37Rv and three MDR-TB isolates, respectively. It also displayed low toxicity following 14 days of oral dosing in C57BL6 mice (MTD 700 mg/kg). Comparative assessment of **100** and EMB in an acute *Mtb* infection C57BL6 mouse model found that oral dosing of both compounds at 20 mg/kg for 42 days gave equivalent, albeit modest efficacy (a ~0.5 $\log_{10}$ CFU decrease in lung bacterial burden, relative to the untreated control).

Phenotypic screening against *M. bovis* BCG rediscovered nitrophenanthroline **101** (**Figure 14**) as a useful hit (MIC_{99} 0.78 μM vs *Mtb* H37Rv; CC_{50} >25 μM vs THP-1 macrophages).[280] Mechanistic studies suggested that it may be activated by an F_{420}-dependent nitroreductase different to the one employed by drugs **2** and **3** to release nitrous acid. Mycolic acid biosynthesis was also inhibited, and there was an induction of autophagy in host macrophages that augmented *Mtb* killing. Interestingly,

metal chelation was not involved in the activity. An SAR study identified methyl derivative **102** (**Figure 14**) as the best lead, having an MIC_{99} value of 0.20 μM against *Mtb* H37Rv. This lead was further tested in a BALB/c mouse model of chronic *Mtb* infection, where oral dosing at 100 mg/kg for 4 weeks reduced the bacterial load in lungs by ~1.0 log_{10} CFU, compared to the untreated control.

Jin et al. (2020) reported thienothiazole amide derivative **104** (**Figure 15**) as an exciting new anti-TB lead, which they obtained by optimising the HTS hit **103** (**Figure 15**).[281] Compound **104** displayed good activity against *Mtb* H37Rv expressing green fluorescent protein (GFP), both in broth and in macrophages (MIC_{50} values 0.76 and 0.19 μM, respectively), and against a panel of MDR clinical isolates (MICs 2-4 μM). It also showed no cytotoxicity toward HepG2 cells (CC_{50} >50 μM) and modest inhibition of hERG (IC_{50} 28 μM) and CYPs 3A4, 2D6 and 2C9 (IC_{50}s ~7 μM). Lead **104** further exhibited high binding to human plasma proteins (99.8%) and better solubility at pH 2.1 than at pH 7.4 (90 vs 1.6 μM). Importantly, this molecule demonstrated an excellent mouse PK profile, with an oral half-life of 2.3 h, an oral bioavailability of 100%, and substantial accumulation in lung tissue over plasma (4.8:1). An *in vivo* efficacy study was conducted using the chronic *Mtb* infection model in BALB/c mice. Remarkably, oral dosing of **104** at 50 and 100 mg/kg for 4 weeks led to reductions in lung mycobacterial load of >2.0 and >4.5 log_{10} CFU, respectively, relative to the vehicle control. Based on these findings, **104** is now being evaluated as a possible future clinical candidate.

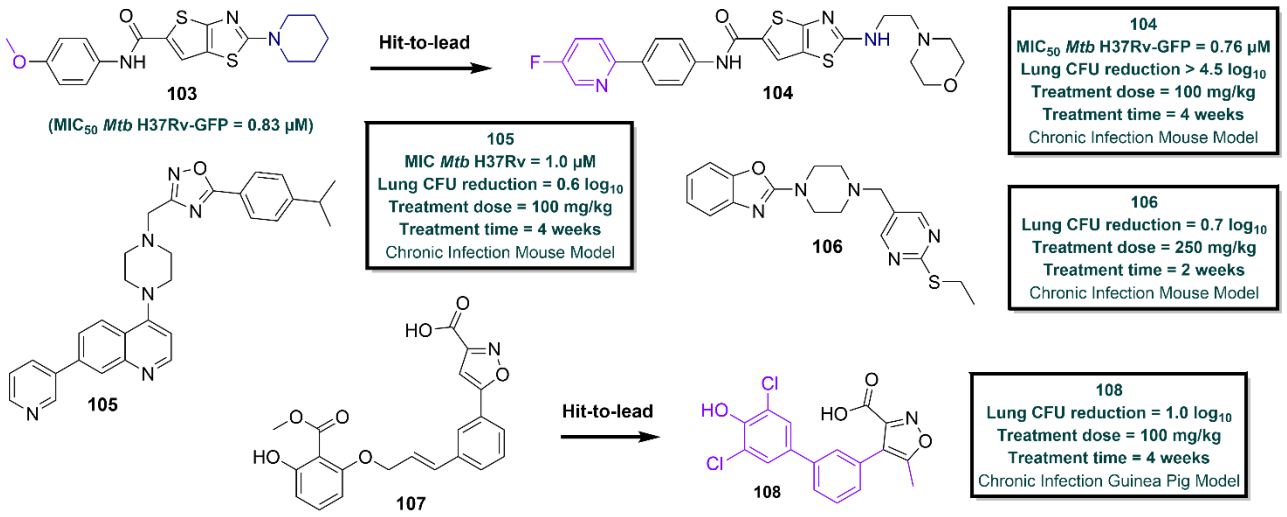

Figure 15. Thienothiazole **104**, quinoline **105**, benzoxazole **106**, and isoxazole **108** with *in vivo* anti-TB activity.

More recently, Kaur et al. disclosed further assessments of the preclinical lead FNDR-20081 (**105**) (Figure **15**), a quinoline derivative selected from their combinatorial synthesis-based SAR study.[282,283] This lead exhibited an MIC value of 1.0 μM against *Mtb* H37Rv but was not active against a panel of Gram-positive and Gram-negative bacteria (MICs >65 μM). Compound **105** had no toxic effects on HepG2 cells (CC_{50} >130 μM), did not inhibit CYP3A4 (IC_{50} >25 μM), and was moderately stable toward human but not mouse liver microsomes (40% and 1.2% parent remained after 1 h). However, a mouse PK study of **105** demonstrated adequate oral absorption and a half-life of 63 min,[283] justifying further *in vivo* assessment in a chronic *Mtb* infection BALB/c mouse experiment. Here, oral dosing of **105** at 100 mg/kg for 4 weeks led to a modest 0.6 $\log_{10}$ CFU decrease in lung bacterial burden, compared to the vehicle control.[282] Mode of action studies revealed that **105** did not target DprE1 and was unlikely to inhibit cell wall biosynthesis; resistant *Mtb* mutants instead mapped to a regulator of the efflux transporter MmpL5 (Rv0678) and a metallophosphoesterase (Rv3683).

Using a new strategy aimed at disrupting *Mtb* response to high chloride concentration (low pH), Lavin et al. identified the piperazinyl-benzoxazole **106** (**Figure 15**) as an *in vivo* active hit from a reporter-based library screen.[284] Compound **106** prevented *Mtb* growth in mouse macrophages (54% at 20 μM) and cholesterol media but not in standard media. It displayed no cytotoxicity to Vero cells (CC_{50} >141 μM) and minimal CYP inhibition (IC_{50}s >10 μM against five isoforms) but it did block hERG (IC_{50} 1.2 μM). This molecule also showed good aqueous solubility (76 μM), reasonable stability toward mouse liver microsomes ($t_{1/2}$ 49 min), and acceptable mouse plasma protein binding (97%). Furthermore, after oral administration to CD-1 mice, **106** exhibited high plasma exposure and an almost equivalent distribution into lung tissue, motivating an assessment of its *in vivo* efficacy. Two weeks of oral dosing with **106** at 250 mg/kg in an acute *Mtb* infection C3HeB/FeJ mouse model reduced the lung bacterial load by 0.9 $\log_{10}$ CFU, relative to the vehicle control. The compound was

slightly less effective in a chronic *Mtb* infection C3HeB/FeJ mouse experiment (using the same dose and schedule), giving a 0.7 $\log_{10}$ CFU decrease in lung burden, compared to the untreated control. Nevertheless, these data still provide an encouraging proof of concept for this drug discovery ploy.

Finally, another novel approach to tackle TB is to target secreted virulence factors that promote *Mtb* survival by undermining the host immune response in macrophages. In 2018, Vickers et al. reported isoxazole **108** (**Figure 15**) as an inhibitor of one such factor, *Mtb* protein tyrosine phosphatase B (MptpB), which dephosphorylates several critical host signalling molecules.[285] This lead resulted from structure-guided optimisation of a human phosphatase inhibitor hit, **107** (**Figure 15**). Isoxazole **108** displayed an IC_{50} of 3.0 μM against MptpB and did not inhibit two human counterparts, hPTP1B and hVHR (IC_{50}s >100 μM). This compound was non-cytotoxic to J774 cells (CC_{50} >500 μM) and selectively decreased *Mtb* survival inside human THP1 macrophages (dosing at 20 or 100 μM). Furthermore, lead **108** had suitable solubility (200 μM), high permeability, and a first-rate PK profile in guinea pigs (e.g., a half-life of 5.1 h and an oral bioavailability of 100%). In an acute *Mtb* infection guinea pig model, oral dosing of **108** at 100 mg/kg for 4 weeks (starting one day after infection) provided a bacterial burden reduction in the lungs of 0.9 $\log_{10}$ CFU, relative to the vehicle control. Similar dosing of **108** at 100 mg/kg for 4 weeks in a chronic *Mtb* infection guinea pig model also produced a lower lung bacterial load (by 1.0 $\log_{10}$ CFU, relative to the vehicle control). These results show that inhibition of MptpB can be a fruitful new strategy for TB therapy.

5. DISCUSSION AND PERSPECTIVE

The spread of COVID-19 has heavily impacted the diagnosis, reporting and treatment of TB in many high burden countries, and this is predicted to lead to a surge in DS-TB and MDR-TB cases.[10,286] To end the TB pandemic, the WHO has highlighted an urgent need to intensify research to identify and develop new drugs and drug regimens that can lead to treatment shortening.[10] However, based on recent clinical success rates for anti-infectives, less than one in six new chemical

entities will make it through from phase I trials to final marketing approval (although this increases to about one in four entities from phase II).[287] Given some redundancies in *Mtb* targets amongst new agents in the current global pipeline and the approved TB drugs, this suggests the requirement to bring at least 20 novel candidates to clinical assessment as soon as possible. These new candidates would ideally be bactericidal against both replicating and nonreplicating *Mtb*, potent against MDR- and XDR-TB, display sterilizing effects, have novel targets or mechanisms, be orally active with a suitable PK profile, able to be co-dosed with other TB or anti-HIV drugs, and show good safety.[45,288] Low cost and specificity for *Mtb* (to avoid microbiome imbalances) are also desirable attributes.

During the past six years, at least 62 new lead compounds have been reported that demonstrate significant *in vivo* efficacy (at least a 0.5 $\log_{10}$ CFU reduction in lung mycobacterial burden, relative to the untreated control) in an animal model of TB, mostly following oral administration. This testing mainly employed the *Mtb* H37Rv strain; rarely were compounds evaluated against drug-resistant strains. In more than 70% of examples, BALB/c mice were utilized (C57BL/6 mice were the primary alternative), typically for an acute infection model in which *Mtb* are rapidly multiplying. Exact protocols varied considerably, for example, between the 9-day rapid acute assay[167] (where mice were *Mtb*-infected by intratracheal delivery and dosing began one day post-infection), low dose aerosol models (commencing within a few days or up to 10 days post-infection), and high dose aerosol models (beginning after two weeks of infection).[289] Efficacy rankings for compounds in the rapid acute assay were reportedly consistent with the results from other early-phase *in vivo* experiments.[167] However, a histopathological analysis of the BALB/c mouse high dose aerosol method showed the presence of small inflammatory foci at the start of treatment, suggesting the prospect of more efficacy differences in this assay.[160] Varied PK and efficacy outcomes also resulted from changes to the oral formulation.

The acute model is viewed as an excellent initial screen to test for bactericidal activity *in vivo* but it does not predict effectiveness against the slowly growing or nonreplicating *Mtb* that are characteristic of established disease (chronic infection model).[289] However, only 22 compounds were assessed in the latter model, which is better at distinguishing sterilizing efficacy. Also, there were just

four instances of lead assessment in *Mtb*-infected C3HeB/FeJ mice or guinea pigs, in which the lung pathology features necrotic granulomas, a hallmark of TB in humans (together with cavitary lesions and fibrosis).[160,289] This is crucial because highly protein-bound lipophilic molecules, especially those with low solubility and more aromatic rings, typically bind strongly and do not diffuse well through caseum (the core necrotic material) to reach numerous persistent drug-tolerant mycobacteria.[290,291] Therefore, the efficacy of such compounds may be overestimated in models like BALB/c that fail to develop necrotic lesions.[289] Killing these caseum-resident persistent bacteria is also thought to be the key to achieving more rapid cures.[291] Nevertheless, the C3HeB/FeJ mouse model is more challenging to work with because three different categories of lesion develop, including the cellular, inflammatory kind seen in BALB/c mice and the caseous necrotic type.[292] Efficacy studies of TB drugs in this model often result in dichotomous CFU data that link to the presence (or not) of large necrotic granulomas in individual mice, and this high variability reduces the statistical power to distinguish between groups.[293] In the past decade, the lesion-specific distribution of several TB drugs (including RIF, INH, PZA, MOX, BDQ, and CFZ) has been quantified through MALDI-MS imaging.[47,290,294] To achieve better drug diffusion, a new design metric was introduced ("calculated intrinsic property forecast index"), in which caseum binding is proportional to ClogP plus the aromatic ring count.[290]

One question presented at the start of this review related to the number of new agents that were likely to reach clinical trials. To address this, we have summarised the major physicochemical, PK, and biological characteristics of the 39 most active lead candidates described in Section 4 (with $\log_{10}$ CFU counts of ≥1.5 in the acute model or ≥1.0 in the chronic model) in Table 3.

Table 3. Summary of physicochemical, PK, and biological data for the 39 most efficacious new leads (colour coding: green, compound identified as being in preclinical development; pale orange, data outside the recommended lead criteria; darker orange, data of potential concern for a lead candidate).

Cpd	MW	ClogP[a]	Aq. Sol. (μM)	MIC *Mtb* (μM)	CC_{50}[b] (μM)	hERG IC_{50} (μM)	CYP[c] IC_{50} (μM)	PPB[d] (%) M/H	*in vivo* $t_{1/2}$ (h)[e] M (R)	*in vivo* *F* (%)[f] M (R)	Log_{10} CFU Reduction (model)[g]
20	343.4	1.52	152	1.6	ND	>33	>50	ND/68	5.9	(100)	1.5 (B/c, Chr)
22	522.5	4.78	ND	<0.035	811[h]	<10	ND	ND	3.1	ND	3.2 (B/c, Ac)
23	572.5	5.27	ND	<0.028	>112[h]	ND	ND	ND	6.7	42	>5.0 (B/c, Ac)
24	499.5	3.70	ND	0.028	>128[h]	48	7.8	ND	4.9	37 (46)	1.8 (C3H, Chr)
25	433.4	1.74	<2.3	0.046	>231[h]	ND	>10	96/>99	2.5	(44)	3.4 (B/c, Ac)
26	455.5	5.49	<0.2	<0.035	>140	>30	>50	ND	7.3	13	5.4 (B/c, Ac)
29	467.6	2.20	160	0.6	50	ND	ND	ND	0.45	100	2.0 (C57, Ac)
30	469.6	1.14	≥364	1.7	32	ND	ND	ND	1.0	79	2.0 (C57, Ac)
34	376.4	2.55	ND	0.089	>100	>30	0.1	ND	ND	ND	>1.7 (B/c, Chr)
35	415.5	2.17	ND	0.29	>154	23	ND	ND	0.85	7.9	2.0 (B/c, Ac)
37	475.5	6.19	6.0	0.06	36	1.5, 10	ND	ND	3.2	55, 43	4.2 (C57, Ac)
42	332.4	5.74	ND	0.012	≥192[h]	>30	ND	97/ND	ND	22, 96	3.6 (B/c, Ac)
44	340.5	5.77	199	0.15	20	16	ND	ND/94	1.7	1.2	1.5 (C57, Ac)
45	407.5	5.61	152	0.3	32	6.3	ND	ND/96	ND	ND	1.5 (C57, Ac)
47	419.5	0.71	413	0.2	>50	>50	25	ND	0.94	92	3.0 (C57, Chr)
49	441.2	3.46	ND	0.09	>100	ND	ND	99/88	3.5	53	1.5 (C3H, Chr)
53	267.3	2.27	>550	0.8	>100	>50	13	77/92	0.33	92	2.4 (C57, Chr)
54	285.3	2.01	175	0.2	170[h]	>50	>50	63/77	ND	ND	>2.0 (B/c, Chr)

55	253.3	2.47	396	1.2	>100	>50	>20	ND	ND	ND	2.0 (B6, Ac)
57	380.4	2.98	74	0.13	>100	6.9, 21	4.2	73/72	1.0	28	1.9 (B/c, Chr)
58	408.5	1.54	ND	0.65	ND	>30	ND	ND	ND	ND	3.1 (C57, Ac)
59	365.4	4.11	ND	0.011	11[h]	ND	ND	ND	4.5	19	2.2 (B/c, Ac)
62	401.9	5.00	15	0.8	60	ND	ND	ND	ND	ND	4.0 (C57, Ac)
63	262.4	3.72	>3812	3.1	>30	>30	>30	ND	6.7	ND	>1.5 (B/c, Ac)
64	350.4	-8.73	>14000	7.1	ND	ND	ND	ND	0.29	ND	5.3 (B/c, Ac)
67	303.3	-2.95	ND	5.0	ND	ND	ND	ND	0.37	ND	1.7 (129, Ac)
73	294.2	-0.74	ND	1.7	>218	ND	ND	ND	ND	ND	1.7 (B/c, Ac)
75	502.1	8.32	ND	5.0	ND	ND	ND	ND	ND	ND	>1.5 (B/c, Ac)
77	417.3	3.95	ND	4.8	50	ND	0.6	ND	(1.1)	(14)	1.7 (B/c, Ac)
83	538.6	5.67	ND	0.011	>100	>30	>20	ND/100	(19)	(94)	3.9 (B/c, Ac)
91	486.5	6.74	ND	6.2	ND	ND	ND	ND	ND	ND	~1.5 (B/c, Ac)
92	381.4	0.75	ND	0.08	>168	>30	48	ND	15	56	≥3.0 (B/c, Chr)
93	408.3	2.26	ND	1.2	ND	ND	ND	ND/90	1.0	69	2.3 (B/c, Ac)
94	283.2	0.68	ND	1.1	16	ND	15	ND/54	ND	ND	>6.0 (B/c, Ac)
97	465.4	1.05	ND	1.6	30[i]	ND	ND	ND	ND	ND	>6.0 (B/c, Ac)
98	465.4	1.05	ND	1.0	43[i]	ND	ND	ND	ND	ND	>6.0 (B/c, Ac)
102	239.2	2.38	ND	0.20	ND	ND	ND	ND	ND	ND	~1.0 (B/c, Chr)
104	483.6	4.54	1.6	0.76	>50	28	6.9	>99/>99	2.3	100	>4.5 (B/c, Chr)
108	364.2	3.79	200	ND	>500[j]	ND	ND	ND	[5.1][k]	[100][k]	1.0 (G.P., Chr)[k]

[a]Calculated logP values from ChemDraw v19.1. [b]Cytotoxicity against HepG2 cells unless noted (ND means not disclosed). [c]Most potent activity amongst the CYP450 isozymes tested. [d]Percentage binding to mouse (M) or human (H) plasma proteins. [e]Half-life in mice (M) or rats (R). [f]Oral bioavailability in mice (M) or rats (R). [g]Mouse strain employed (B/c: BALB/c; C3H: C3HeB/FeJ; C57: C57BL/6; 129: 129sv) and whether acute or chronic *Mtb* infection. [h]Cytotoxicity against Vero cells. [i]Cytotoxicity against MRC-5 cells. [j]Cytotoxicity against J774A.1 cells. [k]Data for guinea pigs.

According to the latest WGND pipeline update,[75] three highlighted compounds in Table 3, β-lactam antibiotic sanfetrinem (**67**), QcrB inhibitor TB47 (**83**), and sutezolid derivative OTB-658 (**92**), as well as the quinoline FNDR-20081 (**105**), are in late-stage preclinical development and appear likely to commence clinical studies soon. A fifth compound, new TrpAB inhibitor GSK839 (**109**) (**Figure 16**) that exhibits an MIC value of 0.07 μM against *Mtb* H37Rv,[295] has also been in GLP toxicology studies during 2021, but no additional information is available on this molecule. A further two highlighted compounds in Table 3, covalent DprE1 inhibitor TZY-5-84 (**24**) and KasA inhibitor JSF-3285 (**54**), are listed in this pipeline update as being in early-stage preclinical development, together with benzothiopyranone NTB-3119 (probably **26**, which had initially been selected as a potential clinical candidate by the Institute of Materia Medica in China[164,296]). As well as this, two other preclinical leads, MmpL3 inhibitors MPL-446 and MPL-447 (TB Alliance and Innovative Medicines Initiative), have reportedly commenced safety studies.[297] The TB Alliance discovery pipeline[298] indicates that two MmpL3 inhibitors from the indole-carboxamide class are under safety evaluation (possibly **40** and **42**,[180] although this has yet to be confirmed).

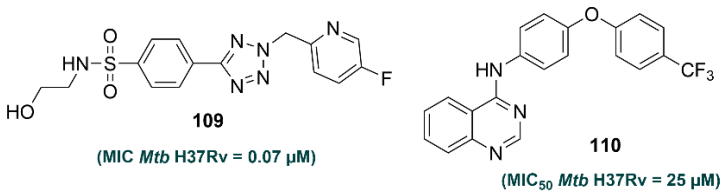

Figure 16. TrpAB inhibitor **109** and cytochrome *bd* inhibitor **110**.

Conversely, the development prospects of a few compounds in Table 3 (e.g., **22**, **29**, **34**, **35**, **37**, **44**, **45**, **53**, **57**, **75**, **77**, **94**, **97**, and **98**) appear to have been diminished by the identification of certain liabilities, e.g., high lipophilicity, cytotoxicity, unfavourable CYP450 or hERG inhibition, suboptimal PK, or chemical stability issues. Various selection criteria have been proposed for TB leads, starting with an MIC value of <1 μM against *Mtb* H37Rv,[299] a CC_{50} value of >20 μM (or SI >20) for cytotoxicity, a hERG IC_{50} value of >30 μM (or SI >100), CYP IC_{50} values >20 μM, and a ≥1.0 $\log_{10}$ CFU reduction in lung mycobacterial burden (relative to the untreated control).[60,300] Other recommendations for infectious disease leads include a logP <5 (preferably <3), solubility at pH 7.4 of >10 μM (or >25 μM[300]), an oral half-life of >2 h, and an oral bioavailability of >25% in mice.[299] It is also worth noting that high PPB and low distribution into lung tissue may limit *in vivo* efficacy. Overall, while strong *in vitro* potency is important, drug experts have argued that this should not be "at the expense of poor physicochemical properties or drug metabolism and PK characteristics".[299] Lipinski's rule of five and Veber's rule around restricting the number of rotatable bonds (<10) and polar surface area (<140 $Å^2$) to achieve good oral bioavailability are often cited in this context.[61,301]

However, one of the peculiarities experienced with lead optimisation of compounds against *Mtb* is that there is generally no correlation between *in vivo* PK and efficacy.[60,301] Candidates with superior *in vivo* efficacy tend to be the exceptions amongst a much larger set of potent analogues, constrained

by only modest PK boundaries, and specific substituents (e.g., 4-OCF_3Ph) may have an extraordinary influence.[302] Furthermore, better *in vitro* potency and *in vivo* efficacy often correlate with higher logP, but excessive lipophilicity negatively impacts solubility and PK and leads to increased toxicity risks; it also results in challenging formulation and drug development hurdles.[60] Metrics like lipophilic efficiency[303] can be helpful as monitoring tools, while *in vitro* microsomal stability testing is frequently employed as an initial screen for metabolism liabilities.[191,300] Nevertheless, agents like BDQ (**1**), delamanid (**2**), SQ109 (**4**), Q203 (**7**), macozinone (**8**), CFZ, TBI-166 (**11**), TBAJ-876 (**16**) and TBAJ-587 (**17**) all have ClogP values in the range of 5 to 8.[61] No drug is perfect and, for transformational agents like BDQ (ClogP 7.25, with a hERG IC_{50} of 1.6 μM[121]), some specific liabilities have been successfully managed at a clinical level. Unfortunately, profiling data on many leads in Table 3 are incomplete (particularly for solubility, hERG and CYP inhibition, and plasma protein binding). However, pending acceptable results, six or seven compounds not already listed in the WGND pipeline update may be worth considering for preclinical development.[304]

Aside from physicochemical, PK and biological properties, commercial factors such as financial resource, timing, and clinical opportunity (versus risk) may also play a major role in deciding which compounds are advanced. For example, MicuRx Pharmaceutical Co. is reportedly focussed solely on the global development of safer LZD analogue contezolid (MRX-I, **93**) against MDR Gram-positive bacterial infections, and has no plans to extend this to TB.[78,270] The current clinical pipeline for TB already includes three oxazolidinones; likewise, there are four DprE1 inhibitors in clinical studies at present, including OPC-167832 (**12**), which was a standout performer *in vivo*. This scenario raises the bar for the advancement of any more DprE1 inhibitors (e.g., **24** or **26**), due to the enormous costs of clinical trials. While an element of competition with “me-too” molecules seems inevitable, ideally,

the focus should be on advancing efficacious leads from novel chemical classes with new mechanisms of action that could contribute greater diversity to future drug regimens against MDR-TB.[64,72]

The success of discovering new agents to tackle TB depends on the generation and selection of high-quality starting hits, ideally acting against novel but essential *Mtb* targets.[45] In this context, acknowledgment should first be made of GSK's efforts to stimulate open-source lead development by publicly disclosing two large sets of small molecule HTS hits with unknown targets (these all had *Mtb* MICs <10 μM and low cytotoxicities against HepG2 cells, giving SI >50 for the main set).[191,305] One of the new hit generation strategies to circumvent the weaknesses of target-based and phenotypic screening methods is target-based whole-cell screening.[45,72] This typically involves phenotypic HTS of compound libraries against *Mtb* strains that have been genetically altered to either overexpress or deplete the target, thus desensitizing or sensitizing them to an inhibitor of that target (causing an MIC shift, relative to wild-type *Mtb*). Other options include developing cellular assays for a target-specific enzyme activity. An innovative large-scale strategy named PROSPECT[73] involves screening chemical libraries against pools of 100-150 barcoded mutant strains, each with a critical target depleted, and deconvoluting the resulting complex "chemical-genetic interaction profiles". This method gave tenfold more hits than using wild-type *Mtb*.

In regard to identifying the best new targets for these novel screening approaches to TB drug discovery, two recent studies using CRISPR interference methods to tune individual gene expression have provided unique insights into the relative vulnerabilities of the essential genes in *Mtb*.[306,307] Within the cell wall biosynthesis class, those genes associated with mycolic acid synthesis were the most vulnerable, with inhibition being strongly bactericidal; *dprE1* was also very susceptible but its inhibition was less bactericidal. Similarly, central process genes for transcription, protein translation

(including tRNA synthetases), DNA gyrase, protein folding, metabolism, and cell division enzymes were highly vulnerable, and their inhibition was strongly bactericidal. Conversely, amino acid biosynthesis and metabolism and oxidative phosphorylation genes were less vulnerable, with inhibition being mainly bacteriostatic, except for *glcB* (malate synthase), *ndh* (NDH-2) and *atpE* (ATP synthase). Intriguingly, a similar analysis[306] using the extremely virulent *Mtb* clinical strain HN878 was generally very consistent with the above trends in H37Rv, but oxidative phosphorylation genes, including *qcrB*, were much more vulnerable and DNA replication (*gyrAB*) was less vulnerable, suggesting the importance of studying additional clinical strains and alternative growth conditions. Therefore, a key priority might be the development of a suitable cytochrome *bd* oxidase inhibitor, as the combination with cytochrome *bcc* inhibitors like Q203 (**7**) should be particularly potent.[96] This has already been shown *in vivo* with a hit compound, ND-011992 (**110**) (**Figure 16**), and Q203.[96] Overall, many still unexploited highly vulnerable targets have now been identified, whose inhibition may induce lower rates of *Mtb* resistance, providing renewed impetus for TB drug discovery.[306]

6. FINAL REMARKS

At the start of this review, we observed that despite increased global efforts in which hundreds of potent and selective small molecules are reported annually as promising agents against TB, few of those compounds ever reach clinical studies. Also, in the last 50 years, only three new TB drugs have been approved. This scenario may be explained by the many challenges encountered in developing a sufficiently efficacious and non-toxic drug candidate with a suitable PK profile and, ideally, a novel mechanism that can be used to treat DS-, MDR- and XDR-TB.[32] The difficulties involving the translational science of converting basic scientific research into clinical research to create new drugs

are acknowledged both in academia and the pharmaceutical industry.[308] Issues can also arise during the late-stage clinical development of a new TB drug, such as how to demonstrate both safety and superior efficacy for a single drug within the context of a novel combination regimen, especially given the better results seen for standard treatment of MDR-TB within the latest WHO guidelines.[54] This may lead to a greater clinical focus on proving "noninferiority" but with treatment shortening.

This review highlights the state-of-the-art regarding small molecules reported in the last six years as potent anti-TB agents that achieved either preclinical development status or could be termed "validated leads" with significant *in vivo* efficacy. For added interest, we included a few *in vivo* active hits; some other compounds are still in the hit-to-lead stage or require further lead optimisation. Encouragingly, several molecules have shown remarkable outcomes and may be suitable for preclinical testing if there are no serious liabilities. Inadequate PK and toxicological profiles can be a bottleneck in preclinical development, and it is not uncommon for *in vivo* active candidates to be abandoned due to PK or toxicity concerns, given the requirement for lengthy treatment times in multi-drug regimens to achieve complete cures. Hence, it is crucial to address such issues and to identify and reduce the likelihood of drug-drug interactions as much as possible during lead optimisation.

However, despite considerable challenges, there have been many recent advancements in the past few years that afford a positive outlook for the future of TB drug discovery. New international consortia are emerging to accelerate the clinical evaluation of new TB drug candidates and drug combinations. There are now 17 compounds in clinical trials for TB, including 10 in phase II, several of which feature new scaffolds and novel targets or mechanisms of action. The number of potential new entrants to the pipeline is building in preclinical development and the identification of a larger pool of novel molecules with good *in vivo* efficacy should ensure that this continues to grow at a faster rate. Investigations into the possibility of repurposing other drugs or drug candidates for TB have unearthed some promising options, e.g., biapenem (**64**), sanfetrinem (**67**), and contezolid (**93**). Innovations in screening, including within infected macrophages or under various stress conditions, are driving the discovery of novel inhibitors for both new and old targets, while efforts are increasing

to verify better which of the latter are both essential and highly vulnerable. Innovative strategies, such as disrupting *Mtb* response to environmental changes or targeting virulence factors, are showing significant promise. Additional advances, such as a better understanding of the complex biology and the development of better mouse models and imaging technologies, are assisting discovery efforts.

Finally, it is worth acknowledging the efforts that partnerships between academia and pharmaceutical companies have achieved in the last few years in TB drug discovery, notably GSK's "Tres Cantos Open Lab for R&D for Diseases of the Developing World", which contributed to the development of some compounds presented here. Likewise, the TB Alliance (and partners) have especially made a massive contribution over two decades to all sections of the TB drug pipeline and spearheaded a recent paradigm shift by focusing late-stage clinical development on new drug combinations (identified *in vivo*), seeking to fast-track the introduction of novel curative treatments. We believe that this review will also bring a fresh perspective into the TB drug discovery landscape and be a ray of hope for those developing better therapeutic alternatives for the treatment of TB.

AUTHOR INFORMATION

Corresponding Authors

Andrew Mark Thompson - Auckland Cancer Society Research Centre, Faculty of Medical and Health Sciences, The University of Auckland, Auckland, 1142, New Zealand; orcid.org/0000-0003-2593-8559; Email: am.thompson@auckland.ac.nz

Guilherme Felipe Santos Fernandes - Department of Chemistry, University College London, 20 Gordon Street, London WC1H 0AJ, United Kingdom; orcid.org/0000-0002-7644-5466; Email: guilherme.fernandes@ucl.ac.uk

Jean Leandro Dos Santos - São Paulo State University (UNESP), School of Pharmaceutical Sciences, Araraquara, 14800903, Brazil; orcid.org/0000-0002-2460-2829; Email: jean.santos@unesp.br

Authors

Daniele Castagnolo - Department of Chemistry, University College London, 20 Gordon Street, London WC1H 0AJ, United Kingdom; orcid.org/0000-0002-7517-5732; Email: d.castagnolo@ucl.ac.uk

William Alexander Denny - Auckland Cancer Society Research Centre, Faculty of Medical and Health Sciences, The University of Auckland, Auckland, 1142, New Zealand; orcid.org/0000-0001-7997-1843; Email: b.denny@auckland.ac.nz

Complete contact information is available at:
https://pubs.acs.org/

Author Contributions

[#]G.F.S.F. and A.M.T. contributed equally.

Notes

The authors declare no competing financial interest.

Biographies

Guilherme Felipe Santos Fernandes received his master's degree in Pharmaceutical Chemistry (2016) and PhD in Medicinal Chemistry (2021) from the São Paulo State University, Brazil under the supervision of Prof. Jean Leandro Dos Santos. During 2015, he was a visiting master student at the University of Navarra, Spain, in the group of Prof. Silvia Pérez Silanes. Throughout 2019, he was a visiting PhD student at the Auckland Cancer Society Research Centre, University of Auckland, New Zealand, under the mentorship of Distinguished Professor William Alexander Denny (Bill).

Currently, Guilherme is a Marie Skłodowska-Curie Research Fellow at the University College London with Dr Daniele Castagnolo. His research interests centre on the design, synthesis, and discovery of novel antimicrobial agents, particularly antitubercular small molecules.

Andrew Mark Thompson is a Senior Research Fellow at the Auckland Cancer Society Research Centre, University of Auckland, New Zealand, where he has been involved in or led numerous drug discovery projects. He obtained his PhD (1991) in marine natural products chemistry from the University of Canterbury, New Zealand. As a research chemist, his early interests (in partnership with Pfizer Global Research and Development) focused on kinase inhibitors for cancer and then inhibitors of DNA gyrase as potential antibacterial agents. Since 2005, his research has centered on the design and synthesis of potential new drugs for tuberculosis and neglected tropical diseases, especially pretomanid derivatives (e.g., DNDI-0690, developed in collaboration with the Global Alliance for TB Drug Development and the Drugs for Neglected Diseases *initiative*).

Daniele Castagnolo obtained his master's degree and PhD (2006) in Pharmaceutical Chemistry at the University of Siena, under the guidance of Prof. Maurizio Botta. He carried out his postdoctoral studies at the Helsinki University of Technology in the group of Prof. Petri Pihko, then at the University of Siena as Research Fellow, and finally at the University of Manchester with Prof. Jonathan Clayden. He began his independent research at Northumbria University Newcastle before relocating to King's College London. In January 2022, he joined University College London as Associate Professor in chemical sustainability. His research interests are focused on the synthesis and discovery of new antimicrobial agents, particularly antitubercular molecules, and developing green and sustainable approaches for the synthesis of drug-like compounds.

William Alexander Denny (Bill) is a Distinguished Professor at the Auckland Cancer Society Research Centre, University of Auckland, New Zealand, where he was Director from 1981-2020. His

research interests comprise the design and development of drugs for cancer (major themes being kinase inhibitors, DNA binding agents, hypoxia-activated prodrugs) and infectious diseases (primary focus being electron transport chain inhibitors for TB). This work, carried out in conjunction with many academic and commercial collaborators, has been reported in 733 papers and 76 granted patent families, and has resulted in 15 drugs brought to clinical trials. Awards include the ACS Medicinal Chemistry Award, the Royal Australian Chemical Institute Adrien Albert Award, the UK Royal Society of Chemistry Adrien Albert Medal, and the University of Auckland Vice-Chancellor's Commercialisation Medal.

Jean Leandro Dos Santos received his master's (2007) and PhD (2009) degrees in Pharmaceutical Chemistry from the São Paulo State University, Brazil. Currently an Associate Professor for the School of Pharmaceutical Science, he was also visiting professor at the Università degli Studi di Torino (Turin, Italy). He carried out his postdoctoral studies (2015) at the University of Minnesota in the research group of Prof. Gunda Georg. His research interests are focused on the drug design of antimicrobial compounds and bioactive agents for hemoglobinopathies.

ACKNOWLEDGMENTS

This investigation has received financial assistance from the European Union's Horizon 2020 research and innovation programme under the Marie Skłodowska-Curie grant agreement (No 101027065) as well as from the Health Research Council of New Zealand (19/259, subaward 5000701). It was also funded by Fundação de Amparo à Pesquisa do Estado de São Paulo (FAPESP grants 2016/09502-7; 2018/17739-2; 2018/11079-0; 2020/13279-7) and Programa de Apoio ao Desenvolvimento Científico da Faculdade de Ciências Farmacêuticas da UNESP-PADC.

ABBREVIATIONS USED

TB, tuberculosis; *Mtb*, *Mycobacterium tuberculosis*; HIV, Human Immunodeficiency Virus; WHO, World Health Organization; MDR-TB, multidrug-resistant tuberculosis; RIF, rifampicin; INH, isoniazid; XDR-TB, extensively drug-resistant tuberculosis; TDR-TB, totally drug-resistant tuberculosis; BDQ, bedaquiline; FDA, Food and Drug Administration; EMA, European Medicines Agency; LZD, linezolid; EBA, early bactericidal activity; MFX, moxifloxacin; UN, United Nations; NIH, National Institutes of Health; PK, pharmacokinetic; DS-TB, drug-susceptible tuberculosis; PZA, pyrazinamide; EMB, ethambutol; WGND, Working Group for New TB Drugs; HTS, high-throughput screening; CFZ, clofazimine; CFU, colony-forming units; BTZ, benzothiazinone; DprE1, decaprenylphosphoryl-β-D-ribose 2'-epimerase; LeuRS, leucyl-tRNA synthetase; ROS, reactive oxygen species; NDH-2, type II NADH dehydrogenase; GSK, GlaxoSmithKline; ETH, ethionamide; DPA, decaprenylphosphoryl-D-arabinose; SI, selectivity index; FAS-II, type II fatty acid synthase; KasA, β-ketoacyl-ACP synthase I; Pks13, polyketide synthase 13; PptT, phosphopantetheinyl transferase; ACP, acyl carrier protein; Ppt, 4′-phosphopantetheine; CoA, coenzyme A; DdlA, D-Alanine-D-alanine ligase A; TrpAB, tryptophan synthase; ASADH, aspartate semialdehyde dehydrogenase; DHFR, dihydrofolate reductase; RLU, relative light units; SD, shikimate dehydrogenase; STPK, Ser/Thr protein kinase; PknD, protein kinase D; PknG, protein kinase G; BCG, Bacillus Calmette-Guérin; PMF, proton motive force; ABT, 1-aminobenzotriazole; GFP, green fluorescent protein; MptpB, *Mtb* protein tyrosine phosphatase B.

REFERENCES

(1) Daniel, T. M. The History of Tuberculosis. *Respir. Med.* **2006**, *100*, 1862–1870.

(2) Barberis, I.; Bragazzi, N. L.; Galluzzo, L.; Martini, M. The History of Tuberculosis: From the First Historical Records to the Isolation of Koch's Bacillus. *J. Prev. Med. Hyg.* **2017**, *58* (1), E9–E12.

(3) Paulson, T. Epidemiology: A Mortal Foe. *Nature* **2013**, *502* (7470), S2-S3.

(4) Public Health Online. *History's Worst Global Pandemics*. 2021. https://www.publichealthonline.org/worst-global-pandemics-in-history/ (accessed October 13, 2021).

(5) Hershkovitz, I.; Donoghue, H. D.; Minnikin, D. E.; Besra, G. S.; Lee, O. Y.-C.; Gernaey, A. M.; Galili, E.; Eshed, V.; Greenblatt, C. L.; Lemma, E.; Bar-Gal, G. K.; Spigelman, M. Detection and Molecular Characterization of 9000-Year-Old *Mycobacterium tuberculosis* From a Neolithic Settlement in the Eastern Mediterranean. *PLoS One* **2008**, *3* (10), e3426.

(6) Kapur, V.; Whittam, T. S.; Musser, J. M. Is *Mycobacterium tuberculosis* 15,000 Years Old? *J. Infect. Dis.* **1994**, *170*, 1348-1349.

(7) Hayman, J. Mycobacterium Ulcerans: An Infection From Jurassic Time? *Lancet* **1984**, *324*, 1015–1016.

(8) World Health Organization. *Global Tuberculosis Report 2017*; Geneva, 2017; p 5.

(9) World Health Organization. *Global Tuberculosis Report 2020*; Geneva, 2020.

(10) World Health Organization. *Global Tuberculosis Report 2021*; Geneva, 2021; pp 1-27.

(11) World Health Organization. WHO Coronavirus (COVID-19) Dashboard. https://covid19.who.int.

(12) Maitre, T.; Aubry, A.; Jarlier, V.; Robert, J.; Veziris, N.; on behalf of the CNR-MyRMA; Bernard, C.; Sougakoff, W.; Brossier, F.; Cambau, E.; Mougari, F.; Raskine, L. Multidrug and Extensively Drug-Resistant Tuberculosis. *Med. Mal. Infect.* **2017**, *47*, 3-10.

(13) Lange, C.; Dheda, K.; Chesov, D.; Mandalakas, A. M.; Udwadia, Z.; Horsburgh, C. R., Jr. Management of Drug-Resistant Tuberculosis. *Lancet* **2019**, *394*, 953-966.

(14) World Health Organization. *WHO Announces Updated Definitions of Extensively Drug-Resistant Tuberculosis.* January 27, 2021. https://www.who.int/news/item/27-01-2021-who-announces-updated-definitions-of-extensively-drug-resistant-tuberculosis#:~:text=The%20definition%20of%20extensively%20drug,of%20these%20forms%20of%20TB (accessed October 13, 2021).

(15) Klopper, M.; Warren, R. M.; Hayes, C.; Gey van Pittius, N. C.; Streicher, E. M.; Muller, B.; Sirgel, F. A.; Chabula-Nxiweni, M.; Hoosain, E.; Coetzee, G.; van Helden, P. D.; Victor, T. C.; Trollip, A. P. Emergence and Spread of Extensively and Totally Drug-Resistant Tuberculosis, South Africa. *Emerg. Infect. Dis.* **2013**, *19*, 449–455.

(16) Parida, S. K.; Axelsson-Robertson, R.; Rao, M. V; Singh, N.; Master, I.; Lutckii, A.; Keshavjee, S.; Andersson, J.; Zumla, A.; Maeurer, M. Totally Drug-Resistant Tuberculosis and Adjunct Therapies. *J. Intern. Med.* **2015**, *277*, 388–405.

(17) Dheda, K.; Gumbo, T.; Maartens, G.; Dooley, K. E.; McNerney, R.; Murray, M.; Furin, J.; Nardell, E. A.; London, L.; Lessem, E.; Theron, G.; van Helden, P.; Niemann, S.; Merker, M.; Dowdy, D.; Van Rie, A.; Siu, G. K. H.; Pasipanodya, J. G.; Rodrigues, C.; Clark, T. G.; Sirgel, F. A.; Esmail, A.; Lin, H.-H.; Atre, S. R.; Schaaf, H. S.; Chang, K. C.; Lange, C.; Nahid, P.; Udwadia, Z. F.; Horsburgh, C. R., Jr.; Churchyard, G. J.; Menzies, D.; Hesseling, A. C.; Nuermberger, E.; McIlleron, H.; Fennelly, K. P.; Goemaere, E.; Jaramillo, E.; Low, M.; Jara, C. M.; Padayatchi, N.; Warren, R. M. The Epidemiology, Pathogenesis, Transmission, Diagnosis, and Management of Multidrug-Resistant, Extensively Drug-Resistant, and Incurable Tuberculosis. *Lancet Respir. Med.* **2017**, *5*, 291–360.

(18) Dheda, K.; Limberis, J. D.; Pietersen, E.; Phelan, J.; Esmail, A.; Lesosky, M.; Fennelly, K. P.; te Riele, J.; Mastrapa, B.; Streicher, E. M.; Dolby, T.; Abdallah, A. M.; Ben-Rached, F.; Simpson, J.; Smith, L.; Gumbo, T.; van Helden, P.; Sirgel, F. A.; McNerney, R.; Theron, G.; Pain, A.; Clark, T. G.; Warren, R. M. Outcomes, Infectiousness, and Transmission Dynamics of Patients With Extensively Drug-Resistant Tuberculosis and Home-Discharged Patients With Programmatically Incurable Tuberculosis: a Prospective Cohort Study. *Lancet Respir. Med.* **2017**, *5*, 269-281.

(19) Hoffmann, H.; Kohl, T. A.; Hofmann-Thiel, S.; Merker, M.; Beckert, P.; Jaton, K.; Nedialkova, L.; Sahalchyk, E.; Rothe, T.; Keller, P. M.; Niemann, S. Delamanid and Bedaquiline Resistance in *Mycobacterium tuberculosis* Ancestral Beijing Genotype Causing Extensively Drug-Resistant Tuberculosis in a Tibetan Refugee. *Am. J. Respir. Crit. Care Med.* **2016**, *193*, 337-340.

(20) Yoshiyama, T.; Takaki, A.; Aono, A.; Mitarai, S.; Okumura, M.; Ohta, K.; Kato, S. Multidrug Resistant Tuberculosis With Simultaneously Acquired Drug Resistance to Bedaquiline and Delamanid. *Clin. Infect. Dis.* **2021**, *73*, 2329-2331.

(21) Andries, K.; Verhasselt, P.; Guillemont, J.; Göhlmann, H. W. H.; Neefs, J.-M.; Winkler, H.; Van Gestel, J.; Timmerman, P.; Zhu, M.; Lee, E.; Williams, P.; de Chaffoy, D.; Huitric, E.; Hoffner, S.; Cambau, E.; Truffot-Pernot, C.; Lounis, N.; Jarlier, V. A Diarylquinoline Drug Active on the ATP Synthase of *Mycobacterium tuberculosis*. *Science* **2005**, *307*, 223–227.

(22) Kakkar, A. K.; Dahiya, N. Bedaquiline for the Treatment of Resistant Tuberculosis: Promises and Pitfalls. *Tuberculosis* **2014**, *94*, 357–362.

(23) Guo, H.; Courbon, G. M.; Bueler, S. A.; Mai, J.; Liu, J.; Rubinstein, J. L. Structure of Mycobacterial ATP Synthase Bound to the Tuberculosis Drug Bedaquiline. *Nature* **2021**, *589*, 143-147.

(24) Ryan, N. J.; Lo, J. H. Delamanid: First Global Approval. *Drugs* **2014**, *74*, 1041-1045.

(25) Keam, S. J. Pretomanid: First Approval. *Drugs* **2019**, *79*, 1797–1803.

(26) Matsumoto, M.; Hashizume, H.; Tomishige, T.; Kawasaki, M.; Tsubouchi, H.; Sasaki, H.; Shimokawa, Y.; Komatsu, M. OPC-67683, a Nitro-Dihydro-Imidazooxazole Derivative With Promising Action Against Tuberculosis In Vitro and In Mice. *PLoS Med.* **2006**, *3* (11), e466.

(27) Manjunatha, U.; Boshoff, H. I.; Barry, C. E. The Mechanism of Action of PA-824. *Commun. Integr. Biol.* **2009**, *2*, 215–218.

(28) Van den Bossche, A.; Varet, H.; Sury, A.; Sismeiro, O.; Legendre, R.; Coppee, J.-Y.; Mathys, V.; Ceyssens, P.-J. Transcriptional Profiling of a Laboratory and Clinical *Mycobacterium tuberculosis* Strain Suggests Respiratory Poisoning Upon Exposure to Delamanid. *Tuberculosis* **2019**, *117*, 18-23.

(29) Hayashi, M.; Nishiyama, A.; Kitamoto, R.; Tateishi, Y.; Osada-Oka, M.; Nishiuchi, Y.; Kaboso, S. A.; Chen, X.; Fujiwara, M.; Inoue, Y.; Kawano, Y.; Kawasaki, M.; Abe, T.; Sato, T.; Kaneko, K.; Itoh, K.; Matsumoto, S.; Matsumoto, M. Adduct Formation of Delamanid With NAD in Mycobacteria. *Antimicrob. Agents Chemother.* **2020**, *64* (5), e01755-19.

(30) Diacon, A. H.; Donald, P. R. The Early Bactericidal Activity of Antituberculosis Drugs. *Expert Rev. Anti Infect. Ther.* **2014**, *12*, 223-237.

(31) Médecins Sans Frontières. *Clinical Trial Results Offer Hope to DR-TB Patients With Short, Effective Treatment.* October 20, 2021. https://www.msf.org/clinical-trial-finds-short-effective-safe-DR-TB-treatment (accessed November 19, 2021).

(32) Dos Santos Fernandes, G. F.; Jornada, D. H.; de Souza, P. C.; Chin, C. M.; Pavan, F. R.; Dos Santos, J. L. Current Advances in Antitubercular Drug Discovery: Potent Prototypes and New Targets. *Curr. Med. Chem.* **2015**, *22*, 3133–3161.

(33) Policy Cures Research 2020 G-FINDER Report. *Neglected Disease Research and Development: Where to Now?* Sydney, 2021.

(34) Treatment Action Group. *Tuberculosis Research Funding Trends, 2005-2019*; New York City, 2020.

(35) United Nations General Assembly. *Political Declaration of the High-Level Meeting of the General Assembly on the Fight Against Tuberculosis. Resolution Adopted by the General Assembly on 10 October 2018*; New York City, 2018. https://www.un.org/en/ga/search/view_doc.asp?symbol=A/RES/73/3 (accessed October 13, 2021).

(36) Stop TB Partnership. *The Paradigm Shift: Global Plan to End TB 2018-2022*; Geneva, 2019.

(37) Riccardi, G.; Old, I. G.; Ekins, S. Raising Awareness of the Importance of Funding for Tuberculosis Small-Molecule Research. *Drug Discov. Today* **2017**, *22*, 487–491.

(38) Cole, S. T. Tuberculosis Drug Discovery Needs Public-Private Consortia. *Drug Discov. Today* **2017**, *22*, 477–478.

(39) *Tackling Drug-Resistant Infections Globally: Final Report and Recommendations. The Review on Antimicrobial Resistance Chaired by Jim O'Neill*; London: Wellcome Trust, HM Government, 2016.

(40) Pai, M.; Behr, M. A.; Dowdy, D.; Dheda, K.; Divangahi, M.; Boehme, C. C.; Ginsberg, A.; Swaminathan, S.; Spigelman, M.; Getahun, H.; Menzies, D.; Raviglione, M. Tuberculosis. *Nat. Rev. Dis. Primers* **2016**, *2*, 16076.

(41) Kumar, A.; Chettiar, S.; Parish, T. Current Challenges in Drug Discovery for Tuberculosis. *Expert Opin. Drug Discov.* **2017**, *12*, 1–4.

(42) Grzelak, E. M.; Choules, M. P.; Gao, W.; Cai, G.; Wan, B.; Wang, Y.; McAlpine, J. B.; Cheng, J.; Jin, Y.; Lee, H.; Suh, J.-W.; Pauli, G. F.; Franzblau, S. G.; Jaki, B. U.; Cho, S. Strategies in Anti-*Mycobacterium tuberculosis* Drug Discovery Based on Phenotypic Screening. *J. Antibiot. (Tokyo)* **2019**, *72*, 719–728.

(43) Queval, C. J.; Brosch, R.; Simeone, R. The Macrophage: A Disputed Fortress in the Battle Against *Mycobacterium tuberculosis*. *Front. Microbiol.* **2017**, *8*, 2284.

(44) Ehrt, S.; Schnappinger, D. Mycobacterial Survival Strategies in the Phagosome: Defence Against Host Stresses. *Cell. Microbiol.* **2009**, *11*, 1170–1178.

(45) Yuan, T.; Sampson, N. S. Hit Generation in TB Drug Discovery: From Genome to Granuloma. *Chem. Rev.* **2018**, *118*, 1887–1916.

(46) Zuniga, E. S.; Early, J.; Parish, T. The Future for Early-Stage Tuberculosis Drug Discovery. *Future Microbiol.* **2015**, *10*, 217–229.

(47) Dartois, V. The Path of Anti-Tuberculosis Drugs: From Blood to Lesions to Mycobacterial Cells. *Nat. Rev. Microbiol.* **2014**, *12*, 159-167.

(48) da Silva, P. E. A.; Von Groll, A.; Martin, A.; Palomino, J. C. Efflux as a Mechanism for Drug Resistance in *Mycobacterium tuberculosis*. *FEMS Immunol. Med. Microbiol*. **2011**, *63*, 1–9.

(49) Balganesh, M.; Dinesh, N.; Sharma, S.; Kuruppath, S.; Nair, A. V.; Sharma, U. Efflux Pumps of *Mycobacterium tuberculosis* Play a Significant Role in Antituberculosis Activity of Potential Drug Candidates. *Antimicrob. Agents Chemother.* **2012**, *56*, 2643–2651.

(50) Tiemersma, E. W.; van der Werf, M. J.; Borgdorff, M. W.; Williams, B. G.; Nagelkerke, N. J. D. Natural History of Tuberculosis: Duration and Fatality of Untreated Pulmonary Tuberculosis in HIV Negative Patients: A Systematic Review. *PLoS One* **2011**, *6* (4), e17601.

(51) Zumla, A.; Nahid, P.; Cole, S. T. Advances in the Development of New Tuberculosis Drugs and Treatment Regimens. *Nat. Rev. Drug Discov.* **2013**, *12*, 388–404.

(52) World Health Organization. *WHO Consolidated Guidelines on Drug-Resistant Tuberculosis Treatment*; Geneva, 2019.

(53) World Health Organization. *WHO Consolidated Guidelines on Tuberculosis. Module 4: Treatment – Drug-Resistant Tuberculosis Treatment.* Geneva, 2020.

(54) Ginsberg, A. M.; Spigelman, M. Challenges in Tuberculosis Drug Research and Development. *Nat. Med*. **2007**, *13*, 290–294.

(55) Gopal, P.; Sarathy, J. P.; Yee, M.; Ragunathan, P.; Shin, J.; Bhushan, S.; Zhu, J.; Akopian, T.; Kandror, O.; Lim, T. K.; Gengenbacher, M.; Lin, Q.; Rubin, E. J.; Grüber, G.; Dick, T. Pyrazinamide Triggers Degradation of its Target Aspartate Decarboxylase. *Nat. Commun.* **2020**, *11* (1), 1661.

(56) Mukonzo, J.; Aklillu, E.; Marconi, V.; Schinazi, R. F. Potential Drug-Drug Interactions Between Antiretroviral Therapy and Treatment Regimens for Multi-Drug Resistant

1956 Tuberculosis: Implications for HIV Care of MDR-TB Co-Infected Individuals. *Int. J. Infect.*
1957 *Dis.* **2019**, *83*, 98–101.
1958 (57) Al-Humadi, H. W.; Al-Saigh, R. J.; Al-Humadi, A. W. Addressing the Challenges of
1959 Tuberculosis: A Brief Historical Account. *Front. Pharmacol.* **2017**, *8*, 689.
1960 (58) la Porte, C. J. L.; Colbers, E. P. H.; Bertz, R.; Voncken, D. S.; Wikstrom, K.; Boeree, M. J.;
1961 Koopmans, P. P.; Hekster, Y. A.; Burger, D. M. Pharmacokinetics of Adjusted-Dose Lopinavir-
1962 Ritonavir Combined With Rifampin in Healthy Volunteers. *Antimicrob. Agents Chemother.*
1963 **2004**, *48*, 1553–1560.
1964 (59) Conradie, F.; Diacon, A. H.; Ngubane, N.; Howell, P.; Everitt, D.; Crook, A. M.; Mendel, C.
1965 M.; Egizi, E.; Moreira, J.; Timm, J.; McHugh, T. D.; Wills, G. H.; Bateson, A.; Hunt, R.; Van
1966 Niekerk, C.; Li, M.; Olugbosi, M.; Spigelman, M. Treatment of Highly Drug-Resistant
1967 Pulmonary Tuberculosis. *N. Engl. J. Med.* **2020**, *382*, 893–902.
1968 (60) Manjunatha, U. H.; Smith, P. W. Perspective: Challenges and Opportunities in TB Drug
1969 Discovery From Phenotypic Screening. *Bioorg. Med. Chem.* **2015**, *23*, 5087–5097.
1970 (61) Machado, D.; Girardini, M.; Viveiros, M.; Pieroni, M. Challenging the Drug-Likeness Dogma
1971 for New Drug Discovery in Tuberculosis. *Front. Microbiol*. **2018**, *9*, 1367.
1972 (62) Degiacomi, G.; Belardinelli, J. M.; Pasca, M. R.; De Rossi, E.; Riccardi, G.; Chiarelli,
1973 L.R. Promiscuous Targets for Antitubercular Drug Discovery: The Paradigm of DprE1 and
1974 MmpL3. *Appl. Sci.* **2020**, *10* (2), 623.
1975 (63) Lee, B. S.; Pethe, K. Therapeutic Potential of Promiscuous Targets in *Mycobacterium*
1976 *tuberculosis*. *Curr. Opin. Pharmacol*. **2018**, *42*, 22-26.

(64) Makarov, V.; Salina, E.; Reynolds, R. C.; Zin, P. P. K.; Ekins, S. Molecule Property Analyses of Active Compounds for *Mycobacterium tuberculosis. J. Med. Chem.* **2020**, *63*, 8917-8955.

(65) Borsari, C.; Ferrari, S.; Venturelli, A.; Costi, M. P. Target-Based Approaches for the Discovery of New Antimycobacterial Drugs. *Drug Discov. Today* **2017**, *22*, 576–584.

(66) Lechartier, B.; Rybniker, J.; Zumla, A.; Cole, S. T. Tuberculosis Drug Discovery in the Post-Post-Genomic Era. *EMBO Mol. Med*. **2014**, *6*, 158–168.

(67) Cole, S. T.; Brosch, R.; Parkhill, J.; Garnier, T.; Churcher, C.; Harris, D.; Gordon, S. V; Eiglmeier, K.; Gas, S.; Barry, C. E. 3rd; Tekaia, F.; Badcock, K.; Basham, D.; Brown, D.; Chillingworth, T.; Connor, R.; Davies, R.; Devlin, K.; Feltwell, T.; Gentles, S.; Hamlin, N.; Holroyd, S.; Hornsby, T.; Jagels, K.; Krogh, A.; McLean, J.; Moule, S.; Murphy, L.; Oliver, K.; Osborne, J.; Quail, M. A.; Rajandream, M.-A.; Rogers, J.; Rutter, S.; Seeger, K.; Skelton, J.; Squares, R.; Squares, S.; Sulston, J. E.; Taylor, K.; Whitehead, S.; Barrell, B. G. Deciphering the Biology of *Mycobacterium tuberculosis* From the Complete Genome Sequence. *Nature* **1998**, *393*, 537–544.

(68) Chiarelli, L. R.; Mori, G.; Esposito, M.; Orena, B. S.; Pasca, M. R. New and Old Hot Drug Targets in Tuberculosis. *Curr. Med. Chem.* **2016**, *23*, 3813–3846.

(69) Wellington, S.; Hung, D. T. The Expanding Diversity of *Mycobacterium tuberculosis* Drug Targets. *ACS Infect. Dis.* **2018**, *4*, 696–714.

(70) Mdluli, K.; Kaneko, T.; Upton, A. The Tuberculosis Drug Discovery and Development Pipeline and Emerging Drug Targets. *Cold Spring Harb. Perspect. Med.* **2015**, *5* (6), a021154.

(71) Campaniço, A.; Moreira, R.; Lopes, F. Drug Discovery in Tuberculosis. New Drug Targets and Antimycobacterial Agents. *Eur. J. Med. Chem*. **2018**, *150*, 525–545.

(72) Huszár, S.; Chibale, K.; Singh, V. The Quest for the Holy Grail: New Antitubercular Chemical Entities, Targets and Strategies. *Drug Discov. Today* **2020**, *25*, 772-780.

(73) Johnson, E. O.; LaVerriere, E.; Office, E.; Stanley, M.; Meyer, E.; Kawate, T.; Gomez, J. E.; Audette, R. E.; Bandyopadhyay, N.; Betancourt, N.; Delano, K.; Da Silva, I.; Davis, J.; Gallo, C.; Gardner, M.; Goals, A. J.; Guinn, K. M.; Kennedy, S.; Korn, R.; McConnell, J. A.; Moss, C. E.; Murphy, K. C.; Nietupski, R. M.; Papavinasasundaram, K. G.; Pinkham, J. T.; Pino, P. A.; Proulx, M. K.; Ruecker, N.; Song, N.; Thompson, M.; Trujillo, C.; Wakabayashi, S.; Wallach, J. B.; Watson, C.; Ioerger, T. R.; Lander, E. S.; Hubbard, B. K.; Serrano-Wu, M. H.; Ehrt, S.; Fitzgerald, M.; Rubin, E. J.; Sassetti, C. M.; Schnappinger, D.; Hung, D. T. Large-Scale Chemical-Genetics Yields New *M. tuberculosis* Inhibitor Classes. *Nature* **2019**, *571*, 72-78.

(74) Zumla, A. I.; Gillespie, S. H.; Hoelscher, M.; Philips, P. P. J.; Cole, S. T.; Abubakar, I.; McHugh, T. D.; Schito, M.; Maeurer, M.; Nunn, A. J. New Antituberculosis Drugs, Regimens, and Adjunct Therapies: Needs, Advances, and Future Prospects. *Lancet Infect. Dis.* **2014**, *14*, 327–340.

(75) Stop TB Partnership's Working Group on New TB Drugs. Clinical Pipeline. https://www.newtbdrugs.org/pipeline/clinical (accessed December 17, 2021).

(76) Raju, T. N. K. The Nobel Chronicles. 1988: James Whyte Black, (b 1924), Gertrude Elion (1918-99), and George H Hitchings (1905-98). *Lancet* **2000**, *355* (9208), 1022.

(77) Brown, D. G.; Bostrom, J. Where Do Recent Small Molecule Clinical Development Candidates Come From? *J. Med. Chem*. **2018**, *61*, 9442-9468.

(78) McKenna, L. *Pipeline Report 2019: Tuberculosis Treatment*. Treatment Action Group, 2019. https://www.treatmentactiongroup.org/wp-content/uploads/2019/12/pipeline_tb_treatment_lm_final.pdf (accessed October 15, 2021).

(79) Egbelowo, O.; Sarathy, J. P.; Gausi, K.; Zimmerman, M. D.; Wang, H.; Wijnant, G. J.; Kaya, F.; Gengenbacher, M.; Van, N.; Degefu, Y.; Nacy, C.; Aldridge, B. B.; Carter, C. L.; Denti, P.; Dartois, V. Pharmacokinetics and Target Attainment of SQ109 in Plasma and Human-Like Tuberculosis Lesions in Rabbits. *Antimicrob. Agents Chemother*. **2021**, *65* (9), e00024-21.

(80) Sacksteder, K. A.; Protopopova, M.; Barry, C. E.; Andries, K.; Nacy, C. A. Discovery and Development of SQ109: A New Antitubercular Drug With a Novel Mechanism of Action. *Future Microbiol.* **2012**, *7*, 823-837.

(81) Tahlan, K.; Wilson, R.; Kastrinsky, D. B.; Arora, K.; Nair, V.; Fischer, E.; Barnes, S. W.; Walker, J. R.; Alland, D.; Barry, C. E.; Boshoff, H. I. SQ109 Targets MmpL3, a Membrane Transporter of Trehalose Monomycolate Involved in Mycolic Acid Donation to the Cell Wall Core of *Mycobacterium tuberculosis*. *Antimicrob. Agents Chemother*. **2012**, *56*, 1797–1809.

(82) Li, W.; Upadhyay, A.; Fontes, F. L.; North, E. J.; Wang, Y.; Crans, D. C.; Grzegorzewicz, A. E.; Jones, V.; Franzblau, S. G.; Lee, R. E.; Crick, D. C.; Jackson, M. Novel Insights into the Mechanism of Inhibition of MmpL3, a Target of Multiple Pharmacophores in *Mycobacterium tuberculosis*. *Antimicrob. Agents Chemother*. **2014**, *58*, 6413–6423.

(83) Li, K.; Schurig-Briccio, L. A.; Feng, X.; Upadhyay, A.; Pujari, V.; Lechartier, B.; Fontes, F. L.; Yang, H.; Rao, G.; Zhu, W.; Gulati, A.; No, J. H.; Cintra, G.; Bogue, S.; Liu, Y.-L.; Molohon, K.; Orlean, P.; Mitchell, D. A.; Freitas-Junior, L.; Ren, F.; Sun, H.; Jiang, T.; Li, Y.;

2041 Guo, R.-T.; Cole, S. T.; Gennis, R. B.; Crick, D. C.; Oldfield, E. Multitarget Drug Discovery
2042 for Tuberculosis and Other Infectious Diseases. *J. Med. Chem*. **2014**, *57*, 3126–3139.
2043 (84) Lee, B.-Y.; Clemens, D. L.; Silva, A.; Dillon, B. J.; Maslesa-Galic, S.; Nava, S.; Ho, C.-M.;
2044 Horwitz, M. A. Ultra-Rapid Near Universal TB Drug Regimen Identified via Parabolic
2045 Response Surface Platform Cures Mice of Both Conventional and High Susceptibility. *PLoS*
2046 *One* **2018**, *13* (11), e0207469.
2047 (85) Malwal, S. R.; Zimmerman, M. D.; Alvarez, N.; Sarathy, J. P.; Dartois, V.; Nacy, C. A.;
2048 Oldfield, E. Structure, *In Vivo* Detection, and Antibacterial Activity of Metabolites of SQ109,
2049 an Anti-Infective Drug Candidate. *ACS Infect. Dis.* **2021**, *7*, 2492-2507.
2050 (86) Fernandes, G. F. S.; Salgado, H. R. N.; Dos Santos, J. L. A Critical Review of HPLC-Based
2051 Analytical Methods for Quantification of Linezolid. *Crit. Rev. Anal. Chem.* **2020**, *50*, 196–211.
2052 (87) Shaw, K. J.; Barbachyn, M. R. The Oxazolidinones: Past, Present, and Future. *Ann. N. Y. Acad.*
2053 *Sci.* **2011**, *1241*, 48-70.
2054 (88) Cho, Y. L.; Jang, J. Development of Delpazolid for the Treatment of Tuberculosis. *Appl. Sci.*
2055 **2020**, *10* (7), 2211.
2056 (89) McKenna, L. *The 2020 Tuberculosis Treatment Pipeline Report.* Treatment Action Group,
2057 2020. https://www.treatmentactiongroup.org/wp-
2058 content/uploads/2020/11/pipeline_tb_treatment_2020_final.pdf (accessed October 15, 2021).
2059 (90) Diacon, A. H.; De Jager, V. R.; Dawson, R.; Narunsky, K.; Vanker, N.; Burger, D. A.; Everitt,
2060 D.; Pappas, F.; Nedelman, J.; Mendel, C. M. Fourteen-Day Bactericidal Activity, Safety, and
2061 Pharmacokinetics of Linezolid in Adults With Drug-Sensitive Pulmonary Tuberculosis.
2062 *Antimicrob. Agents Chemother.* **2020**, *64* (4), e02012-19.

(91) Wallis, R. S.; Dawson, R.; Friedrich, S. O.; Venter, A.; Paige, D.; Zhu, T.; Silvia, A.; Gobey, J.; Ellery, C.; Zhang, Y.; Eisenach, K.; Miller, P.; Diacon, A. H. Mycobactericidal Activity of Sutezolid (PNU-100480) in Sputum (EBA) and Blood (WBA) of Patients With Pulmonary Tuberculosis. *PLoS One* **2014**, *9* (4), e94462.

(92) Shetye, G. S.; Franzblau, S. G.; Cho, S. New Tuberculosis Drug Targets, Their Inhibitors, and Potential Therapeutic Impact. *Transl. Res.* **2020**, *220*, 68–97.

(93) Pethe, K.; Bifani, P.; Jang, J.; Kang, S.; Park, S.; Ahn, S.; Jiricek, J.; Jung, J.; Jeon, H. K.; Cechetto, J.; Christophe, T.; Lee, H.; Kempf, M.; Jackson, M.; Lenaerts, A. J.; Pham, H.; Jones, V.; Seo, M. J.; Kim, Y. M.; Seo, M.; Seo, J. J.; Park, D.; Ko, Y.; Choi, I.; Kim, R.; Kim, S. Y.; Lim, S.; Yim, S.-A.; Nam, J.; Kang, H.; Kwon, H.; Oh, C.-T.; Cho, Y.; Jang, Y.; Kim, J.; Chua, A.; Tan, B. H.; Nanjundappa, M. B.; Rao, S. P. S.; Barnes, W. S.; Wintjens, R.; Walker, J. R.; Alonso, S.; Lee, S.; Kim, J.; Oh, S.; Oh, T.; Nehrbass, U.; Han, S.-J.; No, Z.; Lee, J.; Brodin, P.; Cho, S.-N.; Nam, K.; Kim, J. Discovery of Q203, a Potent Clinical Candidate for the Treatment of Tuberculosis. *Nat. Med.* **2013**, *19*, 1157–1160.

(94) Yanofsy, D. J.; Di Trani, J. M.; Krol, S.; Abdelaziz, R.; Bueler, S. A.; Imming, P.; Brzezinski, P.; Rubinstein, J. L. Structure of Mycobacterial $CIII_2CIV_2$ Respiratory Supercomplex Bound to the Tuberculosis Drug Candidate Telacebec (Q203). *Elife* **2021**, *10*, e71959.

(95) Lamprecht, D. A.; Finin, P. M.; Rahman, M. A.; Cumming, B. M.; Russell, S. L.; Jonnala, S. R.; Adamson, J. H.; Steyn, A. J. C. Turning the Respiratory Flexibility of *Mycobacterium tuberculosis* Against Itself. *Nat. Commun.* **2016**, *7*, 12393.

(96) Lee, B. S.; Hards, K.; Engelhart, C. A.; Hasenoehrl, E. J.; Kalia, N. P.; Mackenzie, J. S.; Sviriaeva, E.; Chong, S. M. S.; Manimekalai, M. S. S.; Koh, V. H.; Chan, J.; Xu, J.; Alonso, S.;

Miller, M. J.; Steyn, A. J. C.; Grüber, G.; Schnappinger, D.; Berney, M.; Cook, G. M.; Moraski, G. C.; Pethe, K. Dual Inhibition of the Terminal Oxidases Eradicates Antibiotic-Tolerant *Mycobacterium tuberculosis. EMBO Mol. Med.* **2021**, *13* (1), e13207.

(97) de Jager, V. R.; Dawson, R.; van Niekerk, C.; Hutchings, J.; Kim, J.; Vanker, N.; van der Merwe, L.; Choi, J.; Nam, K.; Diacon, A. H. Telacebec (Q203), a New Antituberculosis Agent. *N. Engl. J. Med.* **2020**, *382*, 1280–1281.

(98) Almeida, D. V.; Converse, P. J.; Omansen, T. F.; Tyagi, S.; Tasneen, R.; Kim, J.; Nuermberger, E. L. Telacebec for Ultrashort Treatment of Buruli Ulcer in a Mouse Model. *Antimicrob. Agents Chemother.* **2020**, *64* (6), e00259-20.

(99) Makarov, V.; Lechartier, B.; Zhang, M.; Neres, J.; van der Sar, A. M.; Raadsen, S. A.; Hartkoorn, R. C.; Ryabova, O. B.; Vocat, A.; Decosterd, L. A.; Widmer, N.; Buclin, T.; Bitter, W.; Andries, K.; Pojer, F.; Dyson, P. J.; Cole, S. T. Towards a New Combination Therapy for Tuberculosis With Next Generation Benzothiazinones. *EMBO Mol. Med.* **2014**, *6*, 372-383.

(100) Makarov, V.; Mikusova, K. Development of Macozinone for TB Treatment: An Update. *Appl. Sci.* **2020**, *10* (7), 2269.

(101) Lupien, A.; Vocat, A.; Foo, C. S.-Y.; Blattes, E.; Gillon, J.-Y.; Makarov, V.; Cole, S. T. Optimized Background Regimen for Treatment of Active Tuberculosis With the Next-Generation Benzothiazinone Macozinone (PBTZ169). *Antimicrob. Agents Chemother.* **2018**, *62* (11), e00840-18.

(102) Neres, J.; Pojer, F.; Molteni, E.; Chiarelli, L. R.; Dhar, N.; Boy-Röttger, S.; Buroni, S.; Fullam, E.; Degiacomi, G.; Lucarelli, A. P.; Read, R. J.; Zanoni, G.; Edmondson, D. E.; De Rossi, E.; Pasca, M. R.; McKinney, J. D.; Dyson, P. J.; Riccardi, G.; Mattevi, A.; Cole, S. T.; Binda, C.

Structural Basis for Benzothiazinone-Mediated Killing of *Mycobacterium tuberculosis*. *Sci. Transl. Med.* **2012**, *4* (150), 150ra121.

(103) Kloss, F.; Krchnak, V.; Krchnakova, A.; Schieferdecker, S.; Dreisbach, J.; Krone, V.; Möllmann, U.; Hoelscher, M.; Miller, M. J. In Vivo Dearomatization of the Potent Antituberculosis Agent BTZ043 via Meisenheimer Complex Formation. *Angew. Chem. Int. Ed. Engl.* **2017**, *56*, 2187-2191.

(104) Li, X.; Hernandez, V.; Rock, F. L.; Choi, W.; Mak, Y. S. L.; Mohan, M.; Mao, W.; Zhou, Y.; Easom, E. E.; Plattner, J. J.; Zou, W.; Perez-Herran, E.; Giordano, I.; Mendoza-Losana, A.; Alemparte, C.; Rullas, J.; Angulo-Barturen, I.; Crouch, S.; Ortega, F.; Barros, D.; Alley, M. R. K. Discovery of a Potent and Specific *M. tuberculosis* Leucyl-tRNA Synthetase Inhibitor: (S)-3-(Aminomethyl)-4-chloro-7-(2-hydroxyethoxy)benzo[*c*][1,2]oxaborol-1(3*H*)-ol (GSK656). *J. Med. Chem.* **2017**, *60*, 8011–8026.

(105) Palencia, A.; Li, X.; Bu, W.; Choi, W.; Ding, C. Z.; Easom, E. E.; Feng, L.; Hernandez, V.; Houston, P.; Liu, L.; Meewan, M.; Mohan, M.; Rock, F. L.; Sexton, H.; Zhang, S.; Zhou, Y.; Wan, B.; Wang, Y.; Franzblau, S. G.; Woolhiser, L.; Gruppo, V.; Lenaerts, A. J.; O'Malley, T.; Parish, T.; Cooper, C. B.; Waters, M. G.; Ma, Z.; Ioerger, T. R.; Sacchettini, J. C.; Rullas, J.; Angulo-Barturen, I.; Pérez-Herrán, E.; Mendoza, A.; Barros, D.; Cusack, S.; Plattner, J. J.; Alley, M. R. K. Discovery of Novel Oral Protein Synthesis Inhibitors of *Mycobacterium tuberculosis* That Target Leucyl-tRNA Synthetase. *Antimicrob. Agents Chemother*. **2016**, *60*, 6271–6280.

(106) Tenero, D.; Derimanov, G.; Carlton, A.; Tonkyn, J.; Davies, M.; Cozens, S.; Gresham, S.; Gaudion, A.; Puri, A.; Muliaditan, M.; Rullas-Trincado, J.; Mendoza-Losana, A.; Skingsley,

A.; Barros-Aguirre, D. First-Time-in-Human Study and Prediction of Early Bactericidal Activity for GSK3036656, a Potent Leucyl-tRNA Synthetase Inhibitor for Tuberculosis Treatment. *Antimicrob. Agents Chemother.* **2019**, *63* (8), e00240-19.

(107) Shirude, P. S.; Shandil, R.; Sadler, C.; Naik, M.; Hosagrahara, V.; Hameed, S.; Shinde, V.; Bathula, C.; Humnabadkar, V.; Kumar, N.; Reddy, J.; Panduga, V.; Sharma, S.; Ambady, A.; Hegde, N.; Whiteaker, J.; McLaughlin, R. E.; Gardner, H.; Madhavapeddi, P.; Ramachandran, V.; Kaur, P.; Narayan, A.; Guptha, S.; Awasthy, D.; Narayan, C.; Mahadevaswamy, J.; Vishwas, K. G.; Ahuja, V.; Srivastava, A.; Prabhakar, K. R.; Bharath, S.; Kale, R.; Ramaiah, M.; Choudhury, N. R.; Sambandamurthy, V. K.; Solapure, S.; Iyer, P. S.; Narayanan, S.; Chatterji, M. Azaindoles: Noncovalent DprE1 Inhibitors From Scaffold Morphing Efforts, Kill *Mycobacterium tuberculosis* and Are Efficacious *in Vivo*. *J. Med. Chem.* **2013**, *56*, 9701–9708.

(108) Chatterji, M.; Shandil, R.; Manjunatha, M. R.; Solapure, S.; Ramachandran, V.; Kumar, N.; Saralaya, R.; Panduga, V.; Reddy, J.; Prabhakar, K. R.; Sharma, S.; Sadler, C.; Cooper, C. B.; Mdluli, K.; Iyer, P. S.; Narayanan, S.; Shirude, P. S. 1,4-Azaindole, a Potential Drug Candidate for Treatment of Tuberculosis. *Antimicrob. Agents Chemother.* **2014**, *58*, 5325-5331.

(109) Shirude, P. S.; Shandil, R. K.; Manjunatha, M. R.; Sadler, C.; Panda, M.; Panduga, V.; Reddy, J.; Saralaya, R.; Nanduri, R.; Ambady, A.; Ravishankar, S.; Sambandamurthy, V. K.; Humnabadkar, V.; Jena, L. K.; Suresh, R. S.; Srivastava, A.; Prabhakar, K. R.; Whiteaker, J.; McLaughlin, R. E.; Sharma, S.; Cooper, C. B.; Mdluli, K.; Butler, S.; Iyer, P. S.; Narayanan, S.; Chatterji, M. Lead Optimization of 1,4-Azaindoles as Antimycobacterial Agents. *J. Med. Chem.* **2014**, *57*, 5728–5737.

(110) Xu, J.; Wang, B.; Fu, L.; Zhu, H.; Guo, S.; Huang, H.; Yin, D.; Zhang, Y.; Lu, Y. *In Vitro* and *In Vivo* Activities of the Riminophenazine TBI-166 Against *Mycobacterium tuberculosis*. *Antimicrob. Agents Chemother.* **2019**, *63* (5), e02155-18.

(111) Lu, Y.; Zheng, M.; Wang, B.; Fu, L.; Zhao, W.; Li, P.; Xu, J.; Zhu, H.; Jin, H.; Yin, D.; Huang, H.; Upton, A. M.; Ma, Z. Clofazimine Analogs With Efficacy Against Experimental Tuberculosis and Reduced Potential for Accumulation. *Antimicrob. Agents Chemother.* **2011**, *55*, 5185–5193.

(112) Zhang, Y.; Zhu, H.; Fu, L.; Wang, B.; Guo, S.; Chen, X.; Liu, Z.; Huang, H.; Yang, T.; Lu, Y. Identifying Regimens Containing TBI-166, a New Drug Candidate Against *Mycobacterium tuberculosis In Vitro* and *In Vivo*. *Antimicrob. Agents Chemother.* **2019**, *63* (7), e02496-18.

(113) Zhang, D.; Lu, Y.; Liu, K.; Liu, B.; Wang, J.; Zhang, G.; Zhang, H.; Liu, Y.; Wang, B.; Zheng, M.; Fu, L.; Hou, Y.; Gong, N.; Lv, Y.; Li, C.; Cooper, C. B.; Upton, A. M.; Yin, D.; Ma, Z.; Huang, H. Identification of Less Lipophilic Riminophenazine Derivatives for the Treatment of Drug-Resistant Tuberculosis. *J. Med. Chem.* **2012**, *55*, 8409–8417.

(114) Yano, T.; Kassovska-Bratinova, S.; Teh, J. S.; Winkler, J.; Sullivan, K.; Isaacs, A.; Schechter, N. M.; Rubin, H. Reduction of Clofazimine by Mycobacterial Type 2 NADH:Quinone Oxidoreductase: A Pathway for the Generation of Bactericidal Levels of Reactive Oxygen Species. *J. Biol. Chem.* **2011**, *286*, 10276–10287.

(115) Beites, T.; O'Brien, K.; Tiwari, D.; Engelhart, C. A.; Walters, S.; Andrews, J.; Yang, H.-J.; Sutphen, M. L.; Weiner, D. M.; Dayao, E. K.; Zimmerman, M.; Prideaux, B.; Desai, P. V.; Masquelin, T.; Via, L. E.; Dartois, V.; Boshoff, H. I.; Barry, C. E.; Ehrt, S.; Schnappinger, D.

Plasticity of the *Mycobacterium tuberculosis* Respiratory Chain and its Impact on Tuberculosis Drug Development. *Nat. Commun.* **2019**, *10*, 4970.

(116) Hariguchi, N.; Chen, X.; Hayashi, Y.; Kawano, Y.; Fujiwara, M.; Matsuba, M.; Shimizu, H.; Ohba, Y.; Nakamura, I.; Kitamoto, R.; Shinohara, T.; Uematsu, Y.; Ishikawa, S.; Itotani, M.; Haraguchi, Y.; Takemura, I.; Matsumoto, M. OPC-167832, a Novel Carbostyril Derivative With Potent Antituberculosis Activity as a DprE1 Inhibitor. *Antimicrob. Agents Chemother.* **2020**, *64* (6), e02020-19.

(117) Robertson, G. T.; Ramey, M. E.; Massoudi, L. M.; Carter, C. L.; Zimmerman, M.; Kaya, F.; Graham, B. G.; Gruppo, V.; Hastings, C.; Woolhiser, L. K.; Scott, D. W. L.; Asay, B. C.; Eshun-Wilson, F.; Maidj, E.; Podell, B. K.; Vasquez, J. J.; Lyons, M. A.; Dartois, V.; Lenaerts, A. J. Comparative Analysis of Pharmacodynamics in the C3HeB/FeJ Mouse Tuberculosis Model for DprE1 Inhibitors TBA-7371, PBTZ169 and OPC-167832. *Antimicrob. Agents Chemother.* **2021**, *65* (11), e00583-21.

(118) Locher, C. P.; Jones, S. M.; Hanzelka, B. L.; Perola, E.; Shoen, C. M.; Cynamon, M. H.; Ngwane, A. H.; Wild, I. J.; van Helden, P. D.; Betoudji, F.; Nuermberger, E. L.; Thomson, J. A. A Novel Inhibitor of Gyrase B Is a Potent Drug Candidate for Treatment of Tuberculosis and Nontuberculosis Mycobacterial Infections. *Antimicrob. Agents Chemother.* **2015**, *59*, 1455-1465.

(119) Shoen, C. M.; DeStefano, M. S.; Pucci, M. J.; Cynamon, M. H. Evaluating the Sterilizing Activity of SPR720 in Combination Therapy Against *Mycobacterium tuberculosis* Infection in Mice. Poster presentation in ASM Microbe 2019; San Francisco, USA, June 21, 2019. https://sperotherapeutics.com/presentation/evaluating-the-sterilizing-activity-of-spr720-in-

combination-therapy-against-mycobacterium-tuberculosis-infection-in-mice/ (accessed October 15, 2021).

(120) Charifson, P. S.; Grillot, A.-L.; Grossman, T. H.; Parsons, J. D.; Badia, M.; Bellon, S.; Deininger, D. D.; Drumm, J. E.; Gross, C. H.; LeTiran, A.; Liao, Y.; Mani, N.; Nicolau, D. P.; Perola, E.; Ronkin, S.; Shannon, D.; Swenson, L. L.; Tang, Q.; Tessier, P. R.; Tian, S. K.; Trudeau, M.; Wang, T.; Wei, Y.; Zhang, H.; Stamos, D. Novel Dual-Targeting Benzimidazole Urea Inhibitors of DNA Gyrase and Topoisomerase IV Possessing Potent Antibacterial Activity: Intelligent Design and Evolution Through the Judicious Use of Structure-Guided Design and Structure-Activity Relationships. *J. Med. Chem.* **2008**, *51*, 5243-5263.

(121) Sutherland, H. S.; Tong, A. S. T.; Choi, P. J.; Blaser, A.; Conole, D.; Franzblau, S. G.; Lotlikar, M. U.; Cooper, C. B.; Upton, A. M.; Denny, W. A.; Palmer, B. D. 3,5-Dialkoxypyridine Analogues of Bedaquiline Are Potent Antituberculosis Agents With Minimal Inhibition of the HERG Channel. *Bioorg. Med. Chem.* **2019**, *27*, 1292-1307.

(122) Xu, J.; Converse, P. J.; Upton, A. M.; Mdluli, K.; Fotouhi, N.; Nuermberger, E. L. Comparative Efficacy of the Novel Diarylquinoline TBAJ-587 and Bedaquiline Against a Resistant *Rv0678* Mutant in a Mouse Model of Tuberculosis. *Antimicrob. Agents Chemother.* **2021**, *65* (4), e02418-20.

(123) Sarathy, J. P.; Ragunathan, P.; Shin, J.; Cooper, C. B.; Upton, A. M.; Grüber, G.; Dick, T. TBAJ-876 Retains Bedaquiline's Activity Against Subunits c and ε of *Mycobacterium tuberculosis* F-ATP Synthase. *Antimicrob. Agents Chemother.* **2019**, *63* (10), e01191-19.

(124) Sarathy, J. P.; Ragunathan, P.; Cooper, C. B.; Upton, A. M.; Grüber, G.; Dick, T. TBAJ-876 Displays Bedaquiline-Like Mycobactericidal Potency Without Retaining the Parental Drug's Uncoupler Activity. *Antimicrob. Agents Chemother.* **2020**, *64* (2), e01540-19.

(125) Ding, C. Z. The Discovery and Development of a Clinical Candidate WX-081 for MDR-Tuberculosis Therapy. Oral presentation to College of Chemistry, Central China Normal University, November 3, 2016. http://chem.ccnu.edu.cn/info/1233/3230.htm (accessed December 18, 2021).

(126) Huang, Z.; Ding, C. Z.; Tang, D.; Wang, Y.; Li, Z. Preparation Method for Pyridine Derivative Compound, Intermediate and Crystal Form Thereof. Patent WO 2017/121323 A1, 2017.

(127) Aldridge, B. B.; Barros-Aguirre, D.; Barry, C. E.; Bates, R. H.; Berthel, S. J.; Boshoff, H. I.; Chibale, K.; Chu, X.-J.; Cooper, C. B.; Dartois, V.; Duncan, K.; Fotouhi, N.; Gusovsky, F.; Hipskind, P. A.; Kempf, D. J.; Lelièvre, J.; Lenaerts, A. J.; McNamara, C. W.; Mizrahi, V.; Nathan, C.; Olsen, D. B.; Parish, T.; Petrassi, H. M.; Pym, A.; Rhee, K. Y.; Robertson, G. T.; Rock, J. M.; Rubin, E. J.; Russell, B.; Russell, D. G.; Sacchettini, J. C.; Schnappinger, D.; Schrimpf, M.; Upton, A. M.; Warner, P.; Wyatt, P. G.; Yuan, Y. The Tuberculosis Drug Accelerator at Year 10: What Have We Learned? *Nat. Med.* **2021**, *27*, 1333-1337.

(128) VanderVen, B. C.; Fahey, R. J.; Lee, W.; Liu, Y.; Abramovitch, R. B.; Memmott, C.; Crowe, A. M.; Eltis, L. D.; Perola, E.; Deininger, D. D.; Wang, T.; Locher, C. P.; Russell, D. G. Novel Inhibitors of Cholesterol Degradation in *Mycobacterium tuberculosis* Reveal How the Bacterium's Metabolism Is Constrained by the Intracellular Environment. *PLoS Pathog.* **2015**, *11* (2), e1004679.

(129) Bonds, A. C.; Sampson, N. S. More Than Cholesterol Catabolism: Regulatory Vulnerabilities in *Mycobacterium tuberculosis*. *Curr. Opin. Chem. Biol.* **2018**, *44*, 39-46.

(130) Guieu, B.; Jourdan, J.-P.; Dreneau, A.; Willand, N.; Rochais, C.; Dallemagne, P. Desirable Drug-Drug Interactions or When a Matter of Concern Becomes a Renewed Therapeutic Strategy. *Drug Discov. Today* **2021**, *26*, 315-328.

(131) *BioVersys: Saving Lives in Resistant Times*. December 2021. https://media.nature.com/original/magazine-assets/d43747-021-00153-4/d43747-021-00153-4.pdf (accessed January 1, 2022)

(132) Ang, C. W.; Jarrad, A. M.; Cooper, M. A.; Blaskovich, M. A. T. Nitroimidazoles: Molecular Fireworks That Combat a Broad Spectrum of Infectious Diseases. *J. Med. Chem.* **2017**, *60*, 7636-7657.

(133) *Novartis Provides Drug Candidate Compounds to TB Alliance*. TB Alliance, August 18, 2014. https://www.tballiance.org/news/novartis-provides-drug-candidate-compounds-tb-alliance (accessed October 15, 2021)

(134) Kumar, V.; Patel, S.; Jain, R. New Structural Classes of Antituberculosis Agents. *Med. Res. Rev.* **2018**, *38*, 684–740.

(135) Sharma, A.; De Rosa, M.; Singla, N.; Singh, G.; Barnwal, R. P.; Pandey, A. Tuberculosis: An Overview of the Immunogenic Response, Disease Progression, and Medicinal Chemistry Efforts in the Last Decade Toward the Development of Potential Drugs for Extensively Drug-Resistant Tuberculosis Strains. *J. Med. Chem.* **2021**, *64*, 4359–4395.

(136) Atukuri, D.; Gunjal, R.; Holagundi, N.; Korlahalli, B.; Gangannavar, S.; Akkasali, K. Contribution of *N*-Heterocycles Towards Anti-Tubercular Drug Discovery (2014–2019); Predicted and Reengineered Molecular Frameworks. *Drug Dev. Res.* **2021**, *82*, 767-783.

(137) Gatadi, S.; Nanduri, S. New Potential Drug Leads Against MDR-MTB: A Short Review. *Bioorg. Chem.* **2020**, *95*, 103534.

(138) Dos Santos Fernandes, G. F.; Pavan, A. R.; Dos Santos, J. L. Heterocyclic N-Oxides - A Promising Class of Agents Against Tuberculosis, Malaria and Neglected Tropical Diseases. *Curr. Pharm. Des.* **2018**, *24*, 1325–1340.

(139) Oh, S.; Trifonov, L.; Yadav, V. D.; Barry, C. E.; Boshoff, H. I. Tuberculosis Drug Discovery: A Decade of Hit Assessment for Defined Targets. *Front. Cell Infect. Microbiol.* **2021**, *11*, 611304.

(140) Fernandes, G. F. S.; Chin, C. M.; Dos Santos, J. L. Advances in Drug Discovery of New Antitubercular Multidrug-Resistant Compounds. *Pharmaceuticals* **2017**, *10* (2), 51.

(141) Bahuguna, A.; Rawat, D. S. An Overview of New Antitubercular Drugs, Drug Candidates, and Their Targets. *Med. Res. Rev.* **2020**, *40*, 263–292.

(142) Angula, K. T.; Legoabe, L. J.; Beteck, R. M. Chemical Classes Presenting Novel Antituberculosis Agents Currently in Different Phases of Drug Development: A 2010-2020 Review. *Pharmaceuticals* **2021**, *14* (5), 461.

(143) Chiaradia, L.; Lefebvre, C.; Parra, J.; Marcoux, J.; Burlet-Schiltz, O.; Etienne, G.; Tropis, M.; Daffé, M. Dissecting the Mycobacterial Cell Envelope and Defining the Composition of the Native Mycomembrane. *Sci. Rep.* **2017**, *7*, 12807.

(144) Vincent, A. T.; Nyongesa, S.; Morneau, I.; Reed, M. B.; Tocheva, E. I.; Veyrier, F. J. The Mycobacterial Cell Envelope: A Relict From the Past or the Result of Recent Evolution? *Front. Microbiol.* **2018**, *9*, 2341.

(145) Bhat, Z. S.; Rather, M. A.; Maqbool, M.; Lah, H. U.; Yousuf, S. K.; Ahmad, Z. Cell Wall: A Versatile Fountain of Drug Targets in *Mycobacterium tuberculosis*. *Biomed. Pharmacother.* **2017**, *95*, 1520–1534.

(146) Chen, H.; Nyantakyi, S. A.; Li, M.; Gopal, P.; Aziz, D. B.; Yang, T.; Moreira, W.; Gengenbacher, M.; Dick, T.; Go, M. L. The Mycobacterial Membrane: A Novel Target Space for Anti-Tubercular Drugs. *Front. Microbiol.* **2018**, *9*, 1627.

(147) Vilchèze, C. Mycobacterial Cell Wall: A Source of Successful Targets for Old and New Drugs. *Appl. Sci.* **2020**, *10* (7), 2278.

(148) Catalão, M. J.; Filipe, S. R.; Pimentel, M. Revisiting Anti-Tuberculosis Therapeutic Strategies That Target the Peptidoglycan Structure and Synthesis. *Front. Microbiol.* **2019**, *10*, 190.

(149) Barry, C. E.; Crick, D. C.; McNeil, M. R. Targeting the Formation of the Cell Wall Core of *M. tuberculosis. Infect. Disord. Drug Targets* **2007**, *7*, 182–202.

(150) Abrahams, K. A.; Besra, G. S. Mycobacterial Cell Wall Biosynthesis: A Multifaceted Antibiotic Target. *Parasitology* **2018**, *145*, 116–133.

(151) Riccardi, G.; Pasca, M. R.; Chiarelli, L. R.; Manina, G.; Mattevi, A.; Binda, C. The DprE1 Enzyme, One of the Most Vulnerable Targets of *Mycobacterium tuberculosis*. *Appl. Microbiol. Biotechnol.* **2013**, *97*, 8841–8848.

(152) Chikhale, R. V.; Barmade, M. A.; Murumkar, P. R.; Yadav, M. R. Overview of the Development of DprE1 Inhibitors for Combating the Menace of Tuberculosis. *J. Med. Chem.* **2018**, *61*, 8563–8593.

(153) R, M. M.; Shandil, R.; Panda, M.; Sadler, C.; Ambady, A.; Panduga, V.; Kumar, N.; Mahadevaswamy, J.; Sreenivasaiah, M.; Narayan, A.; Guptha, S.; Sharma, S.; Sambandamurthy, V. K.; Ramachandran, V.; Mallya, M.; Cooper, C.; Mdluli, K.; Butler, S.; Tommasi, R.; Iyer, P. S.; Narayanan, S.; Chatterji, M.; Shirude, P. S. Scaffold Morphing to Identify Novel DprE1 Inhibitors With Antimycobacterial Activity. *ACS Med. Chem. Lett.* **2019**, *10*, 1480–1485.

(154) Piton, J.; Vocat, A.; Lupien, A.; Foo, C. S.; Riabova, O.; Makarov, V.; Cole, S. T. Structure-Based Drug Design and Characterization of Sulfonyl-Piperazine Benzothiazinone Inhibitors of DprE1 From *Mycobacterium tuberculosis*. *Antimicrob. Agents Chemother.* **2018**, *62* (10), e00681-18.

(155) Lv, K.; You, X.; Wang, B.; Wei, Z.; Chai, Y.; Wang, B.; Wang, A.; Huang, G.; Liu, M.; Lu, Y. Identification of Better Pharmacokinetic Benzothiazinone Derivatives as New Antitubercular Agents. *ACS Med. Chem. Lett.* **2017**, *8*, 636-641.

(156) Lv, K.; Wang, A.; Tao, Z.; Fu, L.; Liu, H.; Wang, B.; Ma, C.; Wang, H.; Ma, X.; Han, B.; Wang, A.; Zhang, K.; Liu, M.; Lu, Y. hERG Optimizations of IMB1603, Discovery of Alternative Benzothiazinones as New Antitubercular Agents. *Eur. J. Med. Chem.* **2019**, *179*, 208-217.

(157) Wang, A.; Ma, C.; Chai, Y.; Liu, X.; Lv, K.; Fu, L.; Wang, B.; Jia, X.; Liu, M.; Lu, Y. Identification of Benzothiazinones Containing 2-Benzyl-2,7-diazaspiro[3.5]nonane Moieties as New Antitubercular Agents. *Eur. J. Med. Chem.* **2020**, *200*, 112409.

(158) Wang, A.; Lv, K.; Tao, Z.; Gu, J.; Fu, L.; Liu, M.; Wan, B.; Franzblau, S. G.; Ma, C.; Ma, X.; Han, B.; Wang, A.; Xu, S.; Lu, Y. Identification of Benzothiazinones Containing an Oxime Functional Moiety as New Anti-Tuberculosis Agents. *Eur. J. Med. Chem.* **2019**, *181*, 111595.

(159) Guo, S.; Fu, L.; Wang, B.; Chen, X.; Zhao, J.; Liu, M.; Lu, Y. *In Vitro* and *in Vivo* Antimicrobial Activities of a Novel Piperazine-Containing Benzothiazinones Candidate TZY-5-84 Against *Mycobacterium tuberculosis*. *Biomed. Pharmacother.* **2020**, *131*, 110777.

(160) Driver, E. R.; Ryan, G. J.; Hoff, D. R.; Irwin, S. M.; Basaraba, R. J.; Kramnik, I.; Lenaerts, A. J. Evaluation of a Mouse Model of Necrotic Granuloma Formation Using C3HeB/FeJ Mice for Testing of Drugs Against *Mycobacterium tuberculosis*. *Antimicrob. Agents Chemother.* **2012**, *56*, 3181-3195.

(161) Gao, C.; Peng, C.; Shi, Y.; You, X.; Ran, K.; Xiong, L.; Ye, T.-H.; Zhang, L.; Wang, N.; Zhu, Y.; Liu, K.; Zuo, W.; Yu, L.; Wei, Y. Benzothiazinethione is a Potent Preclinical Candidate for the Treatment of Drug-Resistant Tuberculosis. *Sci. Rep.* **2016**, *6*, 29717.

(162) Gao, C.; Ye, T.-H.; Peng, C.-T.; Shi, Y.-J.; You, X.-Y.; Xiong, L.; Ran, K.; Zhang, L.-D.; Zeng, X.-X.; Wang, N.-Y.; Yu, L.-T.; Wei, Y.-Q. A Novel Benzothiazinethione Analogue SKLB-TB1001 Displays Potent Antimycobacterial Activities in a Series of Murine Models. *Biomed. Pharmacother.* **2017**, *88*, 603-609.

(163) Xiong, L.; Gao, C.; Shi, Y.-J.; Tao, X.; Peng, C.-T.; Rong, J.; Liu, K.-L.; Lei, Q.; Zhang, Y.-W.; Wang, N.-Y.; Yu, L.-T. Metabolism of SKLB-TB1001, a Potent Antituberculosis Agent, in Animals. *Antimicrob. Agents Chemother.* **2018**, *62* (7), e02375-17.

(164) Li, P.; Wang, B.; Zhang, X.; Batt, S. M.; Besra, G. S.; Zhang, T.; Ma, C.; Zhang, D.; Lin, Z.; Li, G.; Huang, H.; Lu, Y. Identification of Novel Benzothiopyranone Compounds Against *Mycobacterium tuberculosis* Through Scaffold Morphing From Benzothiazinones. *Eur. J. Med. Chem.* **2018**, *160*, 157-170.

(165) Li, P.; Wang, B.; Fu, L.; Guo, K.; Ma, C.; Wang, B.; Lin, Z.; Li, G.; Huang, H.; Lu, Y. Identification of Novel Benzothiopyranones With Ester and Amide Motifs Derived From Active Metabolite as Promising Leads Against *Mycobacterium tuberculosis. Eur. J. Med. Chem.* **2021**, *222*, 113603.

(166) Borthwick, J. A.; Alemparte, C.; Wall, I.; Whitehurst, B. C.; Argyrou, A.; Burley, G.; de Dios-Anton, P.; Guijarro, L.; Monteiro, M. C.; Ortega, F.; Suckling, C. J.; Pichel, J. C.; Cacho, M.; Young, R. J. *Mycobacterium tuberculosis* Decaprenylphosphoryl-*β*-D-ribose Oxidase Inhibitors: Expeditious Reconstruction of Suboptimal Hits into a Series With Potent in Vivo Activity. *J. Med. Chem.* **2020**, *63*, 2557–2576.

(167) Rullas, J.; García, J. I.; Beltrán, M.; Cardona, P.-J.; Cáceres, N.; García-Bustos, J. F.; Angulo-Barturen, I. Fast Standardized Therapeutic-Efficacy Assay for Drug Discovery Against Tuberculosis. *Antimicrob. Agents Chemother.* **2010**, *54*, 2262-2264.

(168) Balabon, O.; Pitta, E.; Rogacki, M. K.; Meiler, E.; Casanueva, R.; Guijarro, L.; Huss, S.; Lopez-Roman, E. M.; Santos-Villarejo, Á.; Augustyns, K.; Ballell, L.; Barros Aguirre, D.; Bates, R. H.; Cunningham, F.; Cacho, M.; Van der Veken, P. Optimization of Hydantoins as Potent

Antimycobacterial Decaprenylphosphoryl-*β*-D-Ribose Oxidase (DprE1) Inhibitors. *J. Med. Chem.* **2020**, *63*, 5367–5386.

(169) Rogacki, M. K.; Pitta, E.; Balabon, O.; Huss, S.; Lopez-Roman, E. M.; Argyrou, A.; Blanco-Ruano, D.; Cacho, M.; Vande Velde, C. M. L.; Augustyns, K.; Ballell, L.; Barros, D.; Bates, R. H.; Cunningham, F.; Van der Veken, P. Identification and Profiling of Hydantoins—A Novel Class of Potent Antimycobacterial DprE1 Inhibitors. *J. Med. Chem.* **2018**, *61*, 11221–11249.

(170) Liu, R.; Lyu, X.; Batt, S. M.; Hsu, M.-H.; Harbut, M. B.; Vilchèze, C.; Cheng, B.; Ajayi, K.; Yang, B.; Yang, Y.; Guo, H.; Lin, C.; Gan, F.; Wang, C.; Franzblau, S. G.; Jacobs, W. R. Jr.; Besra, G. S.; Johnson, E. F.; Petrassi, M.; Chatterjee, A. K.; Fütterer, K.; Wang, F. Determinants of the Inhibition of DprE1 and CYP2C9 by Antitubercular Thiophenes. *Angew. Chem. Int. Ed. Engl.* **2017**, *56*, 13011-13015.

(171) Wang, F.; Sambandan, D.; Halder, R.; Wang, J.; Batt, S. M.; Weinrick, B.; Ahmad, I.; Yang, P.; Zhang, Y.; Kim, J.; Hassani, M.; Huszar, S.; Trefzer, C.; Ma, Z.; Kaneko, T.; Mdluli, K. E.; Franzblau, S.; Chatterjee, A. K.; Johnsson, K.; Mikusova, K.; Besra, G. S.; Fütterer, K.; Robbins, S. H.; Barnes, S. W.; Walker, J. R.; Jacobs, W. R. Jr.; Schultz, P. G. Identification of a Small Molecule With Activity Against Drug-Resistant and Persistent Tuberculosis. *Proc. Natl. Acad. Sci. U.S.A.* **2013**, *110* (27), E2510–E2517.

(172) Wang, P.; Batt, S. M.; Wang, B.; Fu, L.; Qin, R.; Lu, Y.; Li, G.; Besra, G. S.; Huang, H. Discovery of Novel Thiophene-Arylamide Derivatives as DprE1 Inhibitors With Potent Antimycobacterial Activities. *J. Med. Chem.* **2021**, *64*, 6241-6261.

(173) Degiacomi, G.; Benjak, A.; Madacki, J.; Boldrin, F.; Provvedi, R.; Palu, G.; Kordulakova, J.; Cole, S. T.; Manganelli, R. Essentiality of *mmpL3* and Impact of its Silencing on *Mycobacterium tuberculosis* Gene Expression. *Sci. Rep.* **2017**, *7*, 43495.

(174) Remuiñán, M. J.; Pérez-Herrán, E.; Rullás, J.; Alemparte, C.; Martínez-Hoyos, M.; Dow, D. J.; Afari, J.; Mehta, N.; Esquivias, J.; Jiménez, E.; Ortega-Muro, F.; Fraile-Gabaldón, M. T.; Spivey, V. L.; Loman, N. J.; Pallen, M. J.; Constantinidou, C.; Minick, D. J.; Cacho, M.; Rebollo-López, M. J.; González, C.; Sousa, V.; Angulo-Barturen, I.; Mendoza-Losana, A.; Barros, D.; Besra, G. S.; Ballell, L.; Cammack, N. Tetrahydropyrazolo[1,5-*a*]Pyrimidine-3-Carboxamide and *N*-Benzyl-6′,7′-Dihydrospiro[Piperidine-4,4′-Thieno[3,2-*c*]Pyran] Analogues With Bactericidal Efficacy Against *Mycobacterium tuberculosis* Targeting MmpL3. *PloS One* **2013**, *8* (4), e60933.

(175) Guardia, A.; Baiget, J.; Cacho, M.; Pérez, A.; Ortega-Guerra, M.; Nxumalo, W.; Khanye, S. D.; Rullas, J.; Ortega, F.; Jiménez, E.; Pérez-Herrán, E.; Fraile-Gabaldón, M. T.; Esquivias, J.; Fernández, R.; Porras-De Francisco, E.; Encinas, L.; Alonso, M.; Giordano, I.; Rivero, C.; Miguel-Siles, J.; Osende, J. G.; Badiola, K. A.; Rutledge, P. J.; Todd, M. H.; Remuiñán, M.; Alemparte, C. Easy-To-Synthesize Spirocyclic Compounds Possess Remarkable in Vivo Activity Against *Mycobacterium tuberculosis*. *J. Med. Chem.* **2018**, *61*, 11327-11340.

(176) Ray, P. C.; Huggett, M.; Turner, P. A.; Taylor, M.; Cleghorn, L. A. T.; Early, J.; Kumar, A.; Bonnett, S. A.; Flint, L.; Joerss, D.; Johnson, J.; Korkegian, A.; Mullen, S.; Moure, A. L.; Davis, S. H.; Murugesan, D.; Mathieson, M.; Caldwell, N.; Engelhart, C. A.; Schnappinger, D.; Epemolu, O.; Zuccotto, F.; Riley, J.; Scullion, P.; Stojanovski, L.; Massoudi, L.; Robertson, G. T.; Lenaerts, A. J.; Freiberg, G.; Kempf, D. J.; Masquelin, T.; Hipskind, P. A.; Odingo, J.; Read,

2399 K. D.; Green, S. R.; Wyatt, P. G.; Parish, T. Spirocycle MmpL3 Inhibitors With Improved
2400 hERG and Cytotoxicity Profiles as Inhibitors of *Mycobacterium tuberculosis* Growth. *ACS*
2401 *Omega* **2021**, *6*, 2284-2311.
2402 (177) Nyantakyi, S. A.; Li, M.; Gopal, P.; Zimmerman, M.; Dartois, V.; Gengenbacher, M.; Dick, T.;
2403 Go, M.-L. Indolyl Azaspiroketal Mannich Bases Are Potent Antimycobacterial Agents With
2404 Selective Membrane Permeabilizing Effects and in Vivo Activity. *J. Med. Chem.* **2018**, *61*,
2405 5733–5750.
2406 (178) Li, M.; Phua, Z. Y.; Xi, Y.; Xu, Z.; Nyantakyi, S. A.; Li, W.; Jackson, M.; Wong, M. W.; Lam,
2407 Y.; Chng, S. S.; Go, M. L.; Dick, T. Potency Increase of Spiroketal Analogs of Membrane
2408 Inserting Indolyl Mannich Base Antimycobacterials Is Due to Acquisition of MmpL3
2409 Inhibition. *ACS Infect. Dis.* **2020**, *6*, 1882–1893.
2410 (179) Stec, J.; Onajole, O. K.; Lun, S.; Guo, H.; Merenbloom, B.; Vistoli, G.; Bishai, W. R.;
2411 Kozikowski, A. P. Indole-2-carboxamide-based MmpL3 Inhibitors Show Exceptional
2412 Antitubercular Activity in an Animal Model of Tuberculosis Infection. *J. Med. Chem.* **2016**,
2413 *59*, 6232–6247.
2414 (180) Lun, S.; Tasneen, R.; Chaira, T.; Stec, J.; Onajole, O. K.; Yang, T. J.; Cooper, C. B.; Mdluli,
2415 K.; Converse, P. J.; Nuermberger, E. L.; Raj, V. S.; Kozikowski, A.; Bishai, W. R. Advancing
2416 the Therapeutic Potential of Indoleamides for Tuberculosis. *Antimicrob. Agents Chemother.*
2417 **2019**, *63* (7), e00343-19.
2418 (181) Poce, G.; Bates, R. H.; Alfonso, S.; Cocozza, M.; Porretta, G. C.; Ballell, L.; Rullas, J.; Ortega,
2419 F.; De Logu, A.; Agus, E.; La Rosa, V.; Pasca, M. R.; De Rossi, E.; Wae, B.; Franzblau, S. G.;

2420 Manetti, F.; Botta, M.; Biava, M. Improved BM212 MmpL3 Inhibitor Analogue Shows
2421 Efficacy in Acute Murine Model of Tuberculosis Infection. *PLoS One* **2013**, *8* (2), e56980.
2422 (182) Poce, G.; Cocozza, M.; Alfonso, S.; Consalvi, S.; Venditti, G.; Fernandez-Menendez, R.; Bates,
2423 R. H.; Barros Aguirre, D.; Ballell, L.; De Logu, A.; Vistoli, G.; Biava, M. In Vivo Potent
2424 BM635 Analogue With Improved Drug-like Properties. *Eur. J. Med. Chem.* **2018**, *145*, 539-
2425 550.
2426 (183) Poce, G.; Consalvi, S.; Venditti, G.; Alfonso, S.; Desideri, N.; Fernandez-Menendez, R.; Bates,
2427 R. H.; Ballell, L.; Barros Aguirre, D.; Rullas, J.; De Logu, A.; Gardner, M.; Ioerger, T. R.;
2428 Rubin, E. J.; Biava, M. Novel Pyrazole-Containing Compounds Active Against *Mycobacterium*
2429 *tuberculosis*. *ACS Med. Chem. Lett.* **2019**, *10*, 1423-1429.
2430 (184) Takayama, K.; Wang, C.; Besra, G. S. Pathway to Synthesis and Processing of Mycolic Acids
2431 in *Mycobacterium tuberculosis. Clin. Microbiol. Rev.* **2005**, *18*, 81–101.
2432 (185) Martínez-Hoyos, M.; Perez-Herran, E.; Gulten, G.; Encinas, L.; Álvarez-Gómez, D.; Alvarez,
2433 E.; Ferrer-Bazaga, S.; García-Pérez, A.; Ortega, F.; Angulo-Barturen, I.; Rullas-Trincado, J.;
2434 Blanco Ruano, D.; Torres, P.; Castañeda, P.; Huss, S.; Fernández Menéndez, R.; González Del
2435 Valle, S.; Ballell, L.; Barros, D.; Modha, S.; Dhar, N.; Signorino-Gelo, F.; McKinney, J. D.;
2436 García-Bustos, J. F.; Lavandera, J. L.; Sacchettini, J. C.; Jimenez, M. S.; Martín-Casabona, N.;
2437 Castro-Pichel, J.; Mendoza-Losana, A. Antitubercular Drugs for an Old Target: GSK693 as a
2438 Promising InhA Direct Inhibitor. *EBioMedicine* **2016**, *8*, 291-301.
2439 (186) Xia, Y.; Zhou, Y.; Carter, D. S.; McNeil, M. B.; Choi, W.; Halladay, J.; Berry, P. W.; Mao, W.;
2440 Hernandez, V.; O'Malley, T.; Korkegian, A.; Sunde, B.; Flint, L.; Woolhiser, L. K.; Scherman,
2441 M. S.; Gruppo, V.; Hastings, C.; Robertson, G. T.; Ioerger, T. R.; Sacchettini, J.; Tonge, P. J.;

Lenaerts, A. J.; Parish, T.; Alley, M. R. K. Discovery of a Cofactor-Independent Inhibitor of *Mycobacterium tuberculosis* InhA. *Life Sci. Alliance* **2018**, *1* (3), e201800025.

(187) Robertson, G. T.; Ektnitphong, V. A.; Scherman, M. S.; McNeil, M. B.; Dennison, D.; Korkegian, A.; Smith, A. J.; Halladay, J.; Carter, D. S.; Xia, Y.; Zhou, Y.; Choi, W.; Berry, P. W.; Mao, W.; Hernandez, V.; Alley, M. R. K.; Parish, T.; Lenaerts, A. J. Efficacy and Improved Resistance Potential of a Cofactor-Independent InhA Inhibitor of *Mycobacterium tuberculosis* in the C3HeB/FeJ Mouse Model. *Antimicrob. Agents Chemother.* **2019**, *63* (4), e02071-18.

(188) Blondiaux, N.; Moune, M.; Desroses, M.; Frita, R.; Flipo, M.; Mathys, V.; Soetaert, K.; Kiass, M.; Delorme, V.; Djaout, K.; Trebosc, V.; Kemmer, C.; Wintjens, R.; Wohlkönig, A.; Antoine, R.; Huot, L.; Hot, D.; Coscolla, M.; Feldmann, J.; Gagneux, S.; Locht, C.; Brodin, P.; Gitzinger, M.; Déprez, B.; Willand, N.; Baulard, A. R. Reversion of Antibiotic Resistance in *Mycobacterium tuberculosis* by Spiroisoxazoline SMARt-420. *Science* **2017**, *355*, 1206–1211.

(189) Villemagne, B.; Machelart, A.; Tran, N. C.; Flipo, M.; Moune, M.; Leroux, F.; Piveteau, C.; Wohlkönig, A.; Wintjens, R.; Li, X.; Gref, R.; Brodin, P.; Deprez, B.; Baulard, A. R.; Willand, N. Fragment-Based Optimized EthR Inhibitors With *in Vivo* Ethionamide Boosting Activity. *ACS Infect. Dis.* **2020**, *6*, 366–378.

(190) Costa-Gouveia, J.; Pancani, E.; Jouny, S.; Machelart, A.; Delorme, V.; Salzano, G.; Iantomasi, R.; Piveteau, C.; Queval, C. J.; Song, O.-R.; Flipo, M.; Deprez, B.; Saint-André, J.-P.; Hureaux, J.; Majlessi, L.; Willand, N.; Baulard, A.; Brodin, P.; Gref, R. Combination Therapy for Tuberculosis Treatment: Pulmonary Administration of Ethionamide and Booster Co-loaded Nanoparticles. *Sci. Rep.* **2017**, *7*, 5390.

(191) Ballell, L.; Bates, R. H.; Young, R. J.; Alvarez-Gomez, D.; Alvarez-Ruiz, E.; Barroso, V.; Blanco, D.; Crespo, B.; Escribano, J.; González, R.; Lozano, S.; Huss, S.; Santos-Villarejo, A.; Martín-Plaza, J. J.; Mendoza, A.; Rebollo-Lopez, M. J.; Remuiñan-Blanco, M.; Lavandera, J. L.; Pérez-Herran, E.; Gamo-Benito, F. J.; García-Bustos, J. F.; Barros, D.; Castro, J. P.; Cammack, N. Fueling Open-Source Drug Discovery: 177 Small-Molecule Leads Against Tuberculosis. *ChemMedChem* **2013**, *8*, 313–321.

(192) Abrahams, K. A.; Chung, C. W.; Ghidelli-Disse, S.; Rullas, J.; Rebollo-López, M. J.; Gurcha, S. S.; Cox, J. A. G.; Mendoza, A.; Jiménez-Navarro, E.; Martínez-Martínez, M. S.; Neu, M.; Shillings, A.; Homes, P.; Argyrou, A.; Casanueva, R.; Loman, N. J.; Moynihan, P. J.; Lelièvre, J.; Selenski, C.; Axtman, M.; Kremer, L.; Bantscheff, M.; Angulo-Barturen, I.; Izquierdo, M. C.; Cammack, N. C.; Drewes, G.; Ballell, L.; Barros, D.; Besra, G. S.; Bates, R. H. Identification of KasA as the Cellular Target of an Anti-Tubercular Scaffold. *Nat. Commun.* **2016**, *7*, 12581.

(193) Kumar, P.; Capodagli, G. C.; Awasthi, D.; Shrestha, R.; Maharaja, K.; Sukheja, P.; Li, S.-G.; Inoyama, D.; Zimmerman, M.; Liang, H. P. H.; Sarathy, J.; Mina, M.; Rasic, G.; Russo, R.; Perryman, A. L.; Richmann, T.; Gupta, A.; Singleton, E.; Verma, S.; Husain, S.; Soteropoulos, P.; Wang, Z.; Morris, R.; Porter, G.; Agnihotri, G.; Salgame, P.; Ekins, S.; Rhee, K. Y.; Connell, N.; Dartois, V.; Neiditch, M. B.; Freundlich, J. S.; Alland, D. Synergistic Lethality of a Binary Inhibitor of *Mycobacterium tuberculosis* KasA. *MBio* **2018**, *9* (6), e02101-17.

(194) Inoyama, D.; Awasthi, D.; Capodagli, G. C.; Tsotetsi, K.; Sukheja, P.; Zimmerman, M.; Li, S.-G.; Jadhav, R.; Russo, R.; Wang, X.; Grady, C.; Richmann, T.; Shrestha, R.; Li, L.; Ahn, Y.-M.; Liang, H. P. H.; Mina, M.; Park, S.; Perlin, D. S.; Connell, N.; Dartois, V.; Alland, D.;

2484 Neiditch, M. B.; Kumar, P.; Freundlich, J. S. A Preclinical Candidate Targeting *Mycobacterium*
2485 *tuberculosis* KasA. *Cell Chem. Biol*. **2020**, *27*, 560–570.
2486 (195) Cunningham, F.; Esquivias, J.; Fernández-Menéndez, R.; Pérez, A.; Guardia, A.; Escribano, J.;
2487 Rivero, C.; Vimal, M.; Cacho, M.; de Dios-Antón, P.; Martínez-Martínez, M. S.; Jiménez, E.;
2488 Huertas Valentín, L.; Rebollo-López, M. J.; López-Román, E. M.; Sousa-Morcuende, V.;
2489 Rullás, J.; Neu, M.; Chung, C. W.; Bates, R. H. Exploring the SAR of the *β*-Ketoacyl-ACP
2490 Synthase Inhibitor GSK3011724A and Optimization Around a Genotoxic Metabolite. *ACS*
2491 *Infect. Dis*. **2020**, *6*, 1098-1109.
2492 (196) Portevin, D.; De Sousa-D'Auria, C.; Houssin, C.; Grimaldi, C.; Chami, M.; Daffé, M.; Guilhot,
2493 C. A Polyketide Synthase Catalyzes the Last Condensation Step of Mycolic Acid Biosynthesis
2494 in Mycobacteria and Related Organisms. *Proc. Natl. Acad. Sci. U.S.A.* **2004**, *101*, 314–319.
2495 (197) Aggarwal, A.; Parai, M. K.; Shetty, N.; Wallis, D.; Woolhiser, L.; Hastings, C.; Dutta, N. K.;
2496 Galaviz, S.; Dhakal, R. C.; Shrestha, R.; Wakabayashi, S.; Walpole, C.; Matthews, D.; Floyd,
2497 D.; Scullion, P.; Riley, J.; Epemolu, O.; Norval, S.; Snavely, T.; Robertson, G. T.; Rubin, E. J.;
2498 Ioerger, T. R.; Sirgel, F. A.; van der Merwe, R.; van Helden, P. D.; Keller, P.; Bottger, E. C.;
2499 Karakousis, P. C.; Lenaerts, A. J.; Sacchettini, J. C. Development of a Novel Lead That Targets
2500 *M. tuberculosis* Polyketide Synthase 13. *Cell* **2017**, *170*, 249–259.
2501 (198) Wilson, C.; Ray, P.; Zuccotto, F.; Hernandez, J.; Aggarwal, A.; Mackenzie, C.; Caldwell, N.;
2502 Taylor, M.; Huggett, M.; Mathieson, M.; Murugesan, D.; Smith, A.; Davis, S.; Cocco, M.;
2503 Parai, M. K.; Acharya, A.; Tamaki, F.; Scullion, P.; Epemolu, O.; Riley, J.; Stojanovski, L.;
2504 Lopez-Román, E. M.; Torres-Gómez, P. A.; Toledo, A. M.; Guijarro-Lopez, L.; Camino, I.;
2505 Engelhart, C. A.; Schnappinger, D.; Massoudi, L. M.; Lenaerts, A.; Robertson, G. T.; Walpole,

C.; Matthews, D.; Floyd, D.; Sacchettini, J. C.; Read, K. D.; Encinas, L.; Bates, R. H.; Green, S. R.; Wyatt, P. G. Optimization of TAM16, a Benzofuran That Inhibits the Thioesterase Activity of Pks13; Evaluation Toward a Preclinical Candidate for a Novel Antituberculosis Clinical Target. *J. Med. Chem.* **2022**, *65*, 409-423.

(199) Zhang, W.; Lun, S.; Liu, L.-L.; Xiao, S.; Duan, G.; Gunosewoyo, H.; Yang, F.; Tang, J.; Bishai, W. R.; Yu, L.-F. Identification of Novel Coumestan Derivatives as Polyketide Synthase 13 Inhibitors Against *Mycobacterium tuberculosis*. Part II. *J. Med. Chem.* **2019**, *62*, 3575–3589.

(200) Lun, S.; Xiao, S.; Zhang, W.; Wang, S.; Gunosewoyo, H.; Yu, L.-F.; Bishai, W. R. Therapeutic Potential of Coumestan Pks13 Inhibitors for Tuberculosis. *Antimicrob. Agents Chemother.* **2021**, *65* (5), e02190-20.

(201) Zhao, W.; Wang, B.; Liu, Y.; Fu, L.; Sheng, L.; Zhao, H.; Lu, Y.; Zhang, D. Design, Synthesis, and Biological Evaluation of Novel 4*H*-Chromen-4-one Derivatives as Antituberculosis Agents Against Multidrug-Resistant Tuberculosis. *Eur. J. Med. Chem.* **2020**, *189*, 112075.

(202) Wang, X.; Zhao, W.; Wang, B.; Ding, W.; Guo, H.; Zhao, H.; Meng, J.; Liu, S.; Lu, Y.; Liu, Y.; Zhang, D. Identification of Inhibitors Targeting Polyketide Synthase 13 of *Mycobacterium tuberculosis* as Antituberculosis Drug Leads. *Bioorg. Chem.* **2021**, *114*, 105110.

(203) Stanley, S. A.; Kawate, T.; Iwase, N.; Shimizu, M.; Clatworthy, A. E.; Kazyanskaya, E.; Sacchettini, J. C.; Ioerger, T. R.; Siddiqi, N. A.; Minami, S.; Aquadro, J. A.; Grant, S. S.; Rubin, E. J.; Hung, D. T. Diarylcoumarins Inhibit Mycolic Acid Biosynthesis and Kill *Mycobacterium tuberculosis* by Targeting FadD32. *Proc. Natl. Acad. Sci. U. S. A.* **2013**, *110*, 11565–11570.

(204) Fang, C.; Lee, K. K.; Nietupski, R.; Bates, R. H.; Fernandez-Menendez, R.; Lopez-Roman, E. M.; Guijarro-Lopez, L.; Yin, Y.; Peng, Z.; Gomez, J. E.; Fisher, S.; Barros-Aguirre, D.;

2528 Hubbard, B. K.; Serrano-Wu, M. H.; Hung, D. T. Discovery of Heterocyclic Replacements for
2529 the Coumarin Core of Antitubercular FadD32 Inhibitors. *Bioorg. Med. Chem. Lett.* **2018**, *28*,
2530 3529–3533.
2531 (205) Vickery, C. R.; Kosa, N. M.; Casavant, E. P.; Duan, S.; Noel, J. P.; Burkart, M. D. Structure,
2532 Biochemistry, and Inhibition of Essential 4′-Phosphopantetheinyl Transferases From Two
2533 Species of *Mycobacteria*. *ACS Chem. Biol.* **2014**, *9*, 1939–1944.
2534 (206) Ballinger, E.; Mosior, J.; Hartman, T.; Burns-Huang, K.; Gold, B.; Morris, R.; Goullieux, L.;
2535 Blanc, I.; Vaubourgeix, J.; Lagrange, S.; Fraisse, L.; Sans, S.; Couturier, C.; Bacqué, E.; Rhee,
2536 K.; Scarry, S. M.; Aubé, J.; Yang, G.; Ouerfelli, O.; Schnappinger, D.; Ioerger, T. R.; Engelhart,
2537 C. A.; McConnell, J. A.; McAulay, K.; Fay, A.; Roubert, C.; Sacchettini, J.; Nathan, C.
2538 Opposing Reactions in Coenzyme A Metabolism Sensitize *Mycobacterium tuberculosis* to
2539 Enzyme Inhibition. *Science* **2019**, *363* (6426), eaau8959.
2540 (207) Ottavi, S.; Scarry, S. M.; Mosior, J.; Ling, Y.; Roberts, J.; Singh, A.; Zhang, D.; Goullieux, L.;
2541 Roubert, C.; Bacqué, E.; Lagiakos, H. R.; Vendome, J.; Moraca, F.; Li, K.; Perkowski, A. J.;
2542 Ramesh, R.; Bowler, M. M.; Tracy, W.; Feher, V. A.; Sacchettini, J. C.; Gold, B. S.; Nathan,
2543 C. F.; Aubé, J. In Vitro and In Vivo Inhibition of the *Mycobacterium*
2544 *tuberculosis* Phosphopantetheinyl Transferase PptT by Amidinoureas. *J. Med. Chem.* **2022** (in
2545 press); doi: 10.1021/acs.jmedchem.1c01565.
2546 (208) Cordillot, M.; Dubée, V.; Triboulet, S.; Dubost, L.; Marie, A.; Hugonnet, J.-E.; Arthur, M.;
2547 Mainardi, J.-L. *In Vitro* Cross-Linking of *Mycobacterium tuberculosis* Peptidoglycan by L,D-
2548 Transpeptidases and Inactivation of These Enzymes by Carbapenems. *Antimicrob. Agents*
2549 *Chemother*. **2013**, *57*, 5940–5945.

(209) Jadhav, R.; Gallardo-Macias, R.; Kumar, G.; Daher, S. S.; Kaushik, A.; Bigelow, K. M.; Nuermberger, E. L.; Lamichhane, G.; Freundlich, J. S. Assessment of Carbapenems in a Mouse Model of *Mycobacterium tuberculosis* Infection. *PLoS One* **2021**, *16* (5), e0249841.

(210) Bianchet, M. A.; Pan, Y. H.; Brammer Basta, L. A.; Saavedra, H.; Lloyd, E. P.; Kumar, P.; Mattoo, R.; Townsend, C. A.; Lamichhane, G. Structural Insight into the Inactivation of *Mycobacterium tuberculosis* Non-classical Transpeptidase Ldt_{Mt2} by Biapenem and Tebipenem. *BMC Biochem.* **2017**, *18* (1), 8.

(211) Kumar, P.; Kaushik, A.; Lloyd, E. P.; Li, S.-G.; Mattoo, R.; Ammerman, N. C.; Bell, D. T.; Perryman, A. L.; Zandi, T. A.; Ekins, S.; Ginell, S. L.; Townsend, C. A.; Freundlich, J. S.; Lamichhane, G. Non-Classical Transpeptidases Yield Insight into New Antibacterials. *Nat. Chem. Biol.* **2017**, *13*, 54–61.

(212) Kaushik, A.; Makkar, N.; Pandey, P.; Parrish, N.; Singh, U.; Lamichhane, G. Carbapenems and Rifampin Exhibit Synergy Against *Mycobacterium tuberculosis* and *Mycobacterium abscessus*. *Antimicrob. Agents Chemother*. **2015**, *59*, 6561–6567.

(213) Kaushik, A.; Ammerman, N. C.; Tasneen, R.; Story-Roller, E.; Dooley, K. E.; Dorman, S. E.; Nuermberger, E. L.; Lamichhane, G. *In Vitro* and *in Vivo* Activity of Biapenem Against Drug-Susceptible and Rifampicin-Resistant *Mycobacterium tuberculosis*. *J. Antimicrob. Chemother.* **2017**, *72*, 2320–2325.

(214) Ramon-Garcia, S.; Bates, R.; González del Río, R.; Gamallo, P.; Mendoza-Losana, A.; Ferrer-Bazaga, S.; Thompson, C.; Barros, D. Sanfetrinem, Repurposing an Oral Beta-Lactam With Intracellular Activity for the Treatment of Tuberculosis. *Abstract Book of the 50th World Conference on Lung Health of the International Union Against Tuberculosis and Lung Disease*

(The Union), Hyderabad, India, 29-30 October 2019, p S591. https://araid.es/sites/default/files/congresos/20191101_union2019_abstracts_final.pdf (accessed October 21, 2021).

(215) Kumagai, T.; Tamai, S.; Abe, T.; Hikida, M. Current Status of Oral Carbapenem Development. *Curr. Med. Chem. – Antiinfect. Agents* **2002**, *1*, 1-14.

(216) Tamura, S.; Miyazaki, S.; Tateda, K.; Ohno, A.; Ishii, Y.; Matsumoto, T.; Furuya, N.; Yamaguchi, K. In Vivo Antibacterial Activities of Sanfetrinem Cilexetil, a New Oral Tricyclic Antibiotic. *Antimicrob. Agents Chemother*. **1998**, *42*, 1858-1861.

(217) Barros Aguirre, D.; Bates, R. H.; Gonzalez del Rio, R.; Mendoza Losana, A.; Ramon Garcia, S. Sanfetrinem or a Salt or Ester Thereof for Use in Treating Mycobacterial Infection. Patent WO 2018/206466 A1, 2018.

(218) Batson, S.; de Chiara, C.; Majce, V.; Lloyd, A. J.; Gobec, S.; Rea, D.; Fülöp, V.; Thoroughgood, C. W.; Simmons, K. J.; Dowson, C. G.; Fishwick, C. W. G.; de Carvalho, L. P. S.; Roper, D. I. Inhibition of D-Ala:D-Ala Ligase Through a Phosphorylated Form of the Antibiotic D-Cycloserine. *Nat. Commun.* **2017**, *8***,** 1939.

(219) Meng, J.; Gao, P.; Wang, X.; Guan, Y.; Liu, Y.; Xiao, C. Digging Deeper to Save the Old Anti-tuberculosis Target: D-Alanine-D-Alanine Ligase With a Novel Inhibitor, IMB-0283. *Front. Microbiol.* **2020**, *10*, 3017.

(220) Zhang, Y. J.; Rubin, E. J. Feast or Famine: The Host-Pathogen Battle Over Amino Acids. *Cell. Microbiol.* **2013**, *15*, 1079-1087.

(221) Lott, J. S. The Tryptophan Biosynthetic Pathway Is Essential for *Mycobacterium tuberculosis* to Cause Disease. *Biochem. Soc. Trans.* **2020**, *48*, 2029–2037.

(222) Wellington, S.; Nag, P. P.; Michalska, K.; Johnston, S. E.; Jedrzejczak, R. P.; Kaushik, V. K.; Clatworthy, A. E.; Siddiqi, N.; McCarren, P.; Bajrami, B.; Maltseva, N. I.; Combs, S.; Fisher, S. L.; Joachimiak, A.; Schreiber, S. L.; Hung, D. T. A Small-Molecule Allosteric Inhibitor of *Mycobacterium tuberculosis* Tryptophan Synthase. *Nat. Chem. Biol*. **2017**, *13*, 943–950.

(223) Abrahams, K. A.; Cox, J. A. G.; Fütterer, K.; Rullas, J.; Ortega-Muro, F.; Loman, N. J.; Moynihan, P. J.; Pérez-Herrán, E.; Jiménez, E.; Esquivias, J.; Barros, D.; Ballell, L.; Alemparte, C.; Besra, G. S. Inhibiting Mycobacterial Tryptophan Synthase by Targeting the Inter-Subunit Interface. *Sci. Rep.* **2017**, *7*, 9430.

(224) Michalska, K.; Chang, C.; Maltseva, N. I.; Jedrzejczak, R.; Robertson, G. T.; Gusovsky, F.; McCarren, P.; Schreiber, S. L.; Nag, P. P.; Joachimiak, A. Allosteric Inhibitors of *Mycobacterium tuberculosis* Tryptophan Synthase. *Protein Sci.* **2020**, *29*, 779-788.

(225) Gupta, P.; Thomas, S. E.; Zaidan, S. A.; Pasillas, M. A.; Cory-Wright, J.; Sebastián-Pérez, V.; Burgess, A.; Cattermole, E.; Meghir, C.; Abell, C.; Coyne, A. G.; Jacobs, W. R. Jr.; Blundell, T. L.; Tiwari, S.; Mendes, V. A Fragment-based Approach to Assess the Ligandability of ArgB, ArgC, ArgD and ArgF in the L-Arginine Biosynthetic Pathway of *Mycobacterium tuberculosis*. *Comput. Struct. Biotechnol. J.* **2021**, *19*, 3491-3506.

(226) Mishra, A.; Mamidi, A. S.; Rajmani, R. S.; Ray, A.; Roy, R.; Surolia, A. An Allosteric Inhibitor of *Mycobacterium tuberculosis* ArgJ: Implications to a Novel Combinatorial Therapy. *EMBO Mol. Med.* **2018**, *10* (4), e8038.

(227) Wang, X.; Yang, R.; Liu, S.; Guan, Y.; Xiao, C.; Li, C.; Meng, J.; Pang, Y.; Liu, Y. IMB-XMA0038, a New Inhibitor Targeting Aspartate-Semialdehyde Dehydrogenase of *Mycobacterium tuberculosis*. *Emerg. Microbes Infect.* **2021**, *10*, 2291-2299.

(228) Hurdle, J. G.; Lee, R. B.; Budha, N. R.; Carson, E. I.; Qi, J.; Scherman, M. S.; Cho, S. H.; McNeil, M. R.; Lenaerts, A. J.; Franzblau, S. G.; Meibohm, B.; Lee, R. E. A Microbiological Assessment of Novel Nitrofuranylamides as Anti-tuberculosis Agents. *J. Antimicrob. Chemother.* **2008**, *62*, 1037-1045.

(229) Hajian, B.; Scocchera, E.; Shoen, C.; Krucinska, J.; Viswanathan, K.; G-Dayanandan, N.; Erlandsen, H.; Estrada, A.; Mikušová, K.; Korduláková, J.; Cynamon, M.; Wright, D. Drugging the Folate Pathway in *Mycobacterium tuberculosis*: The Role of Multi-Targeting Agents. *Cell Chem. Biol.* **2019**, *26*, 781-791.

(230) Nixon, M. R.; Saionz, K. W.; Koo, M.-S.; Szymonifka, M. J.; Jung, H.; Roberts, J. P.; Nandakumar, M.; Kumar, A.; Liao, R.; Rustad, T.; Sacchettini, J. C.; Rhee, K. Y.; Freundlich, J. S.; Sherman, D. R. Folate Pathway Disruption Leads to Critical Disruption of Methionine Derivatives in *Mycobacterium tuberculosis*. *Chem. Biol.* **2014**, *21*, 819-830.

(231) Liu, P.; Yang, Y.; Tang, Y.; Yang, T.; Sang, Z.; Liu, Z.; Zhang, T.; Luo, Y. Design and Synthesis of Novel Pyrimidine Derivatives as Potent Antitubercular Agents. *Eur. J. Med. Chem.* **2019**, *163*, 169–182.

(232) Nunes, J. E. S.; Duque, M. A.; de Freitas, T. F.; Galina, L.; Timmers, L. F. S. M.; Bizarro, C. V.; Machado, P.; Basso, L. A.; Ducati, R. G. *Mycobacterium tuberculosis* Shikimate Pathway Enzymes as Targets for the Rational Design of Anti-Tuberculosis Drugs. *Molecules* **2020**, *25* (6), 1259.

(233) Deng, Q.; Meng, J.; Liu, Y.; Guan, Y.; Xiao, C. IMB-SD62, a Triazolothiadiazoles Derivative With Promising Action Against Tuberculosis. *Tuberculosis* **2018**, *112*, 37–44.

(234) Li, Z.; Liu, Y.; Bai, X.; Deng, Q.; Wang, J.; Zhang, G.; Xiao, C.; Mei, Y.; Wang, Y. SAR Studies on 1,2,4-Triazolo[3,4-*b*][1,3,4]thiadiazoles as Inhibitors of *Mtb* Shikimate Dehydrogenase for the Development of Novel Antitubercular Agents. *RSC Adv*. **2015**, *5*, 97089-97101.

(235) Khan, M. Z.; Kaur, P.; Nandicoori, V. K. Targeting the Messengers: Serine/Threonine Protein Kinases as Potential Targets for Antimycobacterial Drug Development. *IUBMB Life* **2018**, *70*, 889–904.

(236) Hatzios, S. K.; Baer, C. E.; Rustad, T. R.; Siegrist, M. S.; Pang, J. M.; Ortega, C.; Alber, T.; Grundner, C.; Sherman, D. R.; Bertozzi, C. R. Osmosensory Signaling in *Mycobacterium tuberculosis* Mediated by a Eukaryotic-like Ser/Thr Protein Kinase. *Proc. Natl. Acad. Sci. U.S.A.* **2013**, *110* (52), E5069-E5077.

(237) Bhattacharyya, N.; Nkumama, I. N.; Newland-Smith, Z.; Lin, L.-Y.; Yin, W.; Cullen, R. E.; Griffiths, J. S.; Jarvis, A. R.; Price, M. J.; Chong, P. Y.; Wallis, R.; O'Hare, H. M. An Aspartate-Specific Solute-Binding Protein Regulates Protein Kinase G Activity to Control Glutamate Metabolism in Mycobacteria. *mBio* **2018**, *9* (4), e00931-18.

(238) Kidwai, S.; Bouzeyen, R.; Chakraborti, S.; Khare, N.; Das, S.; Gosain, T. P.; Behura, A.; Meena, C. L.; Dhiman, R.; Essafi, M.; Bajaj, A.; Saini, D. K.; Srinivasan, N.; Mahajan, D.; Singh, R. NU-6027 Inhibits Growth of *Mycobacterium tuberculosis* by Targeting Protein Kinase D and Protein Kinase G. *Antimicrob. Agents Chemother.* **2019**, *63* (9), e00996-19.

(239) Iqbal, I. K.; Bajeli, S.; Akela, A. K.; Kumar, A. Bioenergetics of *Mycobacterium*: An Emerging Landscape for Drug Discovery. *Pathogens* **2018**, *7* (1), 24.

(240) Thompson, A. M.; Denny, W. A. Chapter Four - Inhibitors of Enzymes in the Electron Transport Chain of *Mycobacterium tuberculosis.* In *Annual Reports in Medicinal Chemistry: Medicinal Chemistry Approaches to Tuberculosis and Trypanosomiasis*, Chibale, K., Ed.; Academic Press: Cambridge, MA, USA, 2019; Volume 52, pp 97-130.

(241) Foo, C. S.-Y.; Pethe, K.; Lupien, A. Oxidative Phosphorylation – an Update on a New, Essential Target Space for Drug Discovery in *Mycobacterium tuberculosis. Appl. Sci.* **2020**, *10* (7), 2339.

(242) Li, Q.; Lu, X. New Antituberculosis Drugs Targeting the Respiratory Chain. *Chin. Chem. Lett.* **2020**, *31*, 1357–1365.

(243) Bald, D.; Villellas, C.; Lu, P.; Koul, A. Targeting Energy Metabolism in *Mycobacterium tuberculosis*, a New Paradigm in Antimycobacterial Drug Discovery. *mBio* **2017**, *8* (2), e00272-17.

(244) Cook, G. M.; Hards, K.; Vilchèze, C.; Hartman, T.; Berney, M. Energetics of Respiration and Oxidative Phosphorylation in Mycobacteria. *Microbiol. Spectr.* **2014**, *2* (3), MGM2-0015–2013.

(245) Gong, H.; Li, J.; Xu, A.; Tang, Y.; Ji, W.; Gao, R.; Wang, S.; Yu, L.; Tian, C.; Li, J.; Yen, H.-Y.; Man Lam, S.; Shui, G.; Yang, X.; Sun, Y.; Li, X.; Jia, M.; Yang, C.; Jiang, B.; Lou, Z.; Robinson, C. V; Wong, L.-L.; Guddat, L. W.; Sun, F.; Wang, Q.; Rao, Z. An Electron Transfer Path Connects Subunits of a Mycobacterial Respiratory Supercomplex. *Science* **2018**, *362* (6418), eaat8923.

(246) Safarian, S.; Opel-Reading, H. K.; Wu, D.; Mehdipour, A. R.; Hards, K.; Harold, L. K.; Radloff, M.; Stewart, I.; Welsch, S.; Hummer, G.; Cook, G. M.; Krause, K. L.; Michel, H. The Cryo-

EM Structure of the *bd* Oxidase From *M. tuberculosis* Reveals a Unique Structural Framework and Enables Rational Drug Design to Combat TB. *Nat. Commun.* **2021**, *12*, 5236.

(247) Mascolo, L.; Bald, D. Cytochrome *bd* in *Mycobacterium tuberculosis*: A Respiratory Chain Protein Involved in the Defense Against Antibacterials. *Prog. Biophys. Mol. Biol.* **2020**, *152*, 55–63.

(248) Bahuguna, A.; Rawat, S.; Rawat, D. S. QcrB in *Mycobacterium tuberculosis*: The New Drug Target of Antitubercular Agents. *Med. Res. Rev.* **2021**, *41*, 2565-2581.

(249) Cleghorn, L. A. T.; Ray, P. C.; Odingo, J.; Kumar, A.; Wescott, H.; Korkegian, A.; Masquelin, T.; Moure, A. L.; Wilson, C.; Davis, S.; Huggett, M.; Turner, P.; Smith, A.; Epemolu, O.; Zuccotto, F.; Riley, J.; Scullion, P.; Shishikura, Y.; Ferguson, L.; Rullas, J.; Guijarro, L.; Read, K. D.; Green, S. R.; Hipskind, P.; Parish, T.; Wyatt, P. G. Identification of Morpholino Thiophenes as Novel *Mycobacterium tuberculosis* Inhibitors, Targeting QcrB. *J. Med. Chem.* **2018**, *61*, 6592–6608.

(250) Foo, C. S.; Lupien, A.; Kienle, M.; Vocat, A.; Benjak, A.; Sommer, R.; Lamprecht, D. A.; Steyn, A. J. C.; Pethe, K.; Piton, J.; Altmann, K.-H.; Cole, S. T. Arylvinylpiperazine Amides, a New Class of Potent Inhibitors Targeting QcrB of *Mycobacterium tuberculosis*. *mBio* **2018**, *9* (5), e01276-18.

(251) Tang, J.; Wang, B.; Wu, T.; Wan, J.; Tu, Z.; Njire, M.; Wan, B.; Franzblau, S. G.; Zhang, T.; Lu, X.; Ding, K. Design, Synthesis, and Biological Evaluation of Pyrazolo[1,5-*a*]pyridine-3-carboxamides as Novel Antitubercular Agents. *ACS Med. Chem. Lett.* **2015**, *6*, 814–818.

(252) Lu, X.; Williams, Z.; Hards, K.; Tang, J.; Cheung, C.-Y.; Aung, H. L.; Wang, B.; Liu, Z.; Hu, X.; Lenaerts, A.; Woolhiser, L.; Hastings, C.; Zhang, X.; Wang, Z.; Rhee, K.; Ding, K.; Zhang,

T.; Cook, G. M. Pyrazolo[1,5-*a*]pyridine Inhibitor of the Respiratory Cytochrome *bcc* Complex for the Treatment of Drug-Resistant Tuberculosis. *ACS Infect. Dis.* **2019**, *5*, 239–249.

(253) Yu, W.; Chiwala, G.; Gao, Y.; Liu, Z.; Sapkota, S.; Lu, Z.; Guo, L.; Khan, S. A.; Zhong, N.; Zhang, T. TB47 and Clofazimine Form a Highly Synergistic Sterilizing Block in a Second-Line Regimen for Tuberculosis in Mice. *Biomed. Pharmacother.* **2020**, *131*, 110782.

(254) Yu, W.; Yusuf, B.; Wang, S.; Tian, X.; Hameed, H. M. A.; Lu, Z.; Chiwala, G.; Alam, M. S.; Cook, G. M.; Maslov, D. A.; Zhong, N.; Zhang, T. Sterilizing Effects of Novel Regimens Containing TB47, Clofazimine and Linezolid in a Murine Model of Tuberculosis. *Antimicrob. Agents Chemother.* **2021**, *65* (10), e00706-21.

(255) Liu, Y.; Gao, Y.; Liu, J.; Tan, Y.; Liu, Z.; Chhotaray, C.; Jiang, H.; Lu, Z.; Chiwala, G.; Wang, S.; Makafe, G.; Islam, M. M.; Hameed, H. M. A.; Cai, X.; Wang, C.; Li, X.; Tan, S.; Zhang, T. The Compound TB47 Is Highly Bactericidal Against *Mycobacterium ulcerans* in a Buruli Ulcer Mouse Model. *Nat. Commun.* **2019**, *10*, 524.

(256) Zhou, S.; Wang, W.; Zhou, X.; Zhang, Y.; Lai, Y.; Tang, Y.; Xu, J.; Li, D.; Lin, J.; Yang, X.; Ran, T.; Chen, H.; Guddat, L. W.; Wang, Q.; Gao, Y.; Rao, Z.; Gong, H. Structure of *Mycobacterium tuberculosis* Cytochrome *bcc* in Complex With Q203 and TB47, Two Anti-TB Drug Candidates. *Elife* **2021**, *10*, e69418.

(257) Hu, X.; Wan, B.; Liu, Y.; Shen, J.; Franzblau, S. G.; Zhang, T.; Ding, K.; Lu, X. Identification of Pyrazolo[1,5-*a*]pyridine-3-carboxamide Diaryl Derivatives as Drug Resistant Antituberculosis Agents. *ACS Med. Chem. Lett.* **2019**, *10*, 295–299.

(258) Moraski, G. C.; Seeger, N.; Miller, P. A.; Oliver, A. G.; Boshoff, H. I.; Cho, S.; Mulugeta, S.; Anderson, J. R.; Franzblau, S. G.; Miller, M. J. Arrival of Imidazo[2,1-*b*]thiazole-5-

carboxamides: Potent Antituberculosis Agents That Target QcrB. *ACS Infect. Dis.* **2016**, *2*, 393–398.

(259) Moraski, G. C.; Deboosère, N.; Marshall, K. L.; Weaver, H. A.; Vandeputte, A.; Hastings, C.; Woolhiser, L.; Lenaerts, A. J.; Brodin, P.; Miller, M. J. Intracellular and *in Vivo* Evaluation of Imidazo[2,1-*b*]thiazole-5-carboxamide Anti-Tuberculosis Compounds. *PLoS One* **2020**, *15* (1), e0227224.

(260) Lupien, A.; Foo, C. S.; Savina, S.; Vocat, A.; Piton, J.; Monakhova, N.; Benjak, A.; Lamprecht, D. A.; Steyn, A. J. C.; Pethe, K.; Makarov, V. A.; Cole, S. T. New 2-Ethylthio-4-methylaminoquinazoline Derivatives Inhibiting Two Subunits of Cytochrome *bc1* in *Mycobacterium tuberculosis*. *PLoS Pathog.* **2020**, *16* (1), e1008270.

(261) Tantry, S. J.; Markad, S. D.; Shinde, V.; Bhat, J.; Balakrishnan, G.; Gupta, A. K.; Ambady, A.; Raichurkar, A.; Kedari, C.; Sharma, S.; Mudugal, N. V.; Narayan, A.; Naveen Kumar, C. N.; Nanduri, R.; Bharath, S.; Reddy, J.; Panduga, V.; Prabhakar, K. R.; Kandaswamy, K.; Saralaya, R.; Kaur, P.; Dinesh, N.; Guptha, S.; Rich, K.; Murray, D.; Plant, H.; Preston, M.; Ashton, H.; Plant, D.; Walsh, J.; Alcock, P.; Naylor, K.; Collier, M.; Whiteaker, J.; McLaughlin, R. E.; Mallya, M.; Panda, M.; Rudrapatna, S.; Ramachandran, V.; Shandil, R.; Sambandamurthy, V. K.; Mdluli, K.; Cooper, C. B.; Rubin, H.; Yano, T.; Iyer, P.; Narayanan, S.; Kavanagh, S.; Mukherjee, K.; Balasubramanian, V.; Hosagrahara, V. P.; Solapure, S.; Ravishankar, S.; Hameed P, S. Discovery of Imidazo[1,2-*a*]pyridine Ethers and Squaramides as Selective and Potent Inhibitors of Mycobacterial Adenosine Triphosphate (ATP) Synthesis. *J. Med. Chem.* **2017**, *60*, 1379-1399.

(262) Tantry, S. J.; Shinde, V.; Balakrishnan, G.; Markad, S. D.; Gupta, A. K.; Bhat, J.; Narayan, A.; Raichurkar, A.; Jena, L. K.; Sharma, S.; Kumar, N.; Nanduri, R.; Bharath, S.; Reddy, J.; Panduga, V.; Prabhakar, K. R.; Kandaswamy, K.; Kaur, P.; Dinesh, N.; Guptha, S.; Saralaya, R.; Panda, M.; Rudrapatna, S.; Mallya, M.; Rubin, H.; Yano, T.; Mdluli, K.; Cooper, C. B.; Balasubramanian, V.; Sambandamurthy, V. K.; Ramachandran, V.; Shandil, R.; Kavanagh, S.; Narayanan, S.; Iyer, P.; Mukherjee, K.; Hosagrahara, V. P.; Solapure, S.; Hameed P, S.; Ravishankar, S. Scaffold Morphing Leading to Evolution of 2,4-Diaminoquinolines and Aminopyrazolopyrimidines as Inhibitors of the ATP Synthesis Pathway. *MedChemComm* **2016**, *7*, 1022-1032.

(263) Sawyer, E. B.; Grabowska, A. D.; Cortes, T. Translational Regulation in Mycobacteria and its Implications for Pathogenicity. *Nucleic Acids Res.* **2018**, *46*, 6950–6961.

(264) Falagas, M. E.; Vardakas, K. Z. Benefit-Risk Assessment of Linezolid for Serious Gram-Positive Bacterial Infections. *Drug Saf.* **2008**, *31*, 753-768.

(265) *New Trial Results Show Effectiveness of BPaL Regimen for Highly Drug-Resistant TB Can Be Maintained With Reduced Dosing of Linezolid*. TB Alliance, July 15, 2021; https://www.tballiance.org.za/news/zenix-press-release-english (accessed October 10, 2021)

(266) Zhao, Q.; Xin, L.; Liu, Y.; Liang, C.; Li, J.; Jian, Y.; Li, H.; Shi, Z.; Liu, H.; Cao, W. Current Landscape and Future Perspective of Oxazolidinone Scaffolds Containing Antibacterial Drugs. *J. Med. Chem.* **2021**, *64*, 10557-10580.

(267) Zhao, H.; Wang, B.; Fu, L.; Li, G.; Lu, H.; Liu, Y.; Sheng, L.; Li, Y.; Zhang, B.; Lu, Y.; Ma, C.; Huang, H.; Zhang, D.; Lu, Y. Discovery of a Conformationally Constrained Oxazolidinone

With Improved Safety and Efficacy Profiles for the Treatment of Multidrug-Resistant Tuberculosis. *J. Med. Chem.* **2020**, *63*, 9316–9339.

(268) Guo, S.; Wang, B.; Fu, L.; Chen, X.; Zhang, W.; Huang, H.; Lu, Y. *In Vitro* and *In Vivo* Activity of Oxazolidinone Candidate OTB-658 Against *Mycobacterium tuberculosis*. *Antimicrob. Agents Chemother.* **2021**, *65* (11), e00974-21.

(269) Shoen, C.; DeStefano, M.; Hafkin, B.; Cynamon, M. *In Vitro* and *In Vivo* Activities of Contezolid (MRX-I) Against *Mycobacterium tuberculosis*. *Antimicrob. Agents Chemother.* **2018**, *62* (8), e00493-18.

(270) Hoy, S. M. Contezolid: First Approval. *Drugs* **2021**, *81*, 1587-1591.

(271) Gordeev, M. F.; Yuan, Z. Y. New Potent Antibacterial Oxazolidinone (MRX-I) With an Improved Class Safety Profile. *J. Med. Chem.* **2014**, *57*, 4487–4497.

(272) Dos Santos Fernandes, G. F.; de Souza, P. C.; Moreno-Viguri, E.; Santivañez-Veliz, M.; Paucar, R.; Pérez-Silanes, S.; Chegaev, K.; Guglielmo, S.; Lazzarato, L.; Fruttero, R.; Chin, C. M.; da Silva, P. B.; Chorilli, M.; Solcia, M. C.; Ribeiro, C. M.; Silva, C. S. P.; Marino, L. B.; Bosquesi, P. L.; Hunt, D. M.; de Carvalho, L. P. S.; de Souza Costa, C. A.; Cho, S. H.; Wang, Y.; Franzblau, S. G.; Pavan, F. R.; Dos Santos, J. L. Design, Synthesis, and Characterization of N-Oxide-Containing Heterocycles With in Vivo Sterilizing Antitubercular Activity. *J. Med. Chem.* **2017**, *60*, 8647–8660.

(273) Fernandes, G. F. S.; Campos, D. L.; Da Silva, I. C.; Prates, J. L. B.; Pavan, A. R.; Pavan, F. R.; Dos Santos, J. L. Benzofuroxan Derivatives as Potent Agents Against Multidrug-Resistant *Mycobacterium tuberculosis*. *ChemMedChem* **2021**, *16*, 1268–1282.

(274) Moffat, J. G.; Vincent, F.; Lee, J. A.; Eder, J.; Prunotto, M. Opportunities and Challenges in Phenotypic Drug Discovery: An Industry Perspective. *Nat. Rev. Drug Discov.* **2017**, *16*, 531–543.

(275) Yuan, T.; Werman, J. M.; Sampson, N. S. The Pursuit of Mechanism of Action: Uncovering Drug Complexity in TB Drug Discovery. *RSC Chem. Biol.* **2021**, *2*, 423-440.

(276) Fernandes, G. F. S.; de Souza, P. C.; Marino, L. B.; Chegaev, K.; Guglielmo, S.; Lazzarato, L.; Fruttero, R.; Chung, M. C.; Pavan, F. R.; Dos Santos, J. L. Synthesis and Biological Activity of Furoxan Derivatives Against *Mycobacterium tuberculosis*. *Eur. J. Med. Chem.* **2016**, *123*, 523–531.

(277) de Souza, P. C.; Fernandes, G. F. S.; Marino, L. B.; Ribeiro, C. M.; da Silva, P. B.; Chorilli, M.; Silva, C. S. P.; Resende, F. A.; Solcia, M. C.; de Grandis, R. A.; Costa, C. A. S.; Cho, S. H.; Wang, Y.; Franzblau, S. G.; Dos Santos, J. L.; Pavan, F. R. Furoxan Derivatives Demonstrated *in Vivo* Efficacy by Reducing *Mycobacterium tuberculosis* to Undetectable Levels in a Mouse Model of Infection. *Biomed. Pharmacother.* **2020**, *130*, 110592.

(278) Cheng, Y.-J.; Liu, Z.-Y.; Liang, H.-J.; Fang, C.-T.; Zhang, N.-N.; Zhang, T.-Y.; Yan, M. Discovery of (3-Benzyl-5-hydroxyphenyl)carbamates as New Antitubercular Agents With Potent In Vitro and In Vivo Efficacy. *Molecules* **2019**, *24* (10), 2021.

(279) Krasavin, M.; Lukin, A.; Vedekhina, T.; Manicheva, O.; Dogonadze, M.; Vinogradova, T.; Zabolotnykh, N.; Rogacheva, E.; Kraeva, L.; Yablonsky, P. Conjugation of a 5-Nitrofuran-2-oyl Moiety to Aminoalkylimidazoles Produces Non-Toxic Nitrofurans That Are Efficacious *in Vitro* and *in Vivo* Against Multidrug-Resistant *Mycobacterium tuberculosis*. *Eur. J. Med. Chem.* **2018**, *157*, 1115–1126.

(280) Kidwai, S.; Park, C.-Y.; Mawatwal, S.; Tiwari, P.; Jung, M. G.; Gosain, T. P.; Kumar, P.; Alland, D.; Kumar, S.; Bajaj, A.; Hwang, Y.-K.; Song, C. S.; Dhiman, R.; Lee, I. Y.; Singh, R. Dual Mechanism of Action of 5-Nitro-1,10-Phenanthroline Against *Mycobacterium tuberculosis. Antimicrob. Agents Chemother.* **2017**, *61* (11), e00969-17.

(281) Jin, G.; Mi Kim, Y.; Lee, A.; Choi, J.; Kang, S.; Seo, M.; Jea Seo, J.; Lee, S.; Kang, J.; Kim, J.; Park, S.; Woo, M.; Falcão, V. C. A.; Lee, H.; Heo, J.; Shum, D.; Park, K.; Delorme, V.; Choi, I. Discovery of Thienothiazolocarboxamide Analogues as Novel Anti-tubercular Agent. *Bioorg. Med. Chem.* **2020**, *28* (23), 115797.

(282) Kaur, P.; Potluri, V.; Ahuja, V. K.; Naveenkumar, C. N.; Krishnamurthy, R. V.; Gangadharaiah, S. T.; Shivarudraiah, P.; Eswaran, S.; Nirmal, C. R.; Mahizhaveni, B.; Dusthackeer, A.; Mondal, R.; Batt, S. M.; Richardson, E. J.; Loman, N. J.; Besra, G. S.; Shandil, R. K.; Narayanan, S. A Multi-Targeting Pre-Clinical Candidate Against Drug-Resistant Tuberculosis. *Tuberculosis* **2021**, *129*, 102104.

(283) Shruthi, T. G.; Eswaran, S.; Shivarudraiah, P.; Narayanan, S.; Subramanian, S. Synthesis, Antituberculosis Studies and Biological Evaluation of New Quinoline Derivatives Carrying 1,2,4-Oxadiazole Moiety. *Bioorg. Med. Chem. Lett.* **2019**, *29*, 97-102.

(284) Lavin, R. C.; Johnson, C.; Ahn, Y.-M.; Kremiller, K. M.; Sherwood, M.; Patel, J. S.; Pan, Y.; Russo, R.; MacGilvary, N. J.; Giacalone, D.; Kevorkian, Y. L.; Zimmerman, M. D.; Glickman, J. F.; Freundlich, J. S.; Tan, S. Targeting *Mycobacterium tuberculosis* Response to Environmental Cues for the Development of Effective Antitubercular Drugs. *PLoS Biol.* **2021**, *19* (7), e3001355.

(285) Vickers, C. F.; Silva, A. P. G.; Chakraborty, A.; Fernandez, P.; Kurepina, N.; Saville, C.; Naranjo, Y.; Pons, M.; Schnettger, L. S.; Gutierrez, M. G.; Park, S.; Kreiswith, B. N.; Perlin, D. S.; Thomas, E. J.; Cavet, J. S.; Tabernero, L. Structure-Based Design of MptpB Inhibitors That Reduce Multidrug-Resistant *Mycobacterium tuberculosis* Survival and Infection Burden in Vivo. *J. Med. Chem.* **2018**, *61*, 8337-8352.

(286) Tiberi, S.; Vjecha, M. J.; Zumla, A.; Galvin, J.; Migliori, G. B.; Zumla, A. Accelerating Development of New Shorter TB Treatment Regimens in Anticipation of a Resurgence of Multi-Drug Resistant TB Due to the COVID-19 Pandemic. *Int. J. Infect. Dis.* **2021**, *113 Suppl. 1*, S96-S99.

(287) Dowden, H.; Munro, J. Trends in Clinical Success Rates and Therapeutic Focus. *Nat. Rev. Drug Discov.* **2019**, *18*, 495-496.

(288) Kaneko, T.; Cooper, C.; Mdluli, K. Challenges and Opportunities in Developing Novel Drugs for TB. *Future Med. Chem.* **2011**, *3*, 1373-1400.

(289) Nuermberger, E. L. Preclinical Efficacy Testing of New Drug Candidates. *Microbiol. Spectr.* **2017**, *5* (3), TBTB2-0034-2017.

(290) Sarathy, J. P.; Zuccotto, F.; Hsinpin, H.; Sandberg, L.; Via, L. E.; Marriner, G. A.; Masquelin, T.; Wyatt, P.; Ray, P.; Dartois, V. Prediction of Drug Penetration in Tuberculosis Lesions. *ACS Infect. Dis.* **2016**, *2*, 552-563.

(291) Sarathy, J. P.; Via, L. E.; Weiner, D.; Blanc, L.; Boshoff, H.; Eugenin, E. A.; Barry, C. E.; Dartois, V. A. Extreme Drug Tolerance of *Mycobacterium tuberculosis* in Caseum. *Antimicrob. Agents Chemother.* **2018**, *62* (2), e02266-17.

(292) Irwin, S. M.; Driver, E.; Lyon, E.; Schrupp, C.; Ryan, G.; Gonzalez-Juarrero, M.; Basaraba, R. J.; Nuermberger, E. L.; Lenaerts, A. J. Presence of Multiple Lesion Types with Vastly Different Microenvironments in C3HeB/FeJ Mice Following Aerosol Infection with *Mycobacterium tuberculosis*. *Dis. Model. Mech.* **2015**, *8*, 591-602.

(293) Lanoix, J.-P.; Lenaerts, A. J.; Nuermberger, E. L. Heterogeneous Disease Progression and Treatment Response in a C3HeB/FeJ Mouse Model of Tuberculosis. *Dis. Model. Mech.* **2015**, *8*, 603-610.

(294) Irwin, S. M.; Prideaux, B.; Lyon, E. R.; Zimmerman, M. D.; Brooks, E. J.; Schrupp, C. A.; Chen, C.; Reichlen, M. J.; Asay, B. C.; Voskuil, M. I.; Nuermberger, E. L, Andries, K.; Lyons, M. A.; Dartois, V.; Lenaerts, A. J. Bedaquiline and Pyrazinamide Treatment Responses Are Affected by Pulmonary Lesion Heterogeneity in *Mycobacterium tuberculosis* Infected C3HeB/FeJ Mice. *ACS Infect. Dis.* **2016**, *2*, 251-267.

(295) Alemparte-Gallardo, C.; Encinas, L.; Esquivias Provencio, J. Novel Tetrazole Compounds and their Use in the Treatment of Tuberculosis. Patent WO 2019/034729 A1, 2019.

(296) Chen, X.; Liu, Z.-Q.; Wang, B.; Zhu, H.; Fu, L.; Li, Y.-Y.; Lu, Y. Evaluation of Antituberculosis Activities of 14 Antituberculosis Drugs in Macrophage. *Chin. J. Antituberc.* **2019**, *41*, 993-998.

(297) Kaneko, T. *About TB Alliance – Global Health Innovative Technology Fund*. GHIT-PDPs Webimar Series, Session 3, TB Alliance; November 19, 2021. GHIT-PDPs-webinar-S3-DrTakushiKaneko.pdf (ghitfund.org) (accessed December 20, 2021)

(298) TB Alliance. *Our Pipeline – MmpL3 Inhibitors*. Compounds | TB Alliance (accessed December 20, 2021)

(299) Katsuno, K.; Burrows, J. N.; Duncan, K.; Hooft van Huijsduijnen, R.; Kaneko, T.; Kita, K.; Mowbray, C. E.; Schmatz, D.; Warner, P.; Slingsby, B. T. Hit and Lead Criteria in Drug Discovery for Infectious Diseases of the Developing World. *Nat. Rev. Drug Discov.* **2015**, *14*, 751-758.

(300) Singh, V.; Chibale, K. Strategies to Combat Multi-Drug Resistance in Tuberculosis. *Acc. Chem. Res.* **2021**, *54*, 2361-2376.

(301) Lakshminarayana, S. B.; Huat, T. B.; Ho, P. C.; Manjunatha, U. H.; Dartois, V.; Dick, T.; Rao, S. P. S. Comprehensive Physicochemical, Pharmacokinetic and Activity Profiling of Anti-TB Agents. *J. Antimicrob. Chemother.* **2015**, *70*, 857-867.

(302) Palmer, B. D.; Sutherland, H. S.; Blaser, A.; Kmentova, I.; Franzblau, S. G.; Wan, B.; Wang, Y.; Ma, Z.; Denny, W. A.; Thompson, A. M. Synthesis and Structure-Activity Relationships for Extended Side Chain Analogues of the Antitubercular Drug (6*S*)-2-Nitro-6-{[4-(trifluoromethoxy)benzyl]oxy}-6,7-dihydro-5*H*-imidazo[2,1-*b*][1,3]oxazine (PA-824). *J. Med. Chem.* **2015**, *58*, 3036-3059.

(303) Johnson, T. W.; Gallego, R. A.; Edwards, M. P. Lipophilic Efficiency as an Important Metric in Drug Design. *J. Med. Chem.* **2018**, *61*, 6401-6420.

(304) Hefti, F. F. Requirements for a Lead Compound to Become a Clinical Candidate. *BMC Neurosci.* **2008**, *9* (Suppl. 3), S7.

(305) Rebollo-Lopez, M. J.; Lelièvre, J.; Alvarez-Gomez, D.; Castro-Pichel, J.; Martínez-Jiménez, F.; Papadatos, G.; Kumar, V.; Colmenarejo, G.; Mugumbate, G.; Hurle, M.; Barroso, V.; Young, R. J.; Martinez-Hoyos, M.; González del Río, R.; Bates, R. H.; Lopez-Roman, E. M.; Mendoza-Losana, A.; Brown, J. R.; Alvarez-Ruiz, E.; Marti-Renom, M. A.; Overington, J. P.;

Cammack, N.; Ballell, L.; Barros-Aguire, D. Release of 50 New, Drug-like Compounds and Their Computational Target Predictions for Open Source Anti-Tubercular Drug Discovery. *PLoS One* **2015**, *10* (12), e0142293.

(306) Bosch, B.; DeJesus, M. A.; Poulton, N. C.; Zhang, W.; Engelhart, C. A.; Zaveri, A.; Lavalette, S.; Ruecker, N.; Trujillo, C.; Wallach, J. B.; Li, S.; Ehrt, S.; Chait, B. T.; Schnappinger, D.; Rock, J. M. Genome-Wide Gene Expression Tuning Reveals Diverse Vulnerabilities of *M. tuberculosis*. *Cell* **2021**, *184*, 4579-4592.

(307) McNeil, M. B.; Keighley, L. M.; Cook, J. R.; Cheung, C.-Y.; Cook, G. M. CRISPR Interference Identifies Vulnerable Cellular Pathways With Bactericidal Phenotypes in *Mycobacterium tuberculosis*. *Mol. Microbiol.* **2021**, *116*, 1033-1043.

(308) Seyhan, A. A. Lost in Translation: The Valley of Death Across Preclinical and Clinical Divide – Identification of Problems and Overcoming Obstacles. *Transl. Med. Commun.* **2019**, *4*, 18.

Table of Contents Graphic